

SURFACE DATA FOR FUSION DEVICES

PROCEEDINGS OF THE U.S.-JAPAN WORKSHOP

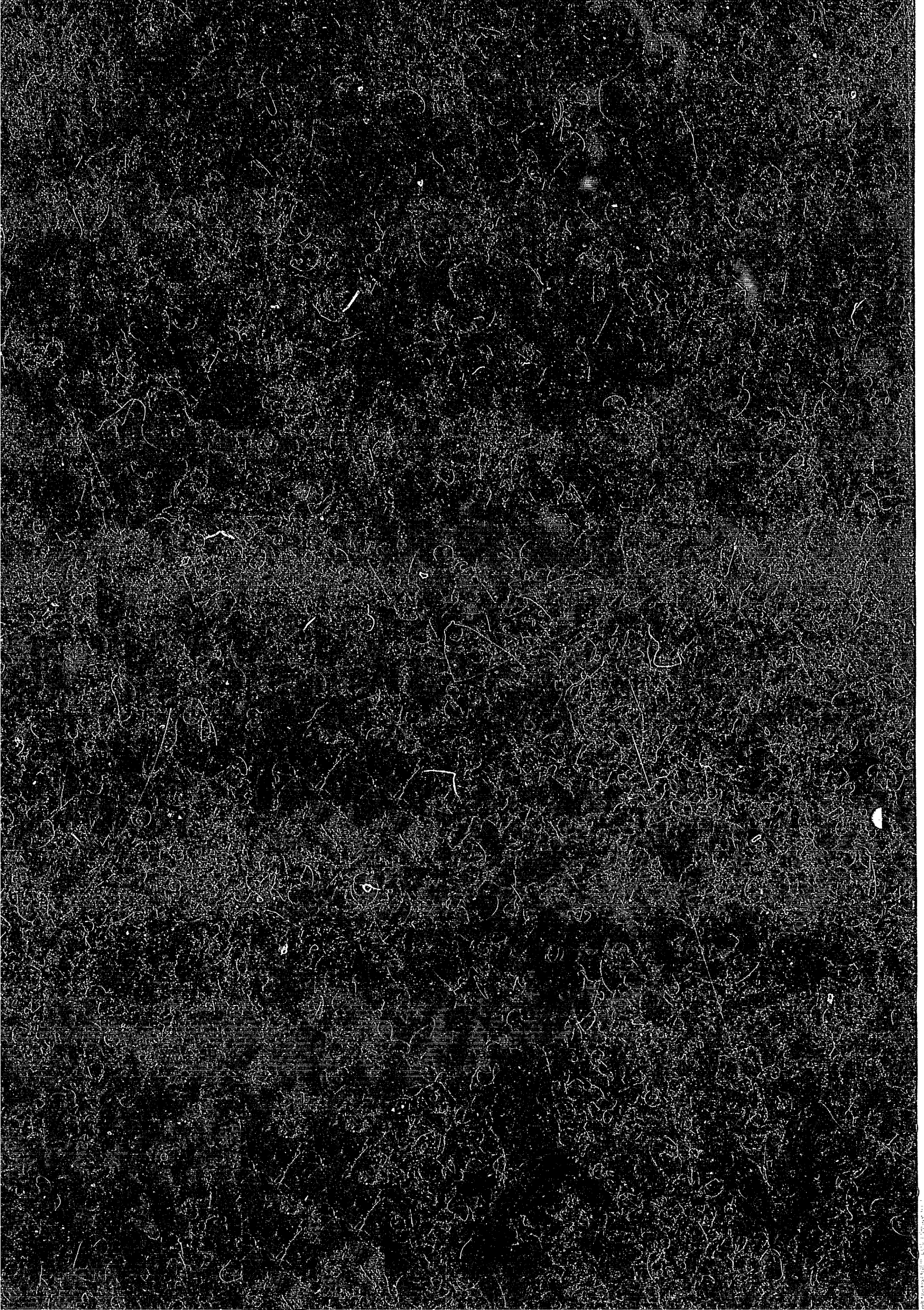
ON

SURFACE DATA REVIEW

INSTITUTE OF PLASMA PHYSICS

NAGOYA UNIVERSITY

NAGOYA, JAPAN



SURFACE DATA FOR FUSION DEVICES

Proceedings of the U.S.—Japan Workshop
on
Surface Data Review

Edited by
Noriaki Itoh¹⁾ and Edward W. Thomas²⁾

Institute of Plasma Physics, Nagoya University
Chikusa-ku, Nagoya 464, Japan

December 14-18, 1981

Permanent address:

- 1) Department of Crystalline Materials Science, Faculty of Engineering, Nagoya University
- 2) School of Physics, Georgia Institute of Technology

This document is prepared as a preprint of compilation of atomic data for fusion research sponsored fully or partly by the IPP/Nagoya University. This is intended for future publication in a journal or will be included in a data book after some evaluations or rearrangements of its contents. This document should not be referred without the agreement of the authors. Enquiries about copyright and reproduction should be addressed to Research Information Center, IPP/Nagoya University, Nagoya, Japan.

PREFACE

U.S.-Japan Workshop on Surface Data Review took place, as one of the activities of the U.S.-Japan Fusion Cooperation program, on December 14 - 18, 1981 at Institute of Plasma Physics, Nagoya University, Nagoya, Japan. This is the second of the U.S.-Japan workshop on fusion-reactor data and is the succession of the "Workshop on Atomic Collision Data for Fusion", held at Boulder, Colorado on October 27-31, 1980. The key persons of present workshop are P.M. Stone and K. Kamada and the organization was made by E.W. Thomas and N. Itoh.

The workshop was intended to survey the present status of the understanding of the mechanisms of the important elementary processes relevant to the plasma-wall interaction (PWI) , to arrive at establishing the methods of the data evaluation and compilation and to promote future cooperation between the data-center activities in U.S. and in Japan. The workshop was divided into five sections:

- I. Overview of PWI Data Needs and Production for Fusion
- II. Mechanism of PWI
- III. Data Center Interactions
- IV. Discussion on PWI Data for Specific Cases
- V. New proposal and Summary

Section II was devoted to understanding of the mechanisms of basic processes of PWI, emphasizing data problems, while section IV was devoted to discussion of data for certain specific reactions.

The proceeding consists of the papers presented in sections I and II and of the summaries of the discussions in sections II, III, IV and V. The entire program and the participants list are attached at the end of the proceedings. The abstract of each contribution was distributed in the workshop.

I would like to express our sincerest gratitude to all participants who gave active contribution not only through the formal presentation of papers but also through discussions in all possible occasions. Thanks are also to Y. Itikawa and K. Morita who helped the organization.

Noriaki Itoh

CONTENTS

Data Needs for Edge Modeling of Tokamak Plasma	
	T. Amano.....i
Plasma-Wall Interaction	
	N. Itoh9
Particle Reflection	
	T. Tabata.....14
Sputtering--- Materials Removal Rate	
	R. Shimizu.....20
Sputtering--- Quantum State of Ejected Material	
	D. Gruen.....25
Chemical Reaction and Chemical Sputtering	
	R. Yamada.....31
Hydrogen Trapping, Detrapping and Re-Emission	
	B. Doyle.....37
Desorption and Adsorption	
	A. Koma73
Review of Discussions on Mechanism of Plasma Wall Interaction	
	B. Doyle.....77
Review of Data Center Activities	
	E.W. Thomas.....80
Review of Discussions on PWI Data for Specific Cases - Reflection and Sputtering -	
	D. M. Gruen.....82
Review of Discussions of PWI Data for Specific Cases - Trapping, Re-Emission, Desorption and Adsorption -	
	K. Kamada.....84
Conclusion	
	E.W. Thomas.....87
Program.....	91
List of Participants.....	95

Data Needs for Edge Modeling of Tokamak Plasmas

Tsuneo Amano

Institute of Plasma Physics

Nagoya University

Nagoya 464 JAPAN

§1. Introduction

Progress achieved in plasma heating and confinement in tokamak experiments during the past decades has brought a number of problems which have to be solved for the development of a tokamak fusion reactor. Among them, the interaction of plasmas with solid surfaces¹⁾ represent a very serious problem in the next generation large tokamaks in which intense neutral beam or RF powers of several tens of MW are injected into the plasmas.

In order to evaluate the role of plasma wall interaction on these large tokamaks, we need an accurate modeling of the edge plasma in the scrape-off region which directly interacts with the limiter (or divertor) and wall. In §2, we attempt a self-consistent modeling of the edge plasma by solving the plasma transport and impurity rate and diffusion equations. We calculate the plasma flow loss to the limiter and the resulting sputtering of the limiter. Sputtering of the wall by charge

exchange fast neutrals is also considered. Sputtered impurity atoms are partly shielded by the plasma in the scrape-off region and partly enter into main plasma region. The cooling of the plasma in the scrape-off region due to impurity radiations is included to obtain the edge electron temperature which governs the sputtering. The data needs for the edge plasma modeling are discussed in §3.

The recycling of working gas between the plasma and the wall plays an important role in the particle and energy balance of the present day tokamaks.¹⁾ In the next generation tokamaks, the understanding of the recycling process becomes more important, particularly when D (deuterium) and T (tritium) fuels are used, for the control of electron density and D, T. Mixture ratio and the tritium inventory in the wall.²⁾ The damage of the wall due to the bombardment of energetic particles and its effect on the recycling must be also assessed. The data needs for the modeling of the plasma wall recycling³⁾ are discussed in §3 together with the data needs for the edge plasma modeling.

At IPPJ, we are now planning to construct a new tokamak called "R tokamak".⁴⁾ Here "R" stands for the "reacting" D-T plasma. The dimensions and physical parameters are listed in Table I. In this device, neutral beam power of 15 MW will be injected to heat a plasma up to 10 keV. Axisymmetric bumper limiters made of T_iC surround the plasma to absorb the major plasma heat load on the order of 15 MW. In §4, we simulate the neutral beam heating of the R tokamak by utilizing the model described in §2 and assess role of the plasma wall interaction in this device.

§2. Edge Plasma Modeling of Tokamaks

We use the following set of transport equations.⁵⁾

$$\frac{\partial n_j}{\partial t} = - \frac{1}{r} \frac{\partial}{\partial r} r \Gamma_j + S_{jI} - \frac{n_j v_f}{L}, \quad j = D, T, He^4, \quad (1)$$

$$\begin{aligned} \frac{3}{2} \frac{\partial}{\partial t} n_e T_e = & - \frac{1}{r} \frac{\partial}{\partial r} (r Q_e) + E_z j_z - \frac{3m_e}{m_i} \frac{n_e}{\tau_e} (T_e - T_i) \\ & + W_{Be} + W_\alpha - W_I - W_R - \frac{2\gamma n_e T_e v_f}{L}, \end{aligned} \quad (2)$$

$$\begin{aligned} \frac{3}{2} \frac{\partial}{\partial t} n_i T_i = & - \frac{1}{r} \frac{\partial}{\partial r} (r Q_i) + \frac{3m_e}{m_i} \frac{n_e}{\tau_e} (T_e - T_i) + W_{Bi} \\ & - W_{cx} - \frac{2n_i T_i v_f}{L}, \end{aligned} \quad (3)$$

$$\frac{\partial B_\theta}{\partial t} = c \frac{\partial E_z}{\partial r}, \quad (4)$$

$$\Gamma_j = - D \frac{\partial n_j}{\partial r} - n_j \frac{c E_z}{B_\theta} L_{14}, \quad j = D, T, He^4, \quad (5)$$

$$Q_e = - \chi_e \frac{\partial T_e}{\partial r} - \frac{3}{2} D T_e \frac{\partial n_e}{\partial r} - n_e T_e \frac{c E_z}{B_\theta} L_{24}, \quad (6)$$

$$Q_i = - \chi_i \frac{\partial T_i}{\partial r} - \frac{3}{2} D T_i \frac{\partial n_i}{\partial r}, \quad (7)$$

$$E_z = n j_z = \frac{cn}{4\pi} \frac{1}{r} \frac{\partial}{\partial r} (r B_\theta), \quad (8)$$

where W_{Be} , W_{Bi} are energy inputs to electrons and ions from neutral beams, respectively. W_α represents Alpha particle heating. W_R , W_I , W_{CX} are radiation, ionization and charge exchange losses, respectively. Terms with L_{14} , L_{24} represent the Ware pinch effects. Particle and energy loss terms proportional to v_f/L in Eqs. (1), (2) and (3) are present only in the scrape-off region of the plasma in the shadow of the limiter. Here L and v_f are the average distance to the limiter and the flow velocity to the limiter, respectively.

The impurity transport equations (or diffusion-rate eqs.) are given by

$$\frac{\partial n_k}{\partial t} = - \frac{1}{r} \frac{\partial}{\partial r} r \Gamma_k + n_e (n_{k-1} S_{k-1} - n_k S_k + n_{k+1} \alpha_{k+1} - n_k \alpha_k), \quad (9)$$

where n_k and Γ_k are the number density and radial diffusion flux of the k -th ion, and S_k and α_k are the ionization and recombination rate coefficients, respectively.⁶⁾ For Γ_k , we assume the form

$$\Gamma_k = \Gamma_k^N + \Gamma_k^A, \quad (10)$$

where Γ_k^N is the neoclassical diffusion flux and Γ_k^A is an empirical diffusion flux,

$$\Gamma_k^A = - D_A \frac{dn_k}{dr}. \quad (11)$$

For D_A , we take the same as the electron density anomalous diffusion coefficient. From n_k , we can calculate the ionization and line radiation

losses W_I and W_R in Eq. (2).

The charged particles in the scrape-off region hit the wall with the energy,

$$E_I = \frac{1}{2} M_i v_f^2 + 3.5 Z T_e, \quad (12)$$

where M and Z are the mass and the charge of the particle, respectively. The second term in Eq. (12) comes from the energy gained due to the sheath potential acceleration in front of the limiter. From the energy and particle flux to the limiter, we can calculate the sputtering of the limiter. In §3, we will consider $T_i C$ coated limiters for the "R" tokamak. We take into account the sputtering processes; $D \rightarrow T_i C$, $T \rightarrow T_i C$ and $T_i \rightarrow T_i C$. For $D \rightarrow T_i C$, we take the sputtering yield data from Ref. (7). For $T \rightarrow T_i C$, we interpolate from the data of $D \rightarrow T_i C$ and $He \rightarrow T_i C$. For $T_i \rightarrow T_i C$ we assume the yield is the same as $T_i \rightarrow T_i$ and use the empirical formula given in Ref. (8). We assume no preferential sputtering of the carbon or titanium. The total sputtering yield is obtained by averaging over the shifted Maxwellian energy distribution,

$$f(E) \propto \exp - \left(\frac{E - E_I}{T_i} \right) \quad (13)$$

where E_I is given by Eq. (12) and T_i is ion temperature.

Most of sputtered particles are emitted as neutrals moving straight in the direction of the emission. The impurity atoms which are ionized during traversing the scrape-off region are swept away back to the limiter. The un-ionized particles either hit the wall or enter the main plasma region.

To simulate this "shielding" effect, we use a Monte Carlo method. The motions of several thousand neutral particles are followed until they are ionized or hit the wall. By use of usual procedure of Monte Carlo method we obtain the neutral particle distribution, which is used as a source term in Eq. (9).

The sputtering yield Y is distributed in energy E in accordance with,

$$dY/dE \propto E/(E + E_B)^{3-m}. \quad (14)$$

Where E_B is the binding energy and $m \approx 0 \sim 1/4$.⁹⁾ There are scarce data for the angular distribution of the sputtered particles for the non-normal incidence. We simply take $\cos\theta$ distribution by assuming the incident charged particles are accelerated with sheath potential in front of the limiter and hit the limiter normally, although this is a dubious assumption for a bumper limiter geometry. The sputtering of the first wall made of T_iC by charge exchange fast neutrals is also considered. Another simple model to consider the shielding effect is simply to assume a fraction γ of the sputtered atoms actually enter the plasma. The value γ is guessed, for instance, from the result of a Monte Carlo simulation.

In §4, we apply the model described in this section to an analysis of "R" tokamak performance.

§3. Data Needs for Edge and Recycling Modeling

In this section, we summarize the data needs for the edge and plasma wall recycling modeling. Data needs in concern with the design of "R"

tokamak are also given. Most of these needs have already been discussed,⁹⁾ however, here we emphasize the importance and the urgency.

I) Edge Modeling

- 1) secondary electron emission rate, T_iC
- 2) self sputtering yield T_iC ($T_i \rightarrow T_iC$, etc.)
- 3) energy distribution of sputtered particles
- 4) angular distribution of sputtered particles for non-normal incidence
- 5) chemical sputtering of C, T_iC preferential sputtering

II) R Tokamak Design

- 1) permeabilities, diffusivities, solubilities of hydrogen, deuterium and tritium in Poco-graphite, T_iC , S_iC
- 2) out gas rate of Poco-graphite, T_iC , S_iC
- 3) values of detrapping energies for the various damage site T_iC , C
- 4) the density of damage site
- 5) those dependence on the energy of injected beam and its fluence
- 6) implantation profile

Table I

R Tokamak Parameters

Major radius	R	2.1 m
Minor radius	a	0.6 m
Plasma current	I_p	1.5 ~ 1.8 MA
Maximum toroidal field B_T		5 Tesla
Injected beam power	W_B	15 MW
Injected beam energy	E_B	120 keV

References

- 1) G. M. McCracken and P. E. Stott : Nucl. Fusion 19 (1979) 927
- 2) J. L. Cecchi : J. Nucl. Mater. 93/94 (1980) 28
- 3) H. C. Howe : J. Nucl. Mater. 93/94 (1980) 17
- 4) A. Miyahara et al. : IPPJ-500 (1981)
- 5) D. F. Duchs et al.: Nucl. Fusion 17 (1977) 3
- 6) T. Amano, E. C. Crume : ORNL/TM-6363 (1978)
M. Sato, T. Amano, K. Sato, K. Miyamoto : J. Phys. Soc. Jpn. 50 (1981) 2114
- 7) J. Roth et al. : IPP 9/26
- 8) N. Matsunami et al. : IPPJ-AM-14
- 9) J. Bohdansky : J. Nucl. Mater. 93/94 (1981) 44

Plasma-Wall Interaction

Noriaki Itoh

Department of Crystalline Materials Science
Faculty of Engineering, Nagoya University
Nagoya 464, Japan

A brief survey is given on the present status of plasma-wall interaction (PWI) emphasizing the available data compilation and feasibility of the data compilation of available data. The PWI is important in three aspects: (1) fuel recycling, (2) impurity generation and (3) possible effect on the wall properties. The third aspect has not been emphasized to a large extent so far but we touch upon this problem briefly.

PWI has been generally divided up into basic processes shown in Table I. The data compilation of each of these problems has been attempted but it has been realized that the data compilation could be carried out only when we understand the mechanisms to some extent. Moreover, recently attention has started to be paid on potential synergisms between each process listed in Table I.

In this review we first take a different approach on PWI, which may be convenient to analyze the present status of understanding of the mechanisms as well as the synergisms. In this approach we consider balances of particles (mainly ions) and energies in the PWI processes. In the particle balance we consider all incident ions (H, D, T, O, C) from the outside of the wall and all atoms ejected from the wall materials. In the energy balance the energy brought from plasma in the form of kinetic energies of ions, electrons and photons should be considered. Most part of the energy may be converted just to heat the wall, but a considerable part, which is of primary concern in the present context, will cause ejection of atoms (sputtering, desorption and de-trapping) from the wall and various stages of the radiation effects in the wall, e.g. defect creation, radiation-enhanced diffusion etc. A series of kinetic equations dealing with the energy and particle balances may be constructed and can be used as a wall modeller.

Generally speaking the energy carried by particles is deposited on the wall in the form of electronic excitation and of the kinetic energy of atoms composing the wall. By virtue of recent development of the experimental and theoretical studies of the stopping power for ions, a reasonably accurate evaluation of the density of the electronic (inelastic) and atomic (elastic) energy deposition on the wall can be made. Electrons and photons may convert its energy only in the form of the electronic excitation. The next problem is to evaluate quantitatively the effects that follow the energy deposition. The effects in which we are interested are sputtering, desorption, detrapping, chemical reaction, segregation, dissolution, diffusion of impurities etc.

On the particle balance, prediction of the behaviors of energetic ions or atoms (above 100 eV) in the wall can be made with a reasonable accuracy again by virtue of the atomic collision theories. Behaviors of thermalized impurity atoms are solid state problems: diffusion, binding with impurities, evaporation, thermal segregation etc. We note again most of these properties are influenced by radiation. The behaviors of low energy atoms (below 100 eV) are unexplored.

Based on the arguments made above we examine each basic process. In table II, we list factors that determine each basic process under three categories: collisions, solid state property and radiation effect.

(1) Reflection: Reflection of incident H^+ , D^+ with energies more than 100 eV is fairly well understood. The total reflection coefficients have been expressed in the form of empirical formulae.¹⁾ The dependence on the incident angle and the angular dependence of reflected ions may be evaluated by computer codes. The behaviors of low energy ions are related to the trapping and detrapping.

(2) Accommodation and desorption: Adsorption of impurities on the surface is a solid-state problem, which has been extensively studied.²⁾ Effect of co-existence of two kinds of atoms (e.g. H_2 and O_2) are not known very well.³⁾ Electronic excitation and elastic collisions with incident ions are known to cause desorption; it may also enhance dissolution into solids or other chemical reaction. Desorption by electronic excitation appears to occur only when excited above a certain threshold energy.⁴⁾ Desorption by elastic collisions of ions may be factorized into the elastic stopping power, probability of the kinetic energy being transferred from the host atoms to the impurities and the binding energy of the impurity at the surface. If the probability of the host-impurity energy transfer is low, the direct ejection of impurities by incident ions will be important.

(3) Trapping and detrapping: Most fundamental problems in trapping and detrapping of hydrogens are the number of the trapping sites in the lattice and the stability of trapping. Various other processes are involved, however, radiation-induced modification of the stability, thermal and radiation-enhanced diffusion, trapping at lattice defects, reaction of hydrogen with other impurities etc. Thus we need more extensive data compilation on thermal processes concerning hydrogen in metals. It is also interesting to note recent observation that motion of hydrogen is enhanced by electronic excitation.⁵⁾

(4) Sputtering: Sputtering in monatomic solids has been characterized reasonably well and empirical equations have been suggested. According to the Sigmund's formula the sputtering yield is proportional to the elastic stopping power and the binding energy of atoms at the surface. This is one of the most simple case in which the "effect" is a linear function of depos-

ited energy. This is the reason why the data compilation has been successful.⁶⁾

Sputtering of alloys is much more complex. It is known that, because of the thermal segregation and radiation-induced segregation, the composition near the surface is not necessarily the same as that in the bulk. Thus the surface composition should be carefully analyzed in order to understand the relation between the sputtering yield of each component and the deposited energy. It is also suggested that the composition change at the surface induces composition change at grain boundaries located relatively deep from the surface. The chemical sputtering is concerned with the chemical reaction (either thermal or radiation-induced) and the behaviors of the reaction products in the bulk and at the surface.

It is clear that most of the basic processes of PWI, except the ion-induced reflection and the sputtering of monatomic solids, are complex mixture of the various thermal processes and radiation-induced processes in solids as listed in Table II. The compilation of existing data on thermal processes involving hydrogen will be useful. Further understanding of each process may be accomplished if the experimental data of the effect of elastic and inelastic energy deposition on well-characterized solid-states is accumulated. One of the main objects of the data compilation is to provide useful data for plasma modellers, in which particle balance and energy balance at the surface and in each segment of materials should be treated.

References

- 1) T. Tabata, R. Itoh, Y. Itikawa, N. Itoh and K. Morita, Inst. Plasma Phys. Nagoya Univ. Rep. IPPJ-AM-18 (1981).
- 2) T. N. Rhodin and G. Ertl(eds), The Nature of the Surface Chemical Bond (North-Holland, Amsterdam, 1979).
- 3) E. I. Ko and R. J. Madix, Surface Science 109, 221 (1981).
- 4) P. J. Feibelman and M. L. Knotek, Phys. Rev. 18, 6531 (1978).
- 5) M. Ikeya and T. Miki, Nature 292, 5824 (1981).
- 6) N. Matsunami, Y. Yamamura, Y. Itikawa, N. Itoh, Y. Kazumata, S. Miyagawa, K. Morita and R. Shimizu, Inst. Plasma Phys. Nagoya Univ. Rep. IPPJ-AM-14 (1980).

Table I. Basic Processes on Plasma Wall Interaction

process	particle	energy
Reflection	hydrogen, helium	100 eV - 10 keV
Accommodation	hydrogen, impurities	1 - 100 eV
Trapping	hydrogen, helium	100 eV - 100 keV
Sputtering	hydrogen, helium impurities	threshold - 20 keV
Desorption by ions	hydrogen, helium impurities	threshold - 20 keV
Desorption by electrons	-	threshold - 100 keV
Desorption by photons	-	threshold - 100 keV
Chemical Reactions		
Arcing		

Table II. Phenomena related to each basic processes of PWI

process	collision	solid state property	radiation effect
Reflection	Scattering		
Accommodation		Binding energy	
Desorption by ions	Elastic energy deposition to host to impurity		Collision cascade Energy-transfer probability to impurity
Desorption by electrons and photons	Inelastic energy deposition	Binding energy	Threshold energy
Trapping and detrapping	Range	Binding energy Diffusion	Hydrogen-defects interaction Diffusion
Sputtering			
Monatomic solids	Elastic energy deposition	Binding energy	Collision cascade
Alloys and compounds	Elastic energy deposition	Binding energy Segregation Diffusion	Collision cascade Energy partition near surface Segregation Diffusion
Practical surface	Elastic energy deposition	Binding energy Adsorption	Collision cascade Energy partition near surface
Chemical	Range Inelastic energy deposition	Binding energy Diffusion	Chemical reaction Diffusion

PARTICLE REFLECTION

Tatsuo Tabata

Radiation Center of Osaka Prefecture, Sakai, Osaka 593, Japan

1. MECHANISM AND RELEVANT PARAMETERS

When an atomic particle impinges on a solid, it undergoes a series of elastic and inelastic collisions with the atoms of the solid. As a result of a large-angle elastic scattering or a cumulative effect of multiple collisions, the particle may emerge from the incident surface in a state with positive or negative charge, or as a neutral atom. This phenomenon is called reflection or backscattering.

The characteristics of reflection are governed by the characteristics of both scattering and energy loss of the particle in the medium. Further details of the mechanism will be touched in Sec. 4.

Let us define:

$$r(E, \theta, \phi, i; E_0, \theta_0) dE \sin \theta d\theta d\phi = \text{probability that a particle impinging with energy } E_0 \text{ and angle of incidence } \theta_0 \text{ is reflected into the energy interval between } E \text{ and } E+dE \text{ and the solid angle } \sin \theta d\theta d\phi \text{ at the colatitude } \theta \text{ and the longitude } \phi, \text{ and leaves the surface with charge state } i, \quad (1)$$

where

$$i = \begin{cases} -1 & \text{for negative charge state} \\ 0 & \text{for neutral state} \\ +1 & \text{for positive charge state.} \end{cases} \quad (2)$$

The function $r(E, \theta, \phi, i; E_0, \theta_0)$ thus defined is called differential reflection coefficient. In practice, it is difficult to have thorough knowledge on the differential reflection coefficient, and it is useful to have some other parameters defined by the integral of the differential coefficient.

Some important integral parameters are:

the number- (or particle-) reflection coefficient

$$R_N(E_0, \theta_0) = \sum_{i=-1}^1 \iiint r(E, \theta, \phi, i; E_0, \theta_0) dE \sin \theta d\theta d\phi, \quad (3)$$

the energy-reflection coefficient

$$R_E(E_0, \theta_0) = \sum_{i=-1}^1 \iiint E r(E, \theta, \phi, i; E_0, \theta_0) dE \sin \theta d\theta d\phi / E_0, \quad (4)$$

the mean fractional energy of reflected particles

$$r_E(E_0, \theta_0) = R_E(E_0, \theta_0) / R_N(E_0, \theta_0), \quad (5)$$

the normalized angular distribution of reflected particles integrated over their energies

$$F_A(\theta, \phi; E_0, \theta_0) = \sum_{i=-1}^1 \int r(E, \theta, \phi, i; E_0, \theta_0) dE / R_N(E_0, \theta_0) , \quad (6)$$

the normalized energy distribution of reflected particles averaged over all ejection angles

$$F_E(E; E_0, \theta_0) = \sum_{i=-1}^1 \iint r(E, \theta, \phi, i; E_0, \theta_0) \sin\theta d\theta d\phi / R_N(E_0, \theta_0) . \quad (7)$$

Other parameters of interest are:

the charge-state fractions

$$f_C(E, \theta, \phi, i; E_0, \theta_0) = r(E, \theta, \phi, i; E_0, \theta_0) / \sum_{i=-1}^1 r(E, \theta, \phi, i; E_0, \theta_0) \quad (i = -1, 0, 1) . \quad (8)$$

In the studies of the reflection coefficients of ions, the reduced energy ϵ defined by the following equation is usually used:

$$\epsilon = 32.5 E_0 M_2 / [(M_1 + M_2) (Z_1^{2/3} + Z_2^{2/3}) Z_1 Z_2] \quad (E_0 \text{ in keV}) , \quad (9)$$

where M_1 and M_2 are the masses and Z_1 and Z_2 are the atomic numbers of the ion and the target atom.

2. RELEVANCE TO PWI

Reflection of particles from the walls of fusion devices is relevant to the process of recycling, which affects the balance of particles and energy in plasma with importance equal to magnetic confinement.

Howe¹⁾ has indicated that in a tokamak with a limiter reflection accounts for 80 to 90% of recycling with re-emission providing an additional 10 to 20%.

3. AVAILABLE DATA BASE

3.1 Coverage Need

The fluxes of hydrogen and its isotopes from the plasmas to the wall are generally about 10^{19} to $10^{20} \text{ m}^{-2} \text{ s}^{-1}$, and the flux of helium is an order of magnitude smaller. Therefore, the data on reflection of hydrogen and its isotopes are of primary importance; the data for helium, of secondary.

The energies of these particles are ranging from several eV to a hundred keV with the energy distribution peaking within the range from a hundred eV to 1 keV (for example, see Fig. 1). For primary energies above 10 keV, fluxes to the wall should be small and the reflection coefficients also becomes small,

so that data on reflection are primarily needed for energies below 10 keV.⁴⁾

3.2 Material Presently Available

Experimental data on reflection of hydrogen, deuterium and helium ions incident on various materials are mostly in the range of energies from 1 to 50 keV. Various parameters of interest have been covered.

Data production by computer simulation has been made down to an energy of 10 eV.

3.3 Available Compendia

Mashkova⁵⁾ has recently given an excellent review article on R_N and R_E of light ions.

There are three major compilations of data on reflection:

ORNL-5207/R1, 1979 (ref. 6) Section D.5: R_N , R_E , angular and energy distributions, and charge state-fractions.

IPP 9/32, 1979 (ref. 7): R_N , R_E , mean energy r_{E0} , some examples of the effect of surface conditions, energy distributions and charge-state fractions.

IPPJ-AM-18, 1981 (ref. 8): R_N , R_E and r_E compared with the empirical formulas proposed by Tabata et al.⁹⁾

3.4 Reliability of Data

The errors assigned to the published experimental data on R_N and R_E lie most frequently in the range from 10 to 30%. The values of relative rms deviation of the experimental data on R_N , R_E and r_E from the empirical formulas of Tabata et al. also indicate that the probable errors of the data are in this range.

3.5 Applicability of Data to Real Machines

In real plasma machines the surface of the walls continually suffers erosion and deposition of materials such as hydrogen isotopes, oxygen, carbon and metals. Therefore, it is necessary to know the effect of these modifications of the surface on the characteristics of particle reflection.

The effects of surface roughness, oxide layers and hydrogen concentration have been investigated by experiment and computer simulation.¹⁰⁻¹²⁾ The results show that these effects reduce the values of R_N and R_E by 20 to 60%. Further study on modified surfaces are considered necessary.

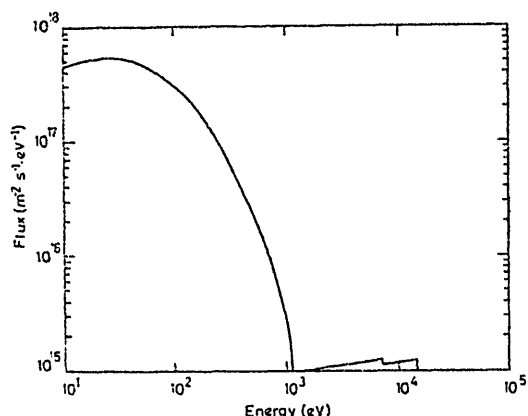


Fig. 1. The calculated energy spectrum of charge exchange neutrals from ATC for a high-power beam-heated discharge (ref. 2; cited from ref. 3).

4. TECHNIQUES FOR PREDICTING, EXTRAPOLATING AND INTERPOLATING DATA

4.1 Theoretical Approaches

Two asymptotic theories have been developed to treat the reflection of light ions from solids. One is the transport theory, in which the reflection is treated as an essentially multiple process by solving the kinetic Boltzmann equation. The other is the single-collision model. In this model, a particle is assumed to move along straight lines in the target both before and after its deflection caused by a single close-collision with a target atom. Using the latter approach, Vukanić and Sigmund¹³⁾ have obtained analytical results for R_N , R_E and other parameters. These results show a rather good agreement with experimental data for $\epsilon \geq 3$. Morita¹⁴⁾ has developed a modified single-collision model in which the angular deviation caused by multiple small-angle collisions is taken into account.

The Monte-Carlo simulation also serves as a useful method for predicting the data on reflection. In most of computer simulations, binary collision approximation has been used. Well-known codes are MARLOWE, TAVERN and TRIM.

From the point of view of modeling the solid, approaches of the computer simulation are classified into a lattice model, a dense-gas model and a "liquid" model. To simulate an amorphous solid with a lattice code, the basic groups of the lattice structure is slid or rotated between successive collisions. Jackson¹⁵⁾ has simulated the reflection of H and He ions using lattice and gas-like codes, and has found that the difference in the short-range crystalline order causes differences in the results. Eckstein et al.¹⁶⁾ have also reported small discrepancies between the results of TRIM (a liquid-like code) and MARLOWE (a lattice code). However, the agreement between the results of experiment and those of the TRIM and MARLOWE programs are reasonable within the experimental accuracy.¹⁷⁾ (For further details of theoretical approaches, see ref. 5.)

4.2 Analytical Representations

Akkerman¹⁷⁾ has analyzed his Monte Carlo results to propose empirical formulas for R_N and R_E as a function of ϵ (from 0.1 to 2) and θ_0 (from 0 to 75°). Tabata et al.⁹⁾ have developed empirical formulas for R_N , R_E and r_E as a function of ϵ (from about 10^{-3} to 10^2) for $\theta_0 = 0^\circ$ (see Fig. 2).

A simple approximate relation to express $R_N(E_0, \theta_0)$ as a function of $R_N(E_0, 0^\circ)$ and θ_0 has been given by Clarke and Sigmar (ref. 18); a refined relation is being developed.¹⁹⁾

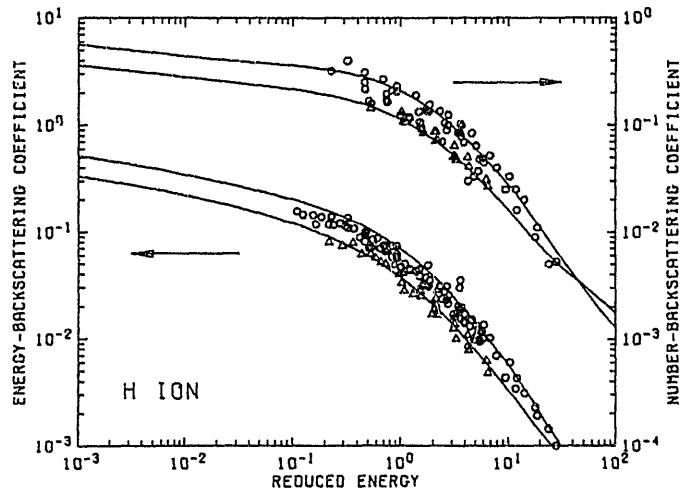
The angular distribution $F_A(\theta; \phi, E_0, 0^\circ)$ is well represented by the cosine law in most cases.

The energy distribution $F_E(E; E_0, 0^\circ)$ has been approximated by Howe¹⁾ as

$$F_E(E; E_0, 0^\circ) = \begin{cases} 2E / \{ \ln[1 + (E_0/E_p)^2] (E_p^2 + E^2) \} & E \leq E_0 \\ 0 & E > E_0 \end{cases} \quad (10)$$

where $E_p \approx 1$ keV.

Fig. 2. $R_N(E_0, 0^\circ)$ and $R_E(E_0, 0^\circ)$ of H ions are plotted as a function of the reduced energy ϵ . o: experimental data for C, Al, Si, Ti, stainless steel, Ni, Cu, Ag, W, Au and Pb; Δ : experimental data for Nb, Mo and Ta; curves: the empirical formulas of Tabata et al. for Fe (the upper of each pair) and Nb (the lower) (from ref. 9).



5. DEFICIENCIES

(1) The empirical formulas for R_N and R_E should be checked and improved for energies below 1 keV.

(2) Estimation and representation of R_N and R_E for wall materials with a saturated hydrogen concentration and for surfaces covered by oxide layers are needed.

(3) A refined analytical representation for the energy distribution is needed.

(4) Analytical representations for R_N and R_E of ions incident with realistic energy and angular distributions (a Maxwell-Boltzmann distribution for energy and a cosine distribution for angle) would be of use.

In relation to item (1), Jackson's work²⁰ should be noted. He used a computer simulation to calculate R_N and R_E of H ions with energies less than 200 eV impinging on Ti in the presence of surface attractive field. The results have indicated that the surface trapping energy from 5 to 20 eV significantly modify both the magnitude and the functional behavior of R_N and R_E , and that such surface fields must be taken into account in models of low energy reflection processes.

REFERENCES

- 1) H. C. Howe, J. Nucl. Mater. 93 & 94, 17 (1980).
- 2) S. A. Cohen, J. Nucl. Mater. 63, 65 (1976).
- 3) G. M. McCracken and P. E. Stott, Nucl. Fusion 19, 889 (1979).
- 4) H. Vernickel, Phys. Rep. 37, 93 (1978).
- 5) E. S. Mashkova, Radiat. Eff. 54, 1 (1981).
- 6) E. W. Thomas, S. W. Hawthorne, F. W. Meyer and B. J. Farmer, Oak Ridge Natl. Labs. Rep. ORNL-5207/R1 (1979).

- 7) W. Eckstein and H. Verbeek, Max-Planck Inst. Plasma Phys. Rep. IPP 9/32 (1979).
- 8) T. Tabata, R. Ito, Y. Itikawa, N. Itoh and K. Morita, Inst. Plasma Phys. Nagoya Univ. Rep. IPPJ-AM-18 (1981).
- 9) T. Tabata, R. Ito, K. Morita and Y. Itikawa, Jpn. J. Appl. Phys. 20, 1929 (1981).
- 10) J. E. Robinson and D. P. Jackson, J. Nucl. Mater. 76 & 77, 353 (1978).
- 11) O. S. Oen and M. T. Robinson, J. Nucl. Mater. 76 & 77, 370 (1978).
- 12) V. M. Sotnikov, Fiz. Plasmy 6, 286 (1980).
- 13) J. Vukanić and P. Sigmund, Appl. Phys. 11, 265 (1976).
- 14) K. Morita, to be published.
- 15) D. P. Jackson, J. Nucl. Mater. 93 & 94, 507 (1980).
- 16) W. Eckstein, H. Verbeek and J. P. Biersack, J. Appl. Phys. 51, 1194 (1980).
- 17) A. F. Akkerman, Phys. Status Solidi a 48, K47 (1978).
- 18) J. F. Clarke and D. J. Sigmar, Proc. 7th European Conf. Plasmas and Cont. Fusion, Lausanne, 1975, p. 134.
- 19) T. Tabata and R. Ito, Preprints of the 42nd Autumn Meeting of Jpn. Soc. Appl. Phys., Fukui, 1981, p. 4.
- 20) D. P. Jackson, Radiat. Eff. 49, 233 (1980).

Sputtering-material removal rate

Ryuichi Shimizu

Department of Applied Physics, Osaka University

The basic processes of sputtering is considered as follows: When an incident projectile impinges on a target, a certain amount of kinetic energy is transferred to target atoms through elastic scattering between the incident and target atoms. If this energy transferred to the target atom exceeds displacement energy, the target atom moves out from the original site undergoing similar scattering processes as does the incident projectile.

This results in so-called collision cascade. Some of recoiled atoms generated in the collision cascade reach the surface to escape from the surface as sputtered atoms if their kinetic energies are large enough to overcome the surface barrier.

This sputtering is measured by the sputtering yield as the mean number of atoms removed from a bombarded surface per incident particle,

$$Y = \frac{\text{atoms removed from the surface}}{\text{incident projectile}} .$$

[Linear Cascade Regime]

(1) Theoretical expression of Y

Sigmund theory based on linear transport equations is well known to describe very well the general features of the sputtering in linear sputtering regime, leading to the equation

$$Y = 0.042 \frac{\alpha(M_1/M_2) S_n(E)}{U_s} \quad (1)$$

for $E \gg E_s$. α is constant given by the ratio of masses of the incident projectile (M_1) and target atom (M_2). $S_n(E)$ is nuclear stopping cross-section and U_s the surface binding energy which is usually taken for sublimation energy.

Yamamura has shown that an extension of this theoretical treatment for energy region where the above assumption $E \gg E_s$ no more holds leads to

$$Y = 0.042 \frac{\alpha(M_1/M_2)}{U_s} S_n(E) [1 - (E_{th}/E)^{1/2}] \quad (2)$$

where E_{th} is the threshold energy.

This equation is the same as that derived first by Matsunami et al, semi-empirically as described below.

(2) Semi-empirical expressions of Y

Bohdansky et al have found the semi-empirical expression

$$Y = 5.5 \times 10^{-3} Q(E/E_{th})^{1/4} [1 - (E_{th}/E)]^{7/2} \quad (3)$$

with

$$\begin{aligned} E_{th}/U_s &= 1/\gamma(1-\gamma), \text{ for } M_1/M_2 \gtrsim 5 \\ &= 8(M_2/M_1)^{-1/3}, \text{ for } M_2/M_1 \lesssim 5 \end{aligned} \quad (4)$$

describing the experimental data for such light incident projectiles as H, D, ^3He , ^4He etc. Q is yield factor and γ the energy transfer factor ($= 4M_1M_2/(M_1+M_2)^2$).

Matsunami et al, on the other hand, have semi-empirically derived an expression

$$Y = 0.042 \frac{\alpha(M_2/M_1)}{U_s} S_n(E) [1 - (E_{th}/E)]^{1/2} \quad (5)$$

from the experimental data over 190 cases. This equation describes the sputtering yields for heavy incident projectile as well and cover the higher energy region with considerable success. Concerning α and E_{th}/U_s in Eq.(5) they have proposed, as the best fit, the expressions as follows;

$$\alpha \begin{cases} = 0.1019 + 0.0842(M_2/M_1)^{0.9805} & \text{for } M_2/M_1 < 2.163 \\ = -0.4137 + 0.6092(M_2/M_1)^{0.1708} & \text{for } M_2/M_1 > 2.163. \end{cases} \quad (6)$$

and

$$\xi (=E_{th}/U_s) \begin{cases} = 4.143 + 11.46(M_2/M_1)^{-0.5004} & \text{for } M_2/M_1 < 3.115 \\ = 5.809 + 2.791(M_2/M_1)^{0.4816} & \text{for } M_2/M_1 > 3.115 \end{cases} \quad (7)$$

Figure 1 shows how the Eq.(5) describes the sputtering yields obtained for Ni. The best fit values of α and ξ obtained are plotted as a function of M_2/M_1 in Figs. 2 and 3, respectively.

[Non-linear Cascade Regime]

In the linear sputtering regime described above the sputtering yield is proportional to $S_n(E)$. Namely linear collision cascades dominate the sputtering process. However, for instance, the sputtering of large Z materials, particularly of low sublimation energy, with heavy ions can no more be considered to be due to linear collision cascade. Those sputterings out of linear sputtering regime is called non-linear sputtering.

Assuming that atoms in spike caused by collision (non-linear) cascade have velocity distribution according to Maxwell distribution Sigmund has derived the sputtering yield in non-linear sputtering regime as

$$Y = \frac{F_D(0) \tau}{(3 M_2 E_S)^{1/2}} \exp(-3 U_S/E_S) \quad (8)$$

$F_D(0)$ is the density of energy deposition at the target surface and τ the average containment time per spike.

Kitazoe et al have proposed another model assuming the generation of shock wave and obtained the expression suggesting

$$Y \propto S_n(E)^{3/2} \quad (9)$$

Even though those theoretical expressions describes some aspects of qualitative tendencies in non-linear sputtering, there is considerable uncertainty as to theoretical evaluation of the sputtering yield in this regime.

[Sputtering Yields of Alloys and Compounds]

The main complication in the sputtering of multicomponent target is that the components are not always sputtered stoichiometrically. The result of this, called preferential sputtering, is that the composition of an alloy can change in a certain depth range beneath the bombarded surface and eventually a stationary state may be reached where the composition of the flux of sputtered articles reflects the bulk composition.

Thus this stationary state allows us to assess the sputtering yield of polyatomic materials.

With respect to theoretical approach to the sputtering of binary medium in linear cascade regime, Andersen and Sigmund have derived in approximation for $E \gg E_0$, the sputtering yield ratio

$$\frac{Y_1}{Y_2} = \frac{C_1 S_{21}(U_{02})}{C_2 S_{12}(U_{01})} \quad (10)$$

Then

$$\frac{Y_1}{Y_2} \Rightarrow \left(\frac{C_1}{C_2} \right)^{2m} \left(\frac{U_{02}}{U_{01}} \right)^{1-2m} \quad \text{for } m_1 = m_2 = m. \quad (11)$$

where C_i is the concentration of i -atom and U_{0i} the surface potential for i -atom in the binary target. S_{ij} is the stopping cross-section for an i -atom hitting a j -atom.

Direct consequence of the above equation is that the lighter component tends to be sputtered preferentially. However, since m is presumably small $0 < m < 0.2$, this effect is less pronounced than that caused by different surface potential.

An simple extension of Monte Carlo simulation have also been done for binary alloys by Shimizu. The result has described the preferential sputtering in Pt-Si alloy with considerable success, leading to conclusion that large mass difference between the components is main factor causing the preferential sputtering of Si-atoms. However, this approach can not explain the preferential sputtering in Cu-Ni alloys even though fairly large surface potential was assumed.

Those collision cascade-calculations, both the analytical and computer simulation, have been done so far for homogeneous multi-component systems. Most measurements, however, were done at steady state region where so-called altered layer is formed and the surface layer concerns the sputtering is no more homogeneous. Thus, calculations for such a multicomponent target having composition change in-depth as the altered layers observed are highly required for assessing the sputtering yield.

Concerning oxide materials Kelly and Ram measured sputtering yields of both metals and their oxides. Their results indicate that the sputtering yield changes drastically from metal to its oxide. Their results are shown in Table I.

In the cases of alloys, on the other hand, no such a systemic measurement of sputtering yields has yet to be done to my knowledge. Saeki and Shimizu measured the sputtering yield of Cu-Ni alloy for 500 eV Ar⁺ ions. The sputtering yield was less than sputtering yields of both pure Cu- and Ni-target and rather agrees well with the result of evaporated Cu-Ni alloy film obtained by Ho.

Furthermore ISS-measurements of uppermost atom layer of the bombarded surfaces have shown that the composition of the uppermost atom layer is almost the same as that of the bulk even though the surface composition obtained by AES under the same condition is clearly of Ni-rich, as reported by Okutani et al. and by Schwartzfager et al.

Consequently those results suggests that the sputtering yields of alloys can not be simply estimated from the sputtering yields of sample-components.

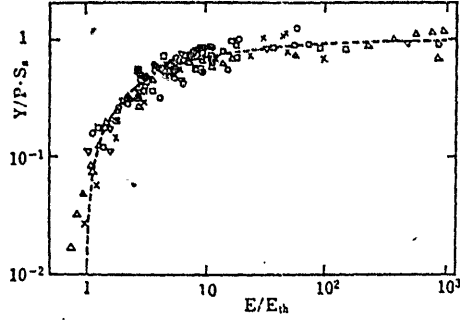


Fig. 1 Energy dependence of the sputtering yields of Ni target for H (x), He (□), Ni (○), Ar (△) and Xe (▽) ions. The yield and energy are normalized by $P=0.042/U_0$ and E_{th} , respectively. The dashed line represents eq. (5).

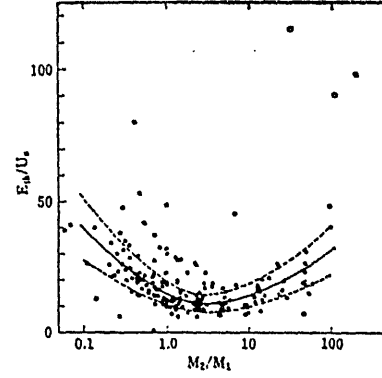


Fig. 3 The $\xi=E_{th}/U_0$ parameter as a function of the mass ratio M_2/M_1 , where M_2 and M_1 are the masses of target atoms and incident ions, respectively. The solid line is drawn by smoothing the averaged values. Multiplying the averaged values by 1.3 and 0.7, broken lines are drawn.

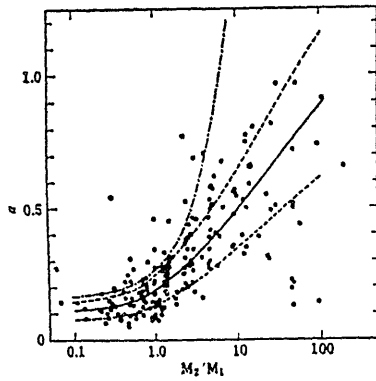


Fig. 2 The α -parameters as a function of the mass ratio M_2/M_1 , where M_2 and M_1 are the masses of target atoms and incident ions, respectively. The solid line is drawn by smoothing the averaged values. Multiplying the averaged values by 1.3 and 0.7, broken lines are drawn. The theoretical values are shown by the dot-dashed.

Table 1 Sputtering yields of oxides and their metals under 10 keV Kr⁺-ion bombardment

Oxide	Y (total atoms/ion) for oxide	Y (atoms/ion) for metal
Al ₂ O ₃	1.5	3.2
MgO	1.8	8.1
MoO ₃	9.6	2.8
Nb ₂ O ₅	3.4	1.8
SiO ₂	3.6	2.1
SnO ₂	15.3	6.5
Ta ₂ O ₅	2.5	1.6
TiO ₂	1.6	2.1
UO ₂	3.8	2.4
V ₂ O ₅	12.7	2.3
WO ₃	9.2	2.6
ZrO ₂	2.8	2.3

Charge, Quantum State and Energy Distributions of Impurities
Released in Plasma-Wall Interaction Processes *

Dieter M. Gruen

Chemistry Division
Argonne National Laboratory, Argonne, IL 60439, USA

Most present day fusion plasma experiments and reactor design studies involve hydrogen plasmas confined by strong magnetic fields. Due to cross-field diffusion and other reasons, confinement is not perfect so that energetic plasma particles bombard limiters, walls and other structural components of the machine. Release of high Z impurities severely limits achievable plasma parameters and may in fact prevent ignition temperatures from being reached as reactor like conditions are approached. These questions require the utmost scrutiny in order to develop effective impurity control methods.

The different possible erosion processes leading to impurity introduction are: (1) Sputtering by D, T, He, impurity ions and neutrons; (2) Arcing between the plasma and various surfaces; (3) Thermal pulses leading to localized power deposition and resulting in evaporation and surface cracking; (4) Implantation of plasma particles leading to blistering, embrittlement or chemical erosion. The latter process is aided by photon, electron, ion bombardment and temperature excursions resulting in desorption of chemical reaction products.

The total erosion rate due to all the various processes acting in concert is of importance for determining wall lifetimes. Impurity levels however depend in detail on the nature of the released products, their energies, angular, spatial and temporal distributions as well as on various transport mechanisms. In order to understand the overall impurity problem, it is necessary to consider each impurity release process separately and in detail. However, certain generic characteristics such as the charges, quantum states and energy distributions of impurities are common to all release mechanisms and play important roles in determining the fractions of the erosion products which, by making their way into the plasma, cause serious plasma energy losses through radiative processes.

For example, the charge state of the impurity species largely determines its fate in the region between the wall or limiter and the plasma edge. Thus, neutral impurities may travel several cm before being ionized very quickly upon entering the plasma edge. The influence of the unipolar sheath potential

*Work performed under the auspices of the Division of Magnetic Fusion Energy,
U. S. Department of Energy

is exerted only within a very short distance of the surface and therefore has no effect on neutral impurity atoms. However, calculations show that secondary ions emanating from the limiter surfaces with kinetic energies less than the sheath potential will have essentially zero probability of traveling more than a few Debye lengths (10^{-2} cm) before being redeposited. Similarly, secondary ions originating at the first wall are redeposited as a result of the deflection produced by the toroidal magnetic field. Impurity influx would therefore be substantially reduced for ejected material possessing a high ion/neutral ratio.

The energy distribution is a function of the charge and quantum state of the impurity as well as the erosion process which gave rise to it. In turn, impurity energy distributions profoundly influence impurity transport in the critical region between the surface of origin and the plasma edge. In the following sections, more detailed considerations will be given to these various parameters as they relate to sputtering only because more is known about this particular erosion process. It should be kept in mind, however, that much of what is said applies, *mutatis mutandis*, to the other erosion processes which have been enumerated above.

When solid surfaces are bombarded by energetic ions, the total yield, S_T , of sputtered particles may be expressed as

$$S_T = S^0 + S^+ + S^- + \sum S_i^* + \sum S_i^M$$

where the partial yields are S^0 = ground state neutral atoms; S^+ = ground state positive ions; S^- = ground state negative ions; S_i^* = neutral or ionized excited atomic species in the i th state; S_i^M = neutral, ionized or excited molecular species. For the purposes of this discussion, S_T is taken to be unity in all cases.

We will now examine the magnitudes of the partial yields to be expected under conditions relevant to fusion machines. Depending on the material and chemical composition of the surface, the principal sputtered species can be either neutral atoms or singly ionized positive ions. In the case of most atomically clean metal surfaces, the predominant yield is S^0 (>0.95). Special surfaces can be prepared however, (e.g. monolayer coverages of alkali metals on metal substrates) for which S^+ is the predominant yield (>0.95) and alkali metal rich surfaces may become of interest for fusion applications if appropriate alloy systems can be developed. Because Ti is a structural or getter material in many Tokamaks, it is of interest that monolayer coverages of oxygen on titanium convert that surface from one with $S^0 \approx 0.95$ to a surface which is predominantly a secondary ion emitter ($S^+ = 0.90$). For these reasons, one needs to pay particular attention to charge transfer processes at surfaces which control the charge state of the sputtered species.

Negatively charged species have been observed primarily as a result of sputtering of oxides. Because oxidic ceramic materials do not constitute important structural components in Tokamaks, the contribution of S^- to S_T is small.

The partial yields of excited atoms or ions, are much lower ($S_i^* \approx 10^{-1}$ - 10^{-2}) than those of neutrals, S^0 , for species in excited states with energies 2 eV or more above ground. Recent laser fluorescence data however

show that the fractions of atoms sputtered in lower lying metastable states can be substantial. Furthermore, atoms sputtered in high energy states have large kinetic energies and are therefore relatively more effective in penetrating the plasma edge. Sputtering in excited states will therefore be considered in somewhat more detail below.

The yields of S_1^M is generally very low except in cases where chemical sputtering of a predominant process (e.g. graphite bombarded by D^0 or D^+ at $\sim 600^\circ C$). The special case of chemical sputtering falls outside the scope of this review.

The Ion/Neutral Ratios

As shown in Fig. 1, the ionization coefficient $R^+ = S^+/S_T$ varies by a factor of $\sim 10^6$ depending on the element and on whether surfaces are clean or covered by oxygen. There are substantial discrepancies in published values presumably due to unknown degrees of surface contamination even under high current density bombardment conditions. In general, there is substantial variation from element to element and from the clean to the oxidized state of a given element.

A number of theories which account for some aspects of secondary ion emission have been advanced but none are completely satisfactory. Because of the remarkable range of values for R^+ , one needs to examine these theories in detail. Several mechanisms of charge transfer such as resonance ionization, deexcitation and neutralization; Auger neutralization or deexcitation; or autoionization processes may be operative singly or in combination.

Secondary ion *yields* seem to be rather insensitive to the actual ionization mechanisms while the kinetic energy distributions contain potentially more information concerning these processes. One therefore wishes to focus attention on $R^+(E)$, the ionization coefficient and its dependence on energy. The ionization probability $R^+(E)$ is defined by the relation

$$N^+(E) = R^+(E)N(E) . \quad (1)$$

For sputtering by random collision cascades,

$$N(E) \sim \frac{E}{(E-E_b)^3} \frac{\cos \theta_e}{\cos \theta_i} \quad (2)$$

where E_b is the surface binding energy, approximately equal to the heat of sublimation, and θ_e and θ_i are the angles of emission and incidence, respectively. This energy spectrum exhibits a peak at $E_b/2$ and has a long high energy tail which falls as E^{-2} . One example of a theoretical approach (Schroeder *et al.*) involves calculating the ionization probability in the adiabatic approximation, assuming that the sputtered atom is initially in a neutral, unexcited state. The resulting expression is:

$$R^+(E) = \left[\frac{E_b}{I-\phi} \right]^2 \left[\frac{h\nu}{a(I-\phi)} \right]^{2m} \quad (3)$$

where I is the ionization potential; ϕ the work function; v the velocity; $m \sim 1.25$ is a fitting parameter, and $a \sim 1.5$ Å. A number of alternative formulations for calculating R^+ have been advanced since the 1973 work of Schroeer. Although able to predict trends, these equations cannot be used to rationalize the experimentally measured values. It must also be borne in mind that small changes in surface composition can drastically alter the distribution among sputtered products. Such changes occur readily because intended or unintended surface modification occurs either as a result of surface contamination or of the bombardment process itself. Careful control of surface conditions must therefore be combined with partial yield measurements to give ultimately a consistent data base against which to test the theoretical apparatus. Only in this way will we enhance our knowledge of the various charge transfer processes which control the charge states and states of excitation of the sputtered species. Although we know in a general way that these processes are strongly dependent on surface composition a detailed understanding is lacking concerning the basis for this extreme sensitivity to surface chemistry.

It is here that Doppler shift laser fluorescence spectroscopy (LFS) can be expected to make a fundamental and potentially far reaching contribution. Laser-induced fluorescence can be used, in principle, to access ground and excited states of neutral and ionized atoms and molecules. Using this technique, it becomes practical for the first time, for example to measure velocity and angular distributions of sputtered neutral atoms and ions under the same experimental conditions while carefully monitoring the chemical state of the surface.

LFS has already been used to measure fluxes and energy distributions of impurity atoms (Fe, Ti, Al, Zr) in the laboratory and as an *in-situ* diagnostic on Tokamaks (APEX, ISX, Doublet-III, ASDEX). Work using this technique is also being done in Japan. LFS provides a new and sensitive method for determining the charge, quantum state, energy distribution, as well as the spatial and temporal evolution of impurities during a single Tokamak pulse. A wealth of new and hitherto inaccessible data on these parameters will become available on a real time basis in operating fusion devices.

Excited Atoms

The yields of excited metal atoms (energy levels ≥ 2 eV), are lower by 1-5 orders of magnitude compared to those for ground state neutrals. The relative yields of excited atoms display an approximately exponential dependence on the excitation energy. The most important characteristic of highly excited sputtered atoms for impurity introduction in Tokamaks however are their very high kinetic energies which are typically 2-3 orders of magnitude greater than target surface binding energies. This fact places excited atoms in a class different from either neutrals or ions since the velocities of the former are perhaps 10 times higher than those of the latter two species. Electron, ion and photo-ionization processes are therefore much less efficient in shielding the plasma from deep penetration by these very energetic neutral impurity atoms. Although produced in relatively low yields, excited atoms can be expected very effectively to be transported to the inner plasma regions.

Excited atom yields show a marked correlation with channeling and with the angle of incidence. Yields fall when the ion beam is incident on an open

crystallographic direction. Yields increase with surface oxygen coverage and there may be an electronegativity correlation similar to that demonstrated for secondary ion sputtering.

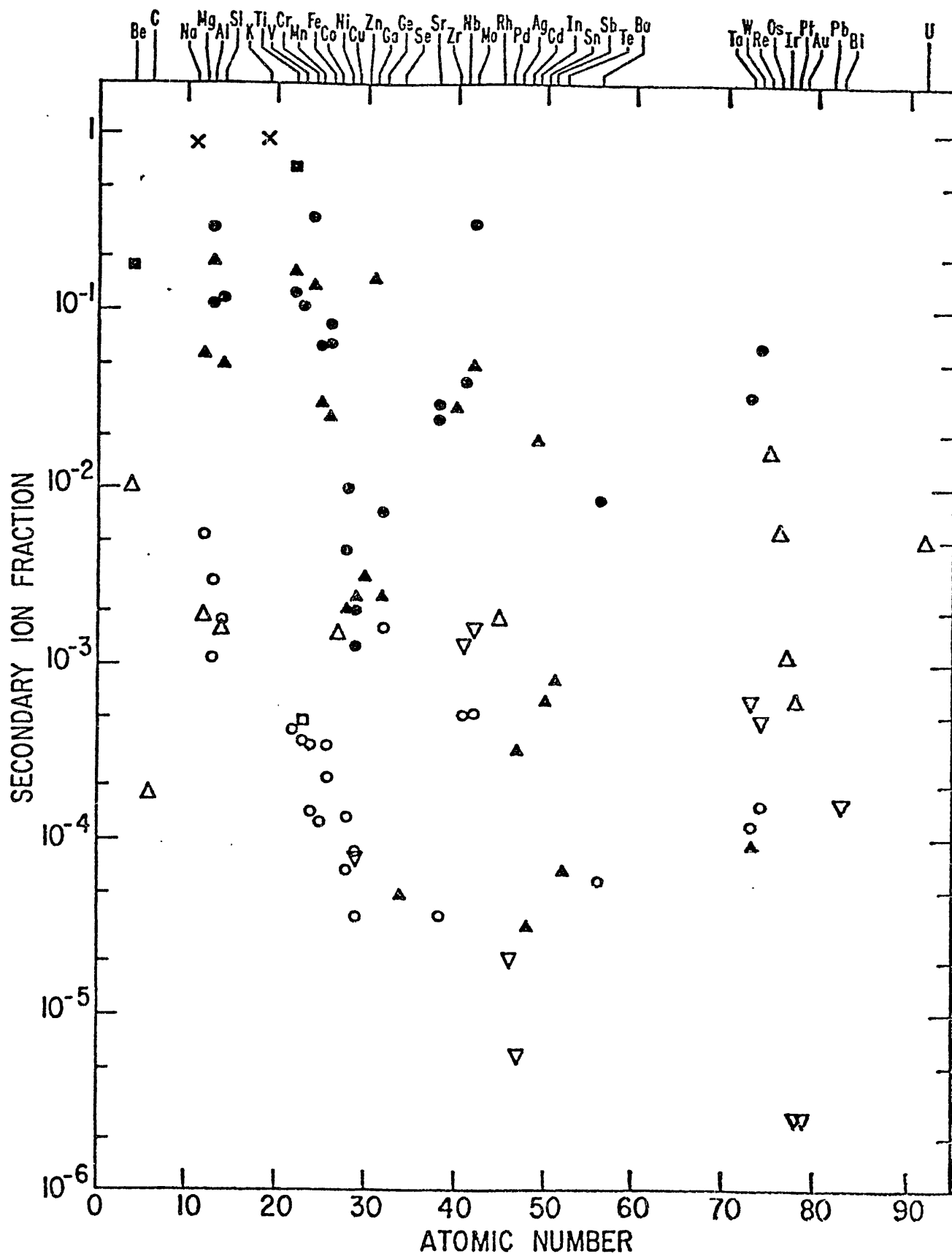
The paucity of information both as concerns yields and energy distributions of sputtered excited atoms reflects the experimental difficulties associated with making these measurements. Again, LFS offers the most hopeful approach to acquiring a good data base in this field.

The mechanism for the production of sputtered atoms in excited electronic states must be one resulting in high kinetic energies and therefore thermal events, either inside or outside the solid appear to be ruled out. Furthermore, excitation within the solid is unlikely because atoms in excited states have radii that are 2-10 times as large as ground state atoms. A likely mechanism involves random inelastic energy transfer either in the same collision leading to sputtering of surface atoms or excitation in a binary encounter just beyond the surface of atoms which were co-sputtered with electron exchange between atoms as they pass each other. A better insight into the excitation mechanisms will clearly be an important side product of these studies.

Conclusions

Conventional wisdom has it that total sputtering yields correlate with high Z-impurity levels found in fusion plasmas. The charge, quantum states and energy distributions of sputtered atoms have been virtually ignored in these considerations. Impurity transport from the wall or limiter to the plasma is however strongly influenced by these factors which may play a crucial role in determining impurity levels in the deeper plasma regions. Preliminary calculations have shown that positively charged impurities would most likely be redeposited on their surfaces of origin.

The conditions leading to charged or excited state atom emission and the energy distributions of such species are reviewed. Techniques for measuring these quantities are discussed and the need for a wider data base in this field is pointed out.



Plot of the secondary ion fraction (R^+) for forty two elements. Open symbols are for nominally clean surfaces and filled symbols are for oxygen-covered surfaces.

CHEMICAL REACTION AND CHEMICAL SPUTTERING

R. YAMADA

Japan Atomic Energy Research Institute

1. Introduction

Low-Z materials have been expected to be used for the first wall of plasma confinement devices because of a large tolerance limit of contamination for the plasma due to a small energy-loss by the line-radiation. Low-Z materials that contain carbon, oxygen, boron and silicon atoms are known to form gaseous molecules, which have lower binding energies than the original surface atoms, by chemical reactions between incident hydrogen atoms or ions and surface atoms. It is essential that such chemical reactions are included into the evaluation of the wall erosion in addition to physical sputtering.

The chemical reaction and chemical sputtering have been reviewed by some authors [1-3]. This report will compile available data of chemical reaction and chemical sputtering of carbon and carbide as a function of target temperature, ion energy, ion dose and dose rate.

2. Important parameters for the chemical sputtering

The chemical sputtering occurs at the surface of target as a result of chemical reaction between the surface atoms and the energetic hydrogen ions diffused from the implanted layer to the surface by ion enhanced and thermal diffusion. From the mechanism of chemical sputtering described above, it will be dependent on target temperature, surface concentration of hydrogen and chemical reactivity of surface.

The surface concentration of hydrogen is dependent on target temperature, dose rate of incident protons and incident energy related to energetic-particle induced diffusion. The surface reactivity is dependent on the chemical nature, which will be changed by bombardment with energetic ions. After all, the chemical sputtering yields must be measured as a function of the following parameters.

- (1) Target: C, TiC, SiC, B₄C, BN, Si₃N₄, Al₂O₃, etc.
- (2) Incident ion: H, D, T, O.
- (3) Target temperature: room temperature to 2000 C.
- (4) Chemical nature: fabrication process, surface structure (crystallographic orientation, topography, contamination).
- (5) Incident energy: thermal energy to 100 keV.
- (6) Incident dose: up to $10^{22}/\text{cm}^2$
- (7) Incident dose rate: up to $10^{18}/\text{cm}^2 \text{ sec.}$
- (8) Synergistic effect: co-operative phenomena between electron, energetic ions and thermal hydrogen.

3. Available data of carbon materials

3.1 Target temperature and surface structure dependence

Among the low-Z materials forming volatile compounds during hydrogen bombardment, the erosion yields of carbon materials have fairly well measured by several laboratories [4-9]. In Fig.1 and 2 are shown temperature dependence of chemical sputtering yields and total erosion yields (physical plus chemical sputtering), respectively due to bombardments with protons, which have been measured up to 1978. The data of the maximum yield and the target temperature at which the maximum yield occurs vary widely among the various authors. The reasons of the scatter have been ascribed to that the yields depend on not the

surface orientation but the fabrication process [4] or depend on the dose rate of impinging protons [8].

The temperature and surface structure dependence of the chemical sputtering have been measured by Yamada et al.[9] using different carbon materials, i.e., two kinds of pyrolytic graphites, isotropic graphite and glassy carbon. In Fig.3 are shown no major differences in the yields for different fabrication processes and structural orientation. The result should be ascribed to the surface damage produced by ion bombardment making the various virgin structures amorphous and any difference between the various crystallographic surfaces vanish.

The thermal atomic hydrogen also reacts with carbon and the erosion rates depend on temperature, as shown in Fig.4. The rates are scattered over three orders of magnitude, and they are a factor about 10^2 to 10^4 smaller than the chemical sputtering yields. This difference is due to the difference between trapping probability for energetic ions and the sticking probability for thermal atomic hydrogen, and also due to different reactivities between non-irradiated and irradiated carbon surface with energetic ions.

The erosion yields of thermal atoms increase by more than an order of magnitude if radiation damage is produced by irradiation with ions in the MeV range [10], as shown in Fig.5, and various carbon materials exposed to the same fluences of 1-2 MeV H_e^+ ions display the same reactivity with atomic hydrogen within about a factor of 3 for them [11].

3.2 Incident energy dependence

The energy dependence of the chemical sputtering yields has been investigated by Roth et al.[4] using 0.7-3 keV H^+ ions, Braganza et al.[7] using 5-30 keV D^+ ions and Yamada et al.[9] using 0.1-6 keV H^+ ions. It has been shown in Fig.6 by Roth et al. that the yield increases with decreasing incident energy and that the yield correlates with the energy deposited in the surface layer, which becomes maximum at incident energy of 150 eV estimated by nuclear collision cross section formulated by LSS theory [12]. It has been shown in Fig.7 by Yamada et al. that the yield has the maximum at energy around 1 keV. This discrepancy may be ascribed by non-negligible number and energy of reflected protons at low incident energy[13].

3.3 Ion dose dependence

The chemical sputtering increases with increasing dose until the saturation of the surface concentration and the steady state of the chemical reactivity are obtained. Fig.8 shows the dose dependence of chemical sputtering yield at bombardments with protons whose energy varies from 100 eV to 6 keV. Fig.9 shows the dose dependence of the yield at subsequent bombardment of pre-bombarded graphite with protons, which reveals that methane production behaves in a different manner, depending on the history of target. A stationary yield is obtained after bombardment with protons more than some times 10^{18} H^+/cm^2 in the energy range used.

3.4 Dose rate dependence

It has been pointed out by Smith and Meyer [8] that chemical sputtering yield decreases and optimum temperature increases with increasing dose rate of protons as shown in Fig.10. The results obtained by Yamada et al.[9] indicates that the above two values are hardly dependent on ion dose at least less than 10^{16} H^+/cm^2 sec. If a dose rate exceeds a certain value, presumably a dose rate more than 10^{17} H^+/cm^2 sec, the total methane produced by impinging protons might not be proportional to the dose rate because of limitation of surface density of carbon atom. As there are no precise measurements of the dose rate

dependence, it is necessary to investigate it in very wide range of ion dose rate.

3.5 Synergistic effect

It is important to investigate the synergistic effect of energetic ions, electrons and atomic hydrogen with respect to chemical reaction with carbon in order to estimate the erosion rate under more realistic conditions. It has been shown by Asby and Rye [14] that methane production due to atomic hydrogen is enhanced by simultaneous bombardment with electrons. The enhanced reaction rate becomes greater than 20 times the rate due to atomic hydrogen only, as shown in Fig.11. There is an electron energy dependence of the synergistic effect, i.e., the reaction rate increases drastically above 100 eV and becomes saturated above 400 eV. Since these energies of electrons are quite lower than the energy necessary for displacement of atoms, the mechanisms of this synergistic effect may be an additional reaction pathway for methane production opened by electron bombardment.

The measurement has been made of the methane production of graphite due to proton bombardment under thermal atomic hydrogen [15], as shown in Fig.12. It is important that the erosive actions of energetic hydrogen ions and atomic hydrogen are additive, even after the equilibrium in the surface hydrogen concentration is established during proton bombardment.

It is necessary to investigate various kinds of synergistic effects in order to understand the mechanisms which are useful for the estimation of synergistic erosive actions at the first wall of plasma confinement devices.

4. Available data of carbides

4.1 SiC and B₄C

A few data of chemical sputtering between carbides and protons are available. Temperature dependence for bulk SiC and B₄C has been reported by Braganza et al. using 20 keV D⁺ ions [16]. The production rates of CD₄ at B₄C and SiC are much smaller than the rates at carbon and also the optimum temperatures are smaller than that of carbon, as shown in Fig.13. It has also been shown by them that the production rate at SiC decays during deuteron bombardment, which is attributed to the depletion of carbon in the surface layer of SiC, whereas such a decay has not been observed at B₄C. It has been reported by Yamashina et al.[17,18] that the depletion depends on the vacuum conditions, i.e., silicon is sputtered more easily than carbon at clean SiC surface by proton bombardment, whereas carbon is more easily sputtered than silicon at oxidized SiC surface. Total erosion yields of bulk and coated SiC measured by Roth et al.[4] and Sone et al.[19], respectively show no temperature dependence, as shown in Fig.14. It has been reported by Veprek et al.[20] that B₄C and SiC show no measurable reactivity with atomic hydrogen at elevated temperature.

4.2 TiC

Energy dependence of total erosion yields of coated TiC has been measured by Bohdanský et al.[21] using 0.3–4 keV H⁺ ions at room temperature. It has been shown by Brossa et al.[22] that the yield at 600 C for 2 keV H⁺ ions is in good agreement with the value at room temperature. Energy, temperature and dose dependence has been recently measured by Yamada et al.[23], as shown in Figs.15–17. The results show that there is little temperature dependence of the yield and that the yield has maximum around 2 keV and that there is strong dose dependence at which pre-bombarded TiC, after being held in air or vacuum at a certain interval, is bombarded with protons. The result may be attributed to the reactivity of Ti with carbon impurity like CO.

5. Conclusion

The following items are not well understood and much investigation is necessary:

- (1) dose rate dependence of chemical sputtering,
- (2) absolute yields of components of alloy which form volatile compounds,
- (3) dose dependence of yields of alloy, especially with respect to preferential sputtering,
- (4) synergistic effect of the chemical reaction,
- (5) model and theory of chemical reaction and chemical sputtering.

References

- [1] G.M. McCracken and P.E. Stott, Nucl. Fusion 19 (1979) 889.
- [2] D.M. Gruen, S. Veprek and R.B. Wright, Plasma Chemistry I (Springer-Verlag, 1980) 47.
- [3] J. Roth, Sputtering by Ion Bombardement III (Springer-Verlag, to be published) Chapter 4.
- [4] J. Roth, J. Bohdansky, W. Poschenrieder and M.K. Sinha, J. Nucl. Mater. 63 (1976) 222.
- [5] N.P. Busharov, E.A. Gorbatov, V.M. Gusev, M.I. Guseva and Yu.V. Martynenko, *ibid.*, 63 (1976) 230.
- [6] K. Sone, H. Ohtsuka, T. Abe, R. Yamada, K. Obara, O. Tsukakoshi, T. Narusawa, T. Satake, M. Mizuno and S. Komiya, in Plasma-Wall Interactions (Pergamon, 1977) 323.
- [7] C.M. Braganza, S.K. Erents and G.M. McCracken, J. Nucl. Mater. 75 (1978) 220.
- [8] J.N. Smith, Jr. and C.H. Meyer, Jr. J. Nucl. Mater. 76&77 (1978) 193.
- [9] R. Yamada, K. Nakamura, K. Sone and M. Saidoh, J. Nucl. Mater. 95 (1980) 278.
- [10] S. Veprek, A.P. Webb, H.R. Oswald and H. Stuessi, J. Nucl. Mater. 68 (1977) 32.
- [11] A.P. Webb, R. Blewer, H. Stuessi and S. Veprek, J. Nucl. Mater. 93&94 (1980) 634.
- [12] J. Lindhard, V. Nielsen, M. Scharff, Mat. Fys. Medd. Dan. Vid. Selsk. 36 No.10 (1980).
- [13] R. Yamada and K. Sone, to be submitted to J. Nucl. Mater.
- [14] C.I.H. Asby and R.R. Rye, J. Nucl. Mater. 92 (1980) 141.
- [15] R. Yamada, K. Nakamura and M. Saidoh, J. Nucl. Mater. 98 (1981) 167 and unpublished data.
- [16] C.M. Braganza, G.M. McCracken and S.K. Erents, in Plasma-Wall Interactions (Proc. Inst. Symp. Julich, (1976), Pergamon, 1977) 257.
- [17] T. Yamashina, M. Mohri, K. Watanabe, H. Doi and K. Hayakawa, J. Nucl. Mater. 76&77 (1978) 202.
- [18] M. Mohri, K. Watanabe and T. Yamashina, J. Nucl. Mater. 75 (1978) 7.
- [19] K. Sone, M. Saidoh, K. Nakamura, R. Yamada, Y. Murakami, T. Shikama, M. Fukutomi, M. Kitajima and M. Okada, J. Nucl. Mater. 98 (1981) 270.
- [20] S. Veprek, M.R. Haque and H.R. Oswald, J. Nucl. Mater. 63 (1976) 405.
- [21] J. Bohdansky, H.L. Bay and W. Ottenberger, J. Nucl. Mater. 76&77 (1978) 163.
- [22] F. Brossa, J. Bohdansky, J. Roth and A.P. Martinelli, J. Nucl. Mater. 93&94 (1980) 474.
- [23] R. Yamada, K. Nakamura, K. Sone and M. Saidoh, To be presented to Fifth Inter. Conf. on Plasma-Surface Interaction, Gatlinburg, (1982).

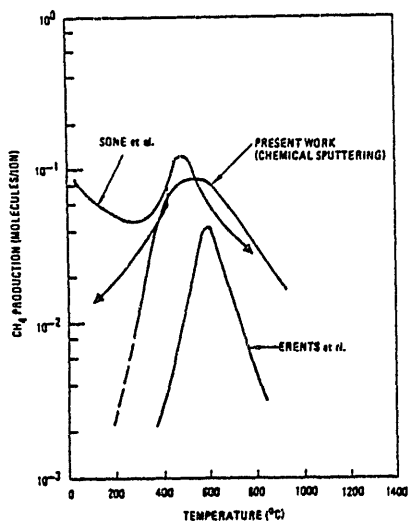


Fig. 1. Temperature dependence of methane production for hydrogen incident on carbon. [8]

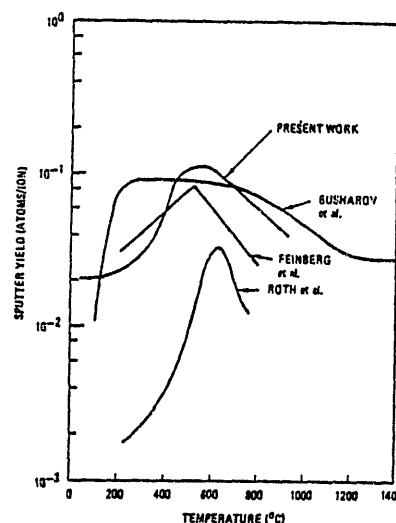


Fig. 2. Temperature dependence of carbon erosion by hydrogen. [8]

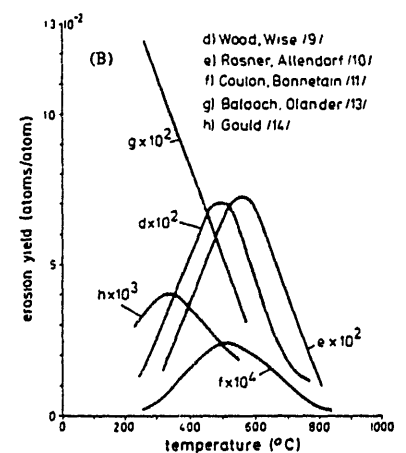


Fig. 4. Temperature dependence of the erosion yield of carbon with hydrogen atoms at thermal energies. [4]

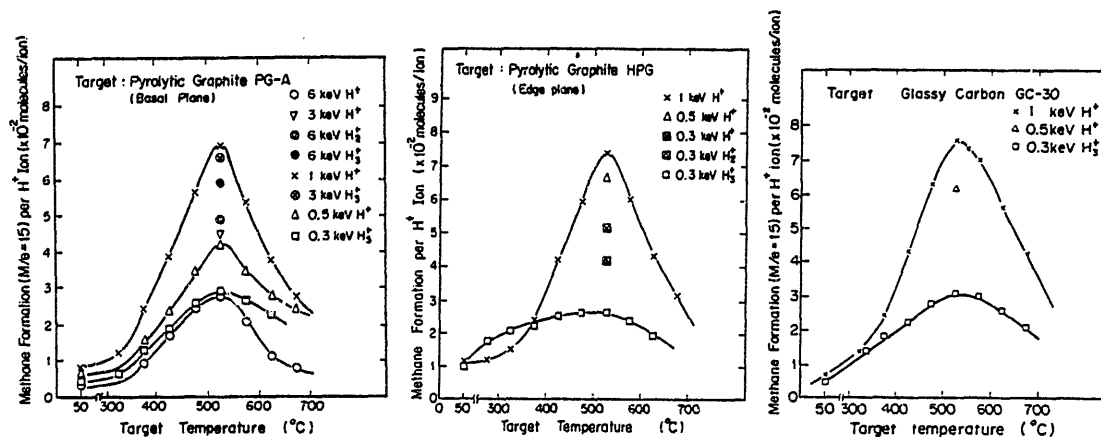


Fig.3. Temperature dependence of methane production rates of carbon materials, i.e., the basal plane of PG-A, the edge plane of HPG and glassy carbon, [9]

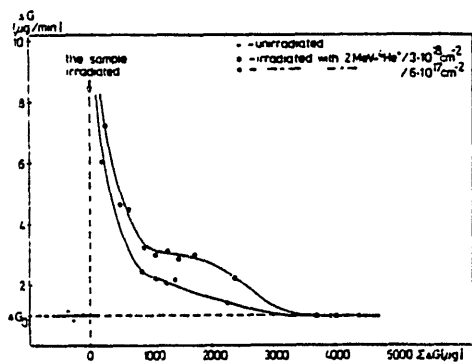


Fig.5. Effect of radiation damage on the reactivity of graphite. [10]

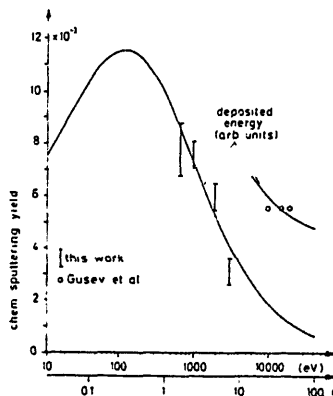


Fig.6. Energy dependence of the erosion due to chemical sputtering for the bombardment of graphite with hydrogen ions at 650 C. For comparison the calculated energy deposited in the surface layer has been introduced. [4]

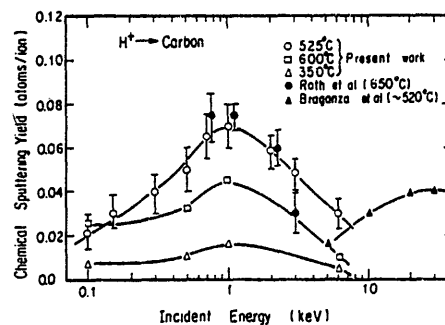


Fig.7. Energy dependence of the chemical sputtering yields of the basal plane of graphite. [9]

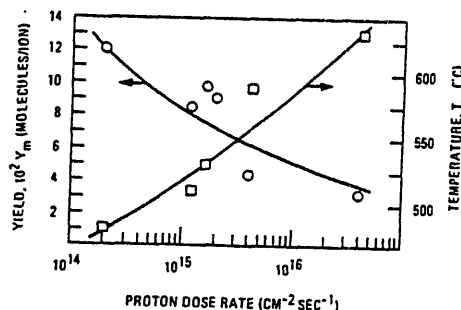


Fig.10. The methane yield Y at the peak temperature, T_m vs. dose rate. [8]

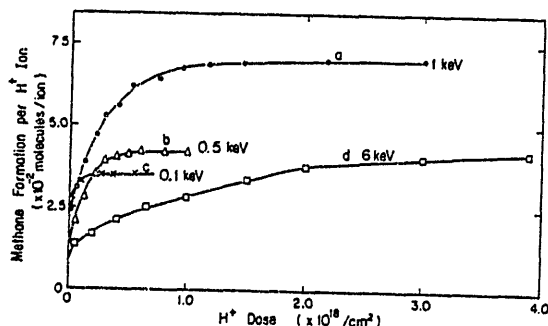


Fig.8. Dose dependence of methane formation of full-annealed samples. Targets of a, b and c were the basal planes of graphite and target of d was the edge plane [9]

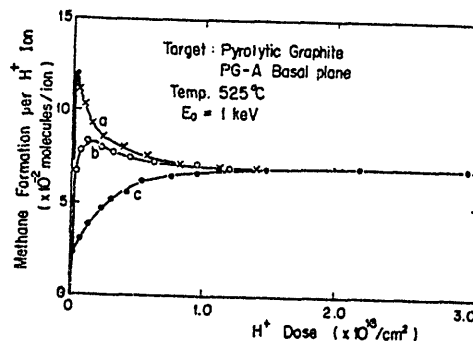


Fig.9. Dose dependence of methane formation of pre-bombarded samples. The individual treatment of targets before the bombardment with 1 keV H^+ at 525 C were as follows. (a) Prebombardment with 1 keV at room temperature. (b) The target of (a) once heated up to 700 C and cooled down to 525 C. (c) prebombardment at room temperature was not done. [9]

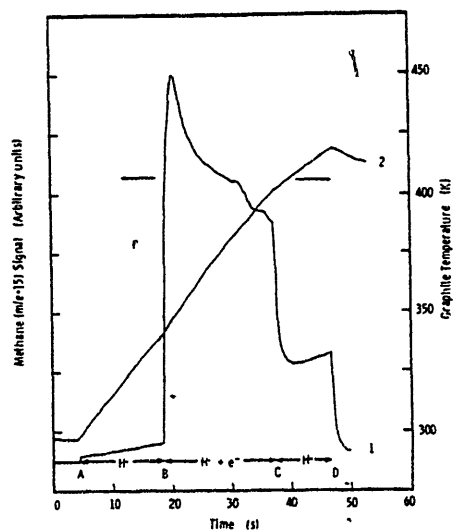


Fig. 11. Effect of electron bombardment on methane production and temperature. At B, electron bombardment is initiated. [14]

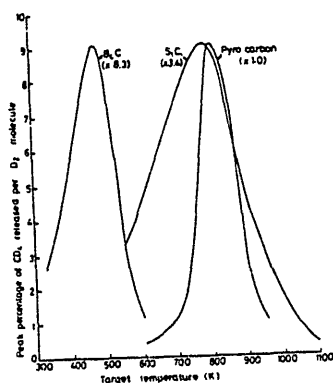


Fig. 13. Temperature dependence of deuterio-methane production due to 20 keV D^+ bombardments of B_4C , SiC and C targets. [16]

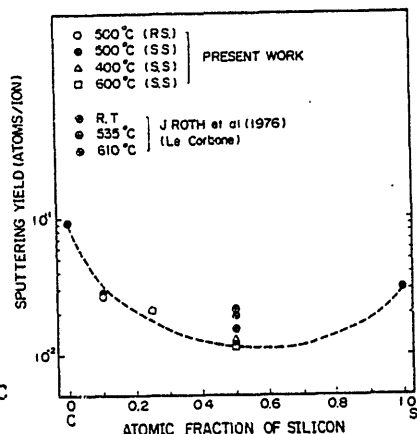


Fig. 14. Sputtering yield of SiC with hydrogen ions as a function of target temperature and atomic fraction of silicon. [19]

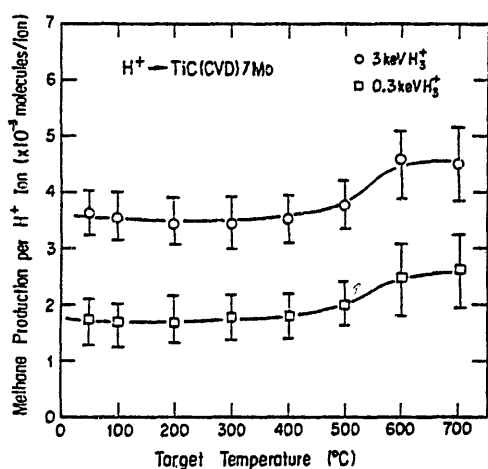


Fig. 16. Temperature dependence of methane production rate of TiC coated on Mo by chemical vapor deposition. [23]

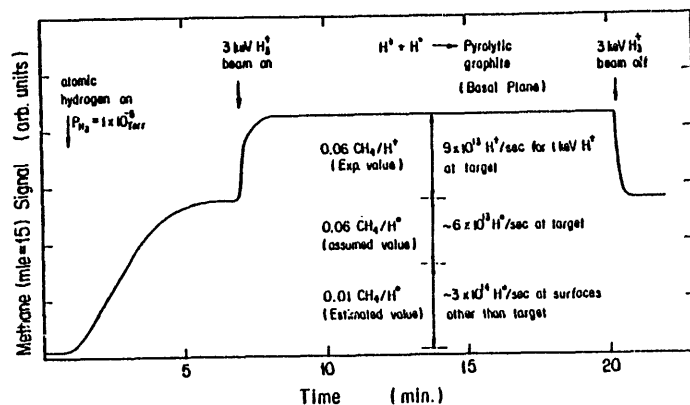


Fig. 12. Methane production rate of graphite due to bombardment with energetic hydrogen ions under atomic hydrogen at thermal energy. [15]

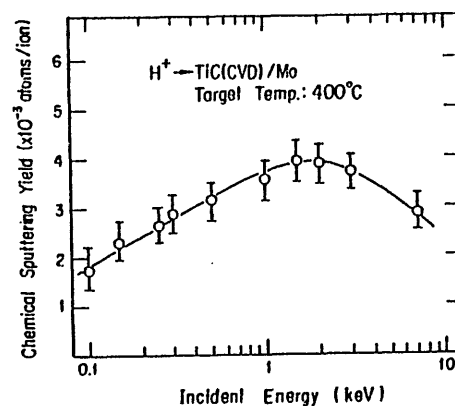


Fig. 15. Energy dependence of methane production rate of TiC coated on Mo by chemical vapor deposition. [23]

Temperature dependence of methane

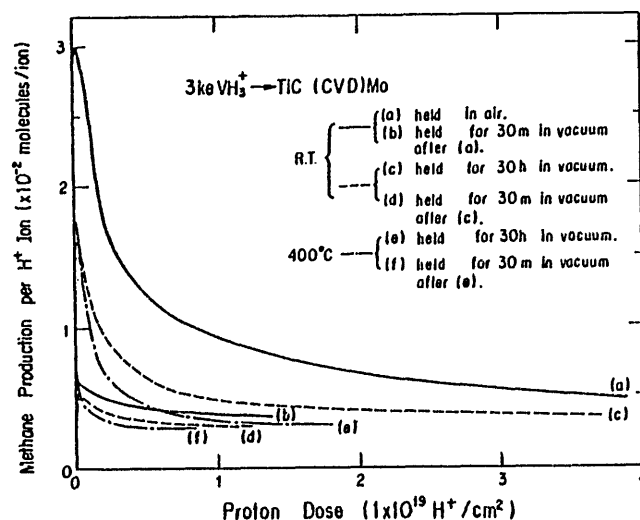


Fig. 17. Dose dependence of methane production rate of pre-bombarded TiC. The targets prior to subsequent bombardment were held in air or vacuum at intervals described in the figure. [23]

HYDROGEN TRAPPING, DETRAPPING AND RE-EMISSION
FROM FUSION FIRST WALLS*

B. L. DOYLE
Sandia National Laboratories,
Albuquerque, New Mexico, USA

ABSTRACT

A review is made of the current status of both the data base and understanding of processes which occur when hydrogen is injected into materials. This review differs from previous ones because equations pertinent to these processes are derived in order to facilitate the assessment of the importance of the various plasma and material parameters which come into play. The response of H injected energetically into materials falls into four categories which depend upon 1) a simple analytic transport parameter W which characterizes either diffusion limited ($W > 1$) or recombination limited ($W < 1$) transport in the material and 2) the temperature, T , which determines the importance of damage trapping.

*This work performed at Sandia National Laboratories supported by the U.S. Department of Energy under contract number DE-AC04-76DP00789.

INTRODUCTION

Significant progress has been made in the past ten years in both the understanding and, in some cases, the control of the plasma surface interaction (PSI) which occurs in magnetically confined plasma devices such as tokamaks. Indeed, this increased knowledge and the subsequent appreciation of PSI related problems has a direct bearing on the design of both present and future fusion reactors.

The regions in the interior of a tokamak where materials-related concerns are important are: 1) the vacuum vessel or liner and 2) components which receive high power deposition (i.e., concentrated plasma flux) such as limiters. In the first case, conventional high vacuum materials are used such as Fe or Ni based alloys. For these components the principle PSI concerns are H trapping, build-up, embrittlement, recycle and permeation together with impurity generation caused by plasma-induced erosion. For the second case, the PSI problems listed above are still important, but the primary concerns are impurity generation and survivability. These components are typically made or coated with low atomic number refractory materials such as C or TiC.

In this review the plasma and material parameters important to the H-related PSI concerns are delineated by introducing an integrated picture of hydrogen transport from a fusion materials viewpoint. The problem is formulated in terms of a normalized transport parameter, W , which results in a natural classification of the behavior of H in materials based on two parameters: W and temperature. An example of the use of this new concept to calculate

H permeation, inventory and recycle under INTOR conditions is given in Appendix B.

This review of H trapping, detrapping and re-emission in fusion first walls covers only a small part of the total PSI picture as can be seen from the diagram of H recycling in Fig. 1. This flow diagram illustrates a comprehensive plasma transport code by Howe⁽¹⁾ which models kinetic reflection, thermal diffusion and beam-induced detrapping in the wall.

In Howe's model, hot H ions [1] diffusing across magnetic field lines eventually strike a limiter [2] and are all neutralized and reinjected into the plasma with ~5 eV energy. Upon reentering the plasma some of the H atoms (~60%) are ionized [3] while others (~40%) undergo Franck-Condon (FC) collisions or charge exchange (CX) [4] with hot H ions in the plasma, giving rise to fluxes of both hot (CX ~100's eV) and cool (FC ~10 eV) H atoms [5] which strike the first wall. It should be noted at this point that this flux will be highly assymmetric (both poloidally and toroidally) with the maximum being near the limiter. Some of the incident H atoms are reflected [6] from the surface back into the plasma while the remainder penetrate [7] into the material of the first wall. Of those H atoms which enter the first wall, some may become trapped at their end of range (EOR) [8] in damage either resident in the material or produced by the particle irradiation. This trapping process may also result in the detrapping [9] of H isotopes already present in the wall. This detrapped H, along with any H which was not trapped, diffuses and [10] eventually permeates either to the back surface [11], or the front surface [12]

or becomes trapped in the bulk [13]. Upon reaching either surface the H can recombine with another H atom and be released as an H₂ molecule to re-enter the plasma [14] or the environment exterior to the first wall [15].

The main scope of this paper was to deal with H trapping, detrapping and release processes [8,9 and 14]; however, in order to get a more complete and accurate picture of H-recycling, wall inventory and permeation flux, it was found necessary to consider all of the processes which can occur once H has penetrated the first wall surface [7-15].

Figure 1 can be used qualitatively to provide insight on how material variables related to H affect important tokamak parameters. Consider H recycling for the case where the wall traps or otherwise retards only 0.1% of the CX or FC neutral flux. In typical tokamaks the confinement time is ~10 ms whereas the pulses endure ~ 1 sec. This means, crudely, that each H atom in the plasma strikes the wall ~100 times during each discharge. The probability that a H gets trapped in the wall during the discharge is $\sim 1 - .999^{100} \approx 10\%$, whereas for a 0.2% trapping coefficient this figure becomes ~18%. This example illustrates how sensitive the "wall confinement," is on H trapping or holdup. Howe⁽¹⁾ has shown that neutral beam induced density clamping⁽²⁾ is the result of a small decrease in the wall recycle coefficient caused by the increased edge plasma energy during neutral beam injection.

Another effect illustrated in Fig. 1 is isotope exchange. If EOR trapping [8] is appreciable, and the tokamak has been operated for a long period of time with just one H isotope, say protium, then

the near surface of the wall saturates with H. Upon changing the working gas to deuterium (D), during the first stages of the D discharge the detrapping [9] which occurs in the wall will be for H, which, as can be seen from the figure, can diffuse [10] to the surface and enter [14] the plasma. Thus the wall initially recycles H, not D, thereby upsetting the isotopic purity of the plasma. This effect has been observed in numerous tokamak devices. (3-6)

The three primary H-material concerns in the PSI are also graphically displayed in Fig. 1, namely: 1) plasma wall recycle effects in Region I, 2) H buildup in the wall (Region II) potentially leading to embrittlement and/or a high T inventory and 3) the possibility that H isotopes (i.e. T) can permeate the wall and enter the environment in Region III. Because of its importance, the PSI has been the subject of several reviews (1,7-22) to which the reader is referred for further details.

EQUATIONS

A set of coupled differential equations can be used to represent the concentration of hydrogen isotopes implanted into a solid. These equations are given in Fig. 2 and the definitions of the various parameters used in this report are given in Appendix A. These differential equations are a hybridization of several theories (1,23-28) plus a modification of the isotope exchange term in Eq. (5) (the second term) from that found in Howe⁽¹⁾. This change is discussed below. Equation 1 is Fick's second law for the diffusing H isotopes with a volume source rate due to implantation and a detrapping term; Eq. 2 defines the time evolution of trapped isotopes; (24,27)

Eq. 3⁽¹⁾ the evolution of empty, but activated, traps and Eq. 4 describes the generation and decomposition of these H traps.⁽²⁸⁾ Eq. 5 gives the detrapping probability (both thermal and ion induced)⁽¹⁾ and Eq. 6 characterizes the diffusivity. The boundary condition in Eq. 7 is valid⁽²⁵⁾ for surface recombination kinetics, and Eq. 8 follows from Eq. 7 for large k_r . The function for k_r given in Eq. 10 comes from Baskes.⁽²⁹⁾ Unfortunately, no analytical solution to these equations has been found and therefore relatively complicated computer codes must be used in the calculations.^(25,27,30)

Special cases of the equations in Fig. 2 are useful to gain insight into 1) the complex interrelationships which exist between the plasma parameters (i.e. flux and energy) and the material's parameters, i.e. D , k_r , and 2) how both sets of these variables affect important issues such as recycle time, T wall inventory and T permeation flux through the wall. Figure 3 gives a schematic representation of the potential, $U(x)$ that a H atom "sees" both in the interior and exterior of A) an endothermic H absorber ($E_s + E_D > 0$) and B) an exothermic H material ($E_s + E_D < 0$) where 0 refers to the energy of a H_2 molecule at rest. The definitions of E_D , E_T and E_s are shown in this figure. The three-dimensional representation is used to show the energetic preference for releasing H_2 molecules rather than H atoms and hence the need to consider recombination. An example of a H atom's trajectory in this energy space is shown as the dashed line. The atom enters with ~ 10 eV energy but rapidly slows down due to atomic collisions and comes to rest on the "roller coaster" shaped potential

surface. From this point on, the H must exercise its motion according to this energy surface and its own Maxwell-Boltzmann (MB) distribution of energies. The MB behavior gives rise to the exponential terms given in Fig. 2. The H motion which is executed in the interior of the two solids is similar but the energetics of release are quite different. In the endothermic case, two H atoms form a molecule and enter the vacuum with excess energy; however, for the exothermic metal each H atom is forced to obtain another E_g worth of energy in order to escape. This makes surface recombination more difficult for the exothermic than for endothermic H materials.

If for the moment we neglect trapping and assume $D \delta c / \delta x \ll 2\sigma k_r c^2$, a steady state (i.e., $\delta c_i / \delta t = 0$), for Eqs. 1 and 7 is given in Eq. 11 in Fig 4(25,26,31) from which Eqs. 12-15 can be derived. When k_r gets very large the boundary condition is better defined by Eq. 8. If we assume that the H atoms are implanted in a delta function distribution at depth R_p , the projected range, (i.e. $G(x) = \alpha \delta(x - R_p)$), then Eq. 1 can be solved⁽³²⁾ yielding the parameters listed in Eqs. 16-20. For the other extreme when $k_r \rightarrow 0$, no H can be re-emitted from the surface and hence the appropriate boundary condition is Eq. 9. If we assume the H is implanted just at the surface, then the terms listed in Eqs. 21-26 result. Another important parameter is the time lag required before a stationary state is set up. This has been written in Eq. 27 in Fig. 4.⁽³³⁾ To include the effect of bulk trapping of H in damage such as dislocations, grain boundaries or strain fields one can use the McNabb & Foster equation^(34,35) (Eq. 28) which accounts for the

reduced diffusivity through the introduction of an effective diffusivity. In their present form it is easy to misinterpret Eqs. 11-28. For example as $k_r \rightarrow \infty$ Eq. 13 states that $\bar{c} = 0$, whereas Eq. 18 has $\bar{c} = \alpha \phi R_p / 2D$. In order to rectify this problem and to help determine the break between recombination and diffusion limited kinetics the dimensionless parameter W is defined in Eq. 29 of Fig. 5. By defining reduced (primed) average H concentrations, permeating fluxes and recycle times, which are reduced relative to their diffusion limited values, the simple equations listed in Fig. 5 result. These equations will approximately account for either recombination or diffusion limited kinetics. The W parameter is similar but not identical to the W' parameter defined by the Julich group.(25,31,36,37) The parameters W and W' share the same properties (Eq. 33) which govern whether diffusion or surface limited effects dominate the H transport. For example, it is easy to show from Wienhold, et al.(25) that when $W < (R_p/X_o)^2$ H release becomes difficult due to the small k_r .

Another assumption which allows a simple solution to Eqs. 1-4 is to let the trapping become so efficient that if any unoccupied traps are located at the end of the H implant trajectory the H will be trapped. If we further assume that the number of such traps saturates at a value of n_{sat} ($\#/cm^3$), which is dependent on the temperature and material, Eq. 34 in Fig. 6 results(38) where the v term contains the potential for isotope exchange addressed above. At this point, the following comment must be made. When isotope exchange was first discovered and treated

experimentally⁽³⁹⁻⁴¹⁾, it was noticed that as the second isotope was implanted, the loss rate of the isotope implanted initially decayed exponentially with fluence. This observation led to the "bath tub" model with the concept of a phenomenological release cross section, σ , which was used to parameterize the data. Unfortunately, the only thing σ has in common with a cross-section is its unit (cm^2). Our group has shown that the correct parameterization is the saturation concentration n_{sat} and that the local mixing model (LMM)⁽³⁸⁾ correctly describes both the saturation process and isotope exchange.⁽⁴²⁻⁴⁵⁾ Möller et al.⁽⁴⁶⁾ have also recently used a slightly modified LMM to describe saturation and exchange profiles of H and D implanted into metals at low temperature. The two models agree for incident particle deposition rates which are constant out to the range R_p (i.e., $G(x) = \alpha\phi/R_p$ for $x < R_p$, $= 0$ else) in which case $n_{\text{sat}} = 1/R_p\sigma$. The main difficulty with σ is that it refers to an interaction volume rather than area and is therefore not well defined. Although the replacement cross-section concept has been used successfully in PSI models^(14,47), in Howe's⁽¹⁾ model, he erroneously defines the second term in Eq. 5 as $\sigma\Gamma$ which resulted from a misinterpretation of σ . The correct term consistent with the LMM has been used in this work.

Figure 6 shows the evolution of first a D profile for 1.5 keV D \rightarrow C at room temperature (solid curve) and then the D profiles upon subsequent replacement by 1.5 keV H (dashed curves). The concentration source term $G(x)$ was calculated using the TRIM partical transport code^(48A). With the LMM it is assumed that diffusion

limited partial transport applies (i.e., $W \gg 1$) and further that D is very large so that $\bar{c}_{\max} \rightarrow 0$ and $\tau \rightarrow 0$. The steady state solution to Eq. 34 gives Eq. 35, although for a MB distribution incident velocities, there is always some portion deep in the tail of the profile which is unsaturated so that steady state is reached only asymptotically. Brice has recently extended the LMM to include trap generation and decay in a trap activation model (TAM)(48b) and has also addressed the generation of traps by neutrons(48c). Other trapping models exist in the literature(48d-f). An example problem using some of the equations derived in this section is given in Appendix B. The current status of data on D and K_T for the special case of H in stainless steel and Ti are summarized in Appendix C.

EXPERIMENTAL

Hydrogen trapping, detrapping, permeation, recombination, diffusion, and release can be studied microscopically by gas re-emission (GR), thermal desorption spectroscopy (TDS) nuclear reaction analysis (NRA) and secondary ion mass spectroscopy (SIMS). Electrochemical techniques are also useful in determining bulk properties such as diffusivity and permeability. Microscopic information as to the actual nature of a H trap can be determined a variety of ways, including Mössbauer shifts, NMR, IR, Raman spectroscopies and nuclear reaction channeling.

DATA

The H transport in various solids will differ because of the individual nature of material characteristics. Nevertheless, materials do tend to sort themselves into four H-retention categories according to the four simplifying assumptions made above in order to solve the general coupled differential Eqs. 1-4. These were: I) recombination (Eq. 11-15), II) diffusion controlled kinetics (Eqs. 16-20), III) total H retention (Eq. 21-26) (a special case of I) and IV. near surface H trapping (EOR trapping) (Eq. 34-37). An example of this categorizing is shown in Fig. 7 where the re-emission rate of H implanted into 304SS, Al, Ti and TiC measured by GR is plotted.^(49,50) These materials are representative of categories I, II, III and IV respectively.

For 304SS, $W \approx .01$ which is in the case I region. Using $D \approx 10^{-9} \text{ cm}^2/\text{s}$ and $2\sigma k_r = 10^{-25} \text{ cm}^4/\text{s}$ as given by Waelbroek, et al.⁽³¹⁾, and letting $R_p = 10^{-5} \text{ cm}$ in Eq. 15, $\tau = 10 \text{ sec}$. This result predicts that the recycle flux should reach half of its maximum for a fluence of 10^{16} D/cm^2 which is in good agreement with Fig. 7.

The class II materials, which are represented by Al in Fig. 7, have $W \geq 1$ and therefore, very low H solubilities and high recombination coefficients. Using the values of Baskes⁽²⁹⁾ for aluminum, $W = 10^5$ and $\tau = 3 \times 10^{-3} \text{ s}$. The H recycle rate data for Al does not increase nearly as rapidly as predicted because of the influence of traps⁽⁵⁰⁾.

For type III materials, Eqs. 24 and 25 indicate that the recycling flux is zero for all times. Indeed the Ti data in Fig.

7 behave this way, with only $\sim 10\%$ (due to reflection) re-emission throughout the course of the implant. The W parameter for Ti in this case is 10^{-10} ; therefore surface recombination severely limits the release. The recycle time τ for Ti is 10^7 s which corresponds to an implant fluence of 10^{22} D/cm², which is orders of magnitude greater than the fluences plotted in Fig. 7.

In the case of TiC the recycle flux is low for implant fluences $< 2 \times 10^{17}$ D/cm²; at higher fluences the recycle flux increases. This behavior is characteristic of a type IV material where initially all of the implanted D atoms are retained in traps; when these traps saturate (see Eq. 37), the recycle flux increases. Using the value⁽⁴³⁾ of $n_{\text{sat}} = 2.5 \times 10^{22}$ and $R_p = 10^{-5}$ cm, Eq. 36 indicates that $\tau \approx \tau_{\text{CO}} = 2.5$ s corresponding to 2.5×10^{17} D/cm² which agrees well with the TiC results plotted Fig. 7. The other types of materials (I, II, and III) may have some degree of type IV behavior as already mentioned for the case of Al (type II).

Of course, the category (I-IV) of a material depends critically on temperature. Using the Baskes calculation of k_r (Eq. 10) along with the diffusion and solubility parameters used by Wilson,⁽⁵¹⁾ W is plotted vs. $1/T$ in Fig. 8 for several materials. The regions in which the various categories apply are also indicated.

The following sections present brief summaries of the more important experimental results concerning each of these four classes of materials. Much of the data base was taken from three excellent reviews recently given by Wilson^(22,51,52).

I. RECOMBINATION LIMITED KINETICS

As can be seen from Fig. 8, a large class of important materials, including stainless steel (SS), Ni and Ni alloys fall into this region over a temperature range which is quite relevant in fusion reactors. A great deal of research on the H retention/release properties of these materials has been published^(22-29,53-103). Two of the more important structural materials in this category are 304 SS and INCONEL (a Ni based alloy). Both materials are assumed to have approximately the same D ^(104,105) and the same k_r , although k_r in INCONEL has yet to be measured. On the other hand, Tanabe, et al.⁽⁹⁴⁾ have measured large differences in D for austenitic steel and Fe-Ni alloys. The E_D for these materials are $\sim .5$ eV or more and H traps have been shown to result from implantation at concentration of ~ 10 at % with $E_T \sim .5$ eV.^(62,67,80,86,88,91) These traps play a small role in the release process at room temperature and the importance of these traps diminishes drastically for higher temperatures where, as can be seen in Fig. 8, recombination becomes more and more important. Unfortunately, there exists a ~ 4 orders of magnitude difference in the measured values of k_r for SS.⁽²²⁾ This wide variation in k_r has been attributed to different surface conditions (oxide layers, contamination, etc.).

Mo is another material which falls into class I for $T >$ room temperature, and has been studied extensively.⁽¹⁰⁶⁻¹¹⁵⁾ In Mo, EOR trapping of H saturates at ~ 5 at % near room temperature with $E_T \sim 1-1.5$ eV,^(107,112,115) but can be increased significantly by prior noble gas implantation.⁽¹¹⁰⁻¹¹²⁾

II. DIFFUSION LIMITED KINETICS

Materials in this class include Al and Cu(116-118) and are characterized by having very low H solubilities and hence very large recombination coefficients and subsequently large W. Because of the low solubility these materials tend to blister by the formation of bubbles when implanted with H. It is easily shown that $r \sim \gamma/(\alpha\phi W)$ where r is the equilibrium bubble diameter. For a material to precipitate H bubbles easily, r should be very small and therefore the conditions conducive to blistering are 1) low surface tension γ , 2) large W and 3) a large $\alpha\phi$ fluence. EOR trapping is observed for Al(119,120) at $\sim 4 \times 10^{18}$ at 374 K with $E_t \sim 1.3$ eV.

III. TOTAL H RETENTION

When $W \ll 1$ H, atoms are essentially prohibited, energetically, from being re-emitted as H_2 molecules. This condition exists for metals with exothermic heats of solution⁽¹²¹⁻¹³⁷⁾ (E_s) for H such as Ti, V, Zr. A phase diagram for the Ti-H system taken from a recent review of H in Ti by Wille and Davis,⁽¹³⁸⁾ is shown in Fig. 9. With the aid of Eq. 26, this diagram provides insight into the hydriding process. Eq. 26 states that the conditions required for forming a hydride are 1) low D and $C_{Hydride}$ and a large $\alpha\phi$. These conditions can be easily met for α -Ti where the $C_{Hydride}$ ($< 10\%$) is low, but becomes more difficult for the β phase where $C_{Hydride} \sim 50\%$. This perhaps explains why ion implantation induced hydriding of Ti has been observed for α -Ti⁽¹³¹⁾ but not in the

Ti-6Al-4V mixed α - β alloy⁽¹³⁰⁾ and also why hydriding is not observed above 200°C (129,130) (D becomes too large).

IV. EOR TRAPPING

As can be seen in Fig. 8 the existence of class IV materials depends not on W but on T; in fact, all materials go into class IV at sufficiently low T. The change over to class IV at low T results from the Boltzman factor in the thermal detrapping term in Eq. 5. When $T < [(E_D + E_T) \cdot 400]^\circ K$, where E_D and E_T have units of eV, the H becomes immobile. Numerous studies of H trapping, detrapping and isotope exchange have been carried out on materials in region IV.^(38-46,139-160) Many of these studies have been on metals at low temperature.^(40,41,46,158-160) In this region W is usually > 1 so that H bubble precipitation or blistering may be anticipated. This has been observed for some cases.^(41,158) Möller,⁽¹⁵⁸⁾ et al. have recently reported data on Ni, Pd, Mo and Ta which shows a significant deformation at the sample surface when it becomes saturated with implanted D. These materials release most of their retained H when warmed to $\sim -100^\circ C$, indicating that $E_D + E_T \sim .5$ eV. For SS $E_D + E_T \sim .74 - .88$ eV.⁽⁸⁰⁾

Another set of class IV materials can efficiently retain implanted H at room temperature and above. C is an example of such a material.^(40,45,139,150) C retains implanted H up to concentrations of ~ 40 at % and does not release H which had been implanted at room temperature until $T > 700^\circ C$ indicating that $E_D + E_T \sim 2.5$ eV. However, when H is implanted at high temperature very little retention is noted above ~ 400 C.⁽⁴⁴⁾ Ion-induced

detrapping has been used to explain this phenomenon. Other C-like class IV materials which have been investigated include several low atomic number refractory metals in use or under consideration for coating applications in regions of tokamaks which are subject to high power deposition (eg. limiters). These materials include TiC, TiB₂, VB₂, SiC, B, and B₄C and Si.⁽¹⁵¹⁻¹⁵⁵⁾ H retention data on fused silicas have also been reported^(156,157). The saturation concentrations have been observed to range from ~ .03 for SiO₂, .16 for TiB₂ and VB₂ .25 for TiC up to ~ .5 for most of the others.

There is unfortunately little or no data for k_T or D in most of these materials and therefore questions as to their suitability for first wall applications in DT tokamaks is still somewhat in doubt. If this class of materials retains H only in the implant region, only relatively low tritium wall inventories would result.

SUMMARY

The response of H injected energetically into materials falls into four categories (see Fig. 8) which depend on 1) a parameter W (Eq. 29) which characterizes either diffusion-limited ($W > 1$) or recombination-limited ($W < 1$) transport in the material and 2) the temperature, T, which determines how important damage trapping is (i.e., for $T < (E_D + E_T) \cdot 400$ K, trapping must be considered). A set of simple equations 30-32 and 34-37 have been derived which can be used to determine approximately the maximum T inventory and permeating flux in the first wall in addition to a characteristic recycle time and an example is worked out in Appendix B. W is

unfortunately either not well-defined or not calculable (i.e., the parameters have not been measured) for most materials relevant for fusion applications, and this situation needs to be rectified quickly to insure continued progress in controlled thermonuclear fusion research.

APPENDIX A

Definition of parameters used in the text in the order of their introduction:

c_i	concentration ($\#/cm^2 \cdot s$) of type i isotope of H
t	time (sec)
D	diffusion coefficient (cm^2/s)
x	distance from surface (cm)
G_i	volume source rate ($\#/cm^3 \cdot s$)
c_{ti}	concentration of trapped H ($\#/cm^3$)
c_e	concentration of empty traps (unitless)
λ	diffusion jump length (cm)
ν	probability for detrapping per second (sec^{-1})
A_n	concentration of sample atoms ($\#/cm^3$)
c_t	saturation concentration for traps (unitless)
b	# traps produced per incident ion
μ	trap decay probability (sec^{-1})
ν_o	jump frequency (sec^{-1})
E_D	diffusion activation energy (eV)
E_T	trap activation energy (eV)
k	Boltzman constant (1/11600 eV/k)
T	temperature (K)
D_o	diffusion prefactor (cm^2/s)
α	penetration probability (unitless)
ϕ	incident particle flux ($\#/cm^2 \cdot s$)
σ	surface roughness factor (unitless)
k_r	surface recombination coefficient (cm^4/s)
c_o	concentration of H at surface ($\#/cm^3$)
m	mass of isotope (amu)
α'	sticking factor (unitless)
c_l	gas constant ($2.635 \times 10^{25} k^{1/2} amu^{1/2} / atm \cdot cm \cdot cm^2$)
c_o^*	solubility prefactor ($\#/cm^3$)
E_s	activation energy for solubility (eV)
x_o	wall thickness (cm)
Φ_{rec}	recycled flux ($\#/cm^2 \cdot s$)
c_{max}	average H concentration in the wall ($\#/cm^3$)
Φ_{in}	permeating flux which passes through wall ($\#/cm^2 \cdot s$)
τ	recycle time - time for Φ_{rec} to reach $\sim \alpha\phi/2$ (s)
R_p	projected range (cm)
$\tau_{Hydride}$	time required for hydriding conditions to be reached (s)
τ_{lag}	time lag (s)
D_{eff}	McNabb-Foster effective diffusion coefficient (cm^2/s)
k	trapping rate coefficient
p	release rate coefficient
W	transport parameter (unitless)
C_{max}	reduced max T concentration (unitless)
Φ_{max}	reduced permeation flux (unitless)
τ_{max}	reduced recycle time (unitless)
n_{sat}	H saturation concentration ($\#/cm^3$)
τ_{co}	change over or saturation time (sec)
γ	surface tension (eV/cm ³)

APPENDIX B

Here a calculation of H recycle, T inventory and wall permeation is made for an INTOR like tokamak using the simple equations in Figure 5. A comparison is made with calculations made by Wienhold, et al., (85c) using the PERI code. The wall material is 304 SS and the pertinent parameters used by Wienhold were:

$$\begin{aligned} x_o &= .5 \text{ cm} \\ T &= 500^\circ C \\ D &\approx 1 \times 10^{-5} \text{ cm}^2/s \\ 2\sigma k_r &\approx 10^{-20} \text{ cm}^4/s \\ \delta &= 1016 \text{ cm}^2/s \end{aligned}$$

The additional assumptions is made that:

$$\begin{aligned} R_p &= 10^{-6} \text{ cm} \\ \text{for } kT_{\text{plasma}} &= 200 \text{ eV} \end{aligned}$$

From these parameters

$$W = R_p^2 \alpha \phi 2\sigma k_r / D^2 = 10^{-6}$$

and therefore

$$\begin{aligned} \bar{c}_{max} &= 10^3 \rightarrow \bar{c}_{max} = 10^3 \cdot \alpha \phi R_p / (2D) = 5 \times 10^{17} / \text{cm}^3 \\ \bar{c}_{max} \text{ (Wienhold)} &\approx 4 \times 10^{17} / \text{cm}^3 \end{aligned}$$

$$\begin{aligned} \Phi_{in} &= 10^3 \rightarrow \Phi_{in} = 10^3 \cdot \alpha \phi R_p / x_o = 2 \times 10^{13} / \text{cm}^2 \cdot s \\ \Phi_{in} \text{ (Wienhold)} &= 1.48 \times 10^{13} / \text{cm}^2 \cdot s \end{aligned}$$

$$\tau = 10^6 \rightarrow \tau = 10^6 R_p^2 / D = .1 \text{ s}$$

τ not calculated by Wienhold.

Good agreement is observed between the two calculations. The results above indicate that for INTOR (surface area = 320 m²), the amount of T in the wall could reach $\sim 8 \times 10^{23} T$ (~ 4 gm or 4×10^4 Ci) which is not so much when one considers the on site inventory of $>10^7$ Ci.

On the other hand, the amount of T permeating the wall per day is $\sim 6 \times 10^{24} T$ atoms (30 gm or 3×10^5 Ci) which is a problem which will have to be dealt with. The recycle time of .1 s is much shorter than the "burn cycle" time of 100 s and therefore isotope exchange and wall hold-up effects should be minimal in INTOR.

APPENDIX C

H Recycle Special Cases - SS and Ti

In order to characterize H recycling retention and release in these materials, the equations developed earlier indicate that D , $2\phi_R$, $\alpha\phi$ and R_p must be known in order to determine W and the rest of the parameters in Figure 5.

Tables 1 and 2 summarize some recent (and not so recent) measurements or uses of D and $2\phi_R$ for stainless steels and Ti, respectively. The references used in these compilations are indicated in these tables. A recent review of H in Ti by Wille and Davis⁽¹³⁸⁾ was used for most of the Ti data. Figures 10-15 are plots of both sets of these data. These calculations were performed assuming 1) a 100 m² wall which is 1 cm thick; 2) $\alpha\phi = 10^{-16}/\text{cm}^2\text{s}$ and 3) $R_p = 10^{-6}$ cm. The scatter which is seen in the parameters plotted in Figs. 10-15 indicate the need for further experimental work for both stainless steel and Ti.


Table 1 - Stainless Steel

$D = D_0 e^{-E_D/kT}$ $K = 2\sigma k_r = (500/T)^{1/2} K_0 e^{-E_K/kT}$						
<u>Ref.</u>	<u>Material</u>	<u>D₀</u> (cm ² /s)	<u>E_D</u> (eV)	<u>K₀</u> (cm ⁴ /s)	<u>E_K</u> (eV)	<u>Sym.</u>
161	310, 304 21-6-9, A-216	4.7(-3)*	.56	1.72(-16)	.50	A
61c	1045	4(-4)	.047	-	-	B
162	α Fe	4.15(-4)	.069	-	-	C
61d	α Fe	1.61(-3)	.073	3.3(-17)	-.23	D
85b	304	2(-2)	.57	3.2(-16) [†]	.72	E
85c	304	9.2(-3)	.45	7.0(-16) [†]	.78	F
84	304	1.8(-1)	.64	5.4(-19) [†]	.68	G
74b	α Fe	3.1(-4)	.048	1.8(-18)	-.28	H
29	α Fe γ Fe	7.8(-4) 6.7(-3)	.08 .47	2.1(-17) 4.2(-18)	-.20 .15	I J
67	304	1.2(-1)	.61	-	-	K
80	304	2.5(-2)	.60	-	-	L
65	304	1.2(-1)	.61	-	-	M
163	300 ser.	1.7(-1)	.61	1.38(-16)	.52	N
73	316	2(-2)	.58	-	-	O
96	316	1.74(-2)	.55	-	-	P
94	α Fe	6.2(-4)	.11	-	-	Q

*4.7(-3) $\equiv 4.7 \times 10^{-3}$

[†]These have been fit to an Arrhenius line where as the rest of the data have resulted from calculations using the Baskes of k_r ²⁹.

Table 2 - Titanium and Alloys

<u>Ref.</u>	<u>Material</u>	<u>D_o</u> (cm ² /s)	<u>E_D</u> (eV)	<u>K_o</u> (cm ⁴ /s)	<u>E_K</u> (eV)	<u>Sym</u>
164,165	α Ti	9(-3)*	.54	1.8(-16)	1.18	A
164,166	α Ti	2.7(-3)	.62	"	"	B
167	α Ti	6(-4)	.63	"	"	C
164,168,169	α Ti	1.8(-2)	.54	"	"	D
164,165	α Ti	1.55(-2)	.56	"	"	E
168,169	β Ti	1.95(-3)	.29	"	"	F
164,170,165	Ti-4Al-4Mn	1.8(-3)	.39	"	"	G
164,170,165	Ti-8Mn	3.6(-3)	.30	"	"	H
171	Ti-13V-11Cr-3Al	1.58(-3)	.22	"	"	I
172	Ti-6Al-4V	1.72(-2)	.49			J
				Ref. 173		

*9(-3) $\equiv 9 \times 10^{-3}$

1. H. C. Howe, J. Nucl. Mater. 93/94 (1980) 17.
2. D. Savain, et al., in Proc. of 9th European Conf. in Cont. Fus., Plasma Physics (Oxford, 1979).
3. G. M. McCracken, S. J. Fielding, S. K. Erents, A. Pospieszczak, P. E. Stott, Nucl. Fusion 18 (1978) 35.
4. TFR Group, J. Nucl. Mater. 93/94 (1980) 173.
5. J. B. Roberto, H. C. Howe, R. C. Isler, and L. E. Murray, 2nd Fus. Mat. Conf. (Seattle, 1981) to be published in J. Nucl. Mat.
6. J. B. Roberto, R. C. Isler, S. Kasai, L. E. Murray, J. E. Simpkins, S. P. Withrow and R. A. Zuhre, AVS (Anaheim, 1981).
7. G. M. McCracken, Reports on Progress in Phys. 38 (1975) 241.
8. S. K. Erents, in B. Navinsek (ed) Physics of Ionized Gases 1976, J. Stefan Institute, Ljubljana, Yugoslavia (1976) 299.
9. G. M. McCracken in Proc. Int. Symp. on Plasma Wall Interaction, Julich, Pergamon Press (1976) 339.
10. B.M.U. Scherzer, J. Vac. Sci. Technol. 13 (1976) 420.
11. R. Behrisch, J. de Physique 38 (1977) C3.
12. W. Bauer, J. Nucl. Mater. 76&77 (1978) 3.
13. K. L. Wilson, IEEE Transactions on Nuclear Science NS-26 (1979) 1296.
14. G. M. McCracken, P. E. Stott, Nuclear Fusion 19 (1979) 889.
15. R. Behrisch in Physics of Plasmas Close to Thermonuclear Conditions, Pergamon Press (1980).
16. E. S. Hotston and G. M. McCracken, J. Nucl. Mater. 63 (1976) 177.
17. E. S. Marmar, J. Nucl. Mater. 76&77 (1978) 59.
18. S. J. Fielding, G. M. McCracken, P. E. Stott, J. Nucl. Mater. 76&77 (1978) 273.
19. G. M. McCracken, J. Nucl. Mater. 85&86 (1979) 943.
20. F. Waelbroeck, I. Ali-Khan, K. J. Dietz and P. Wienhold, J. de Physique C7 (1979) 313.
21. R. W. Conn, 2nd Fusion Materials Conf. (Seattle, 1981) to be published in JNM.
22. K. L. Wilson, (Seattle, 1981).
23. S. M. Myers, S. T. Picraux, and R. E. Stoltz, JAP 50 (1979) 5710.
24. K. L. Wilson and M. I. Baskes, J. Nucl. Mat. 76/77 (1978) 291.
25. P. Wienhold, I. Ali-Khan, K. J. Dietz, M. Profant, F. Waelbroeck, J. Nucl. Mater. 85 & 86 (1979) 1001.
26. P. Wienhold, M. Profant, F. Waelbroeck, J. Winter, J. Nucl. Mater. 93&94 (1980) 866.
27. M. I. Baskes, Sandia Nat. Laboratories, SAND80-8201 (1980).
28. T. Tanabe, N. Saito, Y. Etoh & S. Imoto, (Seattle, 1981).
29. M. I. Baskes, J. Nucl. Mat. 92 (1980) 318.
30. A. C. Hindmarsh, UCID-30001, Rev 3 (LRL, Livermore, CA) 1974.
31. F. Waelbroeck, J. Winter, P. Wienhold, (Seattle, 1981).
32. H. S. Carslaw and J. C. Jaeger, Radiation of Heat in Solids, (University Press, Oxford, 1976) 263.
33. J. Crank, The Mathematics of Diffusion (Clarendon Press, Oxford, 1975) 51.
34. A. McNabb and P. K. Foster, Trans. AIME 227 (1963) 619.
35. C. A. West in Hydrogen in Metals II, ed, G. Alefeld and Volkl (Springer, Berlin, 1978) 305.
36. I. Ali-Khan, K. J. Dietz, F. G. Waelbroeck and P. Wienhold, J. Nucl. Mat. 76&77 (1978) 337.
37. F. Waelbroeck, I. Ali-Khan, K. J. Dietz and P. Wienhold, JNM 85/86 (1979) 345.
38. B. L. Doyle, D. K. Brice and W. R. Wampler, Rad. Eff. Lett. (1980) 81.
39. C. M. Braganza, S. K. Erents and G. M. McCracken, J. Nucl. Mater. 75 (1978) 220.
40. M. Braganza, S. K. Erents, E. S. Hotston and G. M. McCracken, J. Nucl. Mat. 76&77 (1978) 298.
41. R. S. Blewer, R. Behrisch, B.M.U. Scherzer and R. Schulz, J. Nucl. Mat. 76&77 (1978) 305.
42. B. L. Doyle, D. K. Brice and W. R. Wampler, IEEE Trans. Nuc. Science, NS-28 (1981) 1300.
43. B. L. Doyle, W. R. Wampler, D. K. Brice and S. T. Picraux, J. Nuc. Mat. 93&94 (1980) 551.
44. B. L. Doyle, W. R. Wampler and D. K. Brice (Seattle, 1981).
45. W. R. Wampler & C. W. Magee (Seattle, 1981).
46. W. Möller, F. Besenbaches & J. Bottlinger, to be published in Applied Physics.
47. W. Köppendorfer, Nuclear Fusion 19 (1979) 1319.
48. a) J. P. Biersack and L. C. Haggmark, Nucl. Inst. & Mat. 174 (1980) 257.
b) D. K. Brice & B. L. Doyle (Seattle, 1981).
c) D. K. Brice, to be published, JNM.
d) E. S. Hotston, JNM 88 (1980) 279.
e) S. K. Erents and E. S. Hotston, Nucl. Inst. Mat. 170 (1980) 449.
f) S. K. Erents, Nucl. Inst. & Met. 170 (1980) 445.
49. K. L. Wilson, unpublished data.
50. K. L. Wilson and L. G. Haggmark, Thin Solid Films 63 (1979) 282.
51. K. L. Wilson, IAEA (Vienna, 1981).
52. K. L. Wilson, IAEA (Tokyo, 1981).
53. V. A. Simonov, G. F. Kleimonov, A. G. Milehkin and K. A. Kochnev. Nucl. Fusion Suppl. 1 (1962) 325.
54. E. S. Borovik, N. P. Katrich and G. T. Nikolaev, Atomn. Energiya 18 (1965) 91.
55. E. S. Borovik, N. P. Katrich, and G. T. Nikolaev, Atomn. Energiya 21 (1966) 339.
56. N. J. Freeman, I. D. Latimer, and N. R. Daly, Nature 212 (1966) 1346.
57. G. M. McCracken and J.H.C. Maple, Brit. J. Appl. Phys. 18 (1967) 919.
58. A. L. Hunt, C. C. Damm, and R. K. Goodman, Lawrence Livermore Laboratory, UCIL-16408 (1964 Draft; 1973 MS).
59. W. Bauer and G. J. Thomas, J. Nucl. Mat. 53 (1974) 127.
60. K. L. Wilson, G. J. Thomas, and W. Bauer, Nucl. Tech. 29 (1976) 322.
61. a) J. Roth, J. Bohdansky, and W. O. Hofer in Proc. Int. Conf. on Plasma Wall Interaction, Julich, Pergamon Press 309 (1976).
b) W. A. Robertson, Met. Trans. 10A (1979) 489.
c) W. A. Robertson and A. W. Thompson, Met. Trans. 11A (1980) 553.

61. d) N. R. Quick and H. H. Johnson, *Acta. Met.* 26 (1978) 903.
e) J. P. Bugeat and E. Ligeon, *Phys. Lett* 71A (1979) 93.
f) M. R. Loutham and R. G. Derrick, *Corrosion Sci.* 15 (1975) 565.
62. C. J. Altstetter, R. Behrisch, J. Bottiger, F. Pohl, and B.M.U. Scherzer, *Nucl. Instr. and Methods* 149 (1978) 59.
63. T. S. Elleman and K. Verghese, *J. Nucl. Mat.* 53 (1974) 299.
64. R. E. Clausing, L. C. Emerson, L. Heatherly, and R. J. Colchin, in *Proc. Int. Conf. on Plasma Wall Interaction*, Julich, Pergamon Press 573 (1976).
65. K. L. Wilson and M. I. Baskes, *J. Nucl. Mat.* 74 (1978) 179.
66. R. E. Clausing, L. C. Emerson & L. Heatherly *J. Nucl. Mat.* 76&77 (1978) 267.
67. K. L. Wilson and M. I. Baskes, *J. Nucl. Mat.* 76&77 (1978) 291.
68. G. Farrell and S. E. Donnelly, *J. Nucl. Mat.* 76&77 (1978) 332.
69. I. Ali-Khan, K. J. Dietz, F. G. Waelbroeck, and P. Wienhold, *J. Nucl. Mat.* 76&77 (1978) 337.
70. K. J. Dietz and F. Waelbroeck, in *Proc. Int. Conf. on Plasma Wall Interaction*, Julich, Pergamon Press, 445 (1976).
71. R. E. Clausing, L. C. Emerson & L. Heatherly, *J. Nucl. Mat.* 76&77 (1978) 267.
72. G. J. Thomas and K. L. Wilson, *J. Nucl. Mat.* 76&77 (1978) 332.
73. G. W. Look and M. I. Baskes, *J. Nucl. Mat.* 85&86 (1979) 995.
74. a) P. Wienhold, I. Ali-Khan, K. J. Dietz, M. Profant, and F. Waelbroeck, *J. Nucl. Mat.* 85&86 (1979) 1001.
b) F. Waelbroeck, I. Ali-Khan, K. J. Dietz and P. Wienhold, *JNM* 85&86 (1979) 345.
75. I. Ali-Khan, K. J. Dietz, F. G. Waelbroeck, and P. Wienhold, *J. Nucl. Mat.* 85&86 (1979) 1151.
76. P. Wienhold, R. E. Clausing & F. Waelbroeck, *J. Nucl. Mat.* 93&94 (1980) 540.
77. R. E. Clausing, L. C. Emerson & L. Heatherly *J. Nucl. Mat.* 85&86 (1979) 542.
78. K. L. Wilson and A. E. Pontau, *J. Nucl. Mat.* 85&86 (1979) 989.
79. B. Navinsek, M. Peternel, A. Zabkar & S. K. Erents, *J. Nucl. Mat.* 93&94 (1980) 739.
80. J. Bohdanský, K. L. Wilson, A. E. Pontau, L. G. Haggmark, and M. I. Baskes, *J. Nucl. Mat.* 93&94 (1980) 594.
81. E. W. Thomas, *J. Appl. Phys.* 51 (1980) 1176.
82. M. B. Lewis and K. Farrell, *Appl. Phys. Lett.* 51 (1980) 1176.
83. F. Waelbroeck, K. J. Dietz, P. Wienhold, J. Winter, I. Ali-Khan, H. Merken, & E. Rota, *J. Nucl. Mat.* 93&94 (1980) 839.
84. M. Braun, B. Emmoth, F. Waelbroeck, and P. Wienhold, *J. Nucl. Mat.* 93&94 (1980) 861.
85. a) P. Wienhold, M. Profant, F. Waelbroeck & J. Winter, *J. Nucl. Mat.* 93&94 (1980) 866.
b) F. Waelbroeck, J. Winter and P. Wienhold, (Seattle, 1981).
c) P. Wienhold, F. Waelbroeck, J. Winter & I. Ali-Khan, *KFA Report JUL 1694* (1980).
d) I. Ali-Khan, K. J. Dietz, F. Waelbroeck, P. Wienhold, *KFA Report, JUL-1597* (1979).
86. F. Besenbacher, J. Bottiger and S. M. Myers, to be published in *J. App. Phys.*
87. H. K. Perkins and T. Noda, *J. Nucl. Mater.* 71 (1978) 349.
88. S. T. Picraux and W. R. Wampler, *J. Nucl. Mater* 93&94 (1980) 853.
89. K. Erents & G. M. McCracken, *Brit. J. Appl.* 93&94 (1980) 853.
90. K. Erents and G. M. McCracken, *Radiation Effects* 3 (1970) 123.
91. F. Besenbacher, J. Bottiger, T. Laursen & W. Moller, *J. Nucl. Mat.* 93&94 (1980) 617.
92. A. E. Gorodetsky, A. P. Zakharov, V. M. Sharapov, and V. Kh. Alimov, *J. Nucl. Mat.* 93&94 (1980) 588.
93. W. Moller, B.M.U. Scherzer, R. Behrisch, *Nucl. Instr. and Methods* 168 (1980) 289.
94. T. Tanabe and S. Imoto, *JIMIS-2, Hydrogen in Metals* (1980) 109.
95. Y. Etoh, T. Tanabe & S. Imoto, *Osaka Report* 1614 (1981) 1.
96. N. Saitoh, Y. Etoh, T. Tanabe and S. Imoto, *Osaka Report* 30, No. 1564 (1980) 429.
97. T. Tanabe, N. Saito, Y. Etoh & S. Imoto, (Seattle, 1981).
98. R. Yamada, K. Nakamura, K. Saie & M. Saidoh *J. Nucl. Mat.* 101 (1981) 993.
99. Y. Sakamoto & A. Miura, *Nagasaki Report* 13, 109 (1979).
100. Y. Sakamoto and K. Takeuchi, *Japan Materials Research Congress* (1977) 152.
101. Y. Sakamoto and J. Eguchi, *Japan Materials Research Congress* (1976) 91.
102. Y. Sakamoto and T. Matsumoto, in *H Diffusion in Stainless Steel* Ba 68 (1977) H. 4, 285.
103. Y. Sakamoto and T. Mantani, *Trans. JIM* 17 (1976) 743.
104. E. H. VanDevender, V. A. Moroni, *J. Nucl. Mat.* 92 (1980) 103.
105. W. M. Robertson, *Met. Trans.* 9A (1977) 1709.
106. G. M. McCracken and J.H.C. Maple, *Proc. 7th International Conf. on Phenomena in Ionized Gases* (Belgrade) Vol. 1, 137 (1965).
107. G. M. McCracken and S. K. Erents in S. T. Picraux, E. P. EerNisse, & F. L. Vook, (ed.) *Applications of Ion Beams to Metals*, Plenum Press, 585 (1974).
108. S. K. Erents, *Vacuum* 24 (1974) 445.
109. C. Braganza, G. Carter, & G. Farrell, *Nucl. Inst. and Methods* 132 (1976) 679.
110. J. Bottiger, S. T. Picraux, N. Rud, and T. Laursen, *J. Appl. Phys.* 48 (1977) 920.
111. S. T. Picraux, J. Bottiger, & N. Rud., *Appl. Phys. Lett.* 28 (1976) 179.
112. S. T. Picraux, J. Bottiger, and N. Rud, *J. Nucl. Mat.* 63 (1976) 110.
113. G. Carter, D. G. Armour, C. Branganza, S. E. Donnelly, and G. Farrell, in *Physics of Ionized Gases 1976*, edited by B. Navinsek, Univ. Ljubljana 261 (1978).
114. R. Schulz, R. Behrisch, and B.M.U. Scherzer, *J. Nucl. Mat* 93&94 (1980) 608.
115. A. E. Pontau, F. Greulich, and K. L. Wilson, unpublished data.
116. C. E. Ellis and W. Evans, *Trans. Metall. Soc. AIME* 277 (1963) 438.
117. W. R. Wampler, T. Schober, and B. Lengeler, *Phil. Mag.* 34 (1976) 129.

118. a) P. B. Johnson and D. J. Mazey, *J. Nucl. Mat.* 93&94 (1980) 721.
b) P. B. Johnson and T. R. Armstrong, *Appl. Phys. Lett.* 31 (1977) 326.
c) P. B. Johnson, D. J. Mazey, *J. of Nucl. Mat.*, 91 (1980) 41.
d) T. R. Armstrong, R. C. Corliss and P. B. Johnson, *J. of Nucl. Mat.* 98 (1981) 338.
e) P. B. Johnson and T. R. Armstrong, *Nucl. Inst. and Met.* 148 (1978) 85.
119. K. L. Wilson and L. G. Haggmark, *Thin Solid Films* 63 (1979) 283.
120. R. D. Daniels, *J. Appl. Phys.* 42 (1971) 417.
121. E. S. Hotson and G. M. McCracken, *J. Nucl. Mat.* 68 (1977) 277.
122. K. L. Wilson, in G. H. Miley & W. H. Sawyer (ed.) *Proc. of the Inst. on Curriculum Development in Fusion, Center for Educational Affairs ANL Vol. 1, chp. 13* (1976).
123. G. M. McCracken, D. K. Jefferies, and P. Goldsmith, *Proc. 4th Int. Vacuum Congress, Inst. of Physics Conf. Ser. No. 5* 149 (1968).
124. I. Sheft, A. H. Reis, Jr., D. M. Gruen, and S. W. Peterson, *J. Nucl. Mat.* 59 (1976) 1.
125. J. Bohdanský, J. Roth, M. K. Sinha, and W. Ottenberger, *J. Nucl. Mat.* 63 (1976) 115.
126. O. C. Yonts & R. A. Strehlow, *J. Appl. Phys.* 33 (1962) 2903.
127. M. K. Sinha, J. Roth, & J. Bohdanský, *Proc. 9th Symp. Fusion Technology, Garmisch* 41 (1976).
128. J. Bohdanský, J. Roth, & W. Poschenrieder, *Inst. Phys. Conf. Ser.* 28 (1978) 307.
129. J. Roth, W. Eckstein, & J. Bohdanský, *Rad. Effects* 48 (1980) 231.
130. A. E. Pontau, L. G. Haggmark, K. L. Wilson, R. Bastasz, M. E. Malinowski, D. B. Dawson, and W. Bauer, *J. Nucl. Mat.* 85&86 (1979) 1013.
131. A. E. Pontau, K. L. Wilson, I. Greulich & L. G. Haggmark, *J. Nucl. Mat.* 91 (1980) 343.
132. F. Greulich and G. J. Thomas, *SNL Report SAND80-8723*, to be published.
133. R. H. Stulen, *Appl. Surf. Sci.* 5 (1980) 212.
134. K. L. Wilson and A. E. Pontau, *J. Nucl. Mat.* 93&94 (1980) 569.
135. E. Brauer, R. Dunn and H. Zuchner, *Z. Physikalische Chemie* 100 (1976) 109.
136. R. J. Brewer, J. K. Gimzewski & S. Veprek, (Seattle, 1981).
137. J. K. Gimzewski, R. J. Brewer & S. Veprek, *Proc. 5th Int. Symp. on Plasma Chem.*, ed. B. Waldie (Edinburgh, 1981).
138. G. W. Wille and J. W. Davis, *Report DOE/ET/52039-2* (1981).
139. T. R. Armstrong and P. B. Johnson, *J. Nucl. Mat.* 60 (1976) 241.
140. S. K. Erents, C. M. Braganza & G. McCracken *JNM* 63 (1976) 399.
141. B.M.U. Scherzern, R. Behrish, W. Eckstein, U. Littmark, J. Roth, and M. K. Sinha, *JNM* 63 (1976) 100.
142. R. A. Langley, R. S. Blewer and J. Roth, *JNM*, 76&77 (1978) 313.
143. G. Standenmair, et al., *JNM* 84 (1979) 149.
144. S. A. Cohen and G. M. McCracken, *JNM* 84 (1979) 157.
145. S. K. Erents, *Nucl. Instr. and Mat.* 170 (1980) 455.
146. M. C. Underwood, S. K. Erents and E. S. Hotston, *JNM*, 93&94 (1980) 575.
147. P. Hucks, K. Flaskamp and E. Vietzke, *JNM* 93&94 (1980) 558.
148. J. Roth, et al., *JNM* 93/94 (1980) 601.
149. K. L. Wilson and A. E. Pontau, *JNM* 93&94 (1980) 601.
150. B.M.U. Scherzer, et al., to be published *J. Inst. and Met.* (Lyon, 1981).
151. S. T. Picraux and W. R. Wampler, *JNM* 93&94 (1980) 853.
152. A. E. Pontau and K. L. Wilson, *Thin Solid Films* 73 (1980) 109.
153. B. L. Doyle and F. L. Vook, *Thin Solid Films* 63 (1979) 277.
154. B. L. Doyle & F. L. Vook, *JNM* 85/86 (1979) 1019.
155. C. W. Magee, et al., *Nucl. Inst. and Meth.* 168 (1980) 383.
156. G. W. Arnold & B. L. Doyle, to be published (MAS, Boston, 1981).
157. B. L. Doyle & G. W. Arnold, to be published (MAS, Boston, 1981).
158. W. Möller, F. Besenbacher and T. Laursen, *JNM* 93&94 (1980) 750.
159. F. Besenbacher, J. Bottiger, T. Laursen and W. Möller, *JNM* 93&94 (1980) 617.
160. R. Schulz, R. Behrish, and B.M.U. Scherzer, *JNM* 93&94 (1980) 608.
161. M. R. Louthan and D. G. Derrick, *Corrosion Science* 15 (1975) 565.
162. J. Volkl and G. Alefeld in *Hydrogen in Metals I*, eds. Alefeld & Volkl, Springer-Verlag (1978) 321.
163. R. A. Kerst, (Seattle, 1981).
164. D. N. Williams, *TML Report No. 100*, (1958).
165. D. N. Williams, et al., *Report #AF33(616)* 2813 (1957).
166. H. Schliecher and U. Zwicker, (thesis) *Rensselaer Inst.* (1957).
167. L. C. Covington, *NACE* 35 (1979) 378.
168. R. J. Wasilewski and G. L. Kehl, *Metal-lurgia* (1954) 225.
169. R. J. Wasilewski and G. L. Kehl, *Report No. DA-30-069-OR-644* (1953).
170. W. M. Albrecht and M. W. Mallett, *Trans. of Met. Society of AIME*, (1958) 204.
171. W. R. Holman, R. W. Crawford & F. Paredes, *Trans. of Met. Society of AIME* 233 (1965) 1836.
172. J. L. Waisman, G. Stines and R. F. Toosky, *2nd Int. Cong. on H in Metals*, (Paris, 1977)

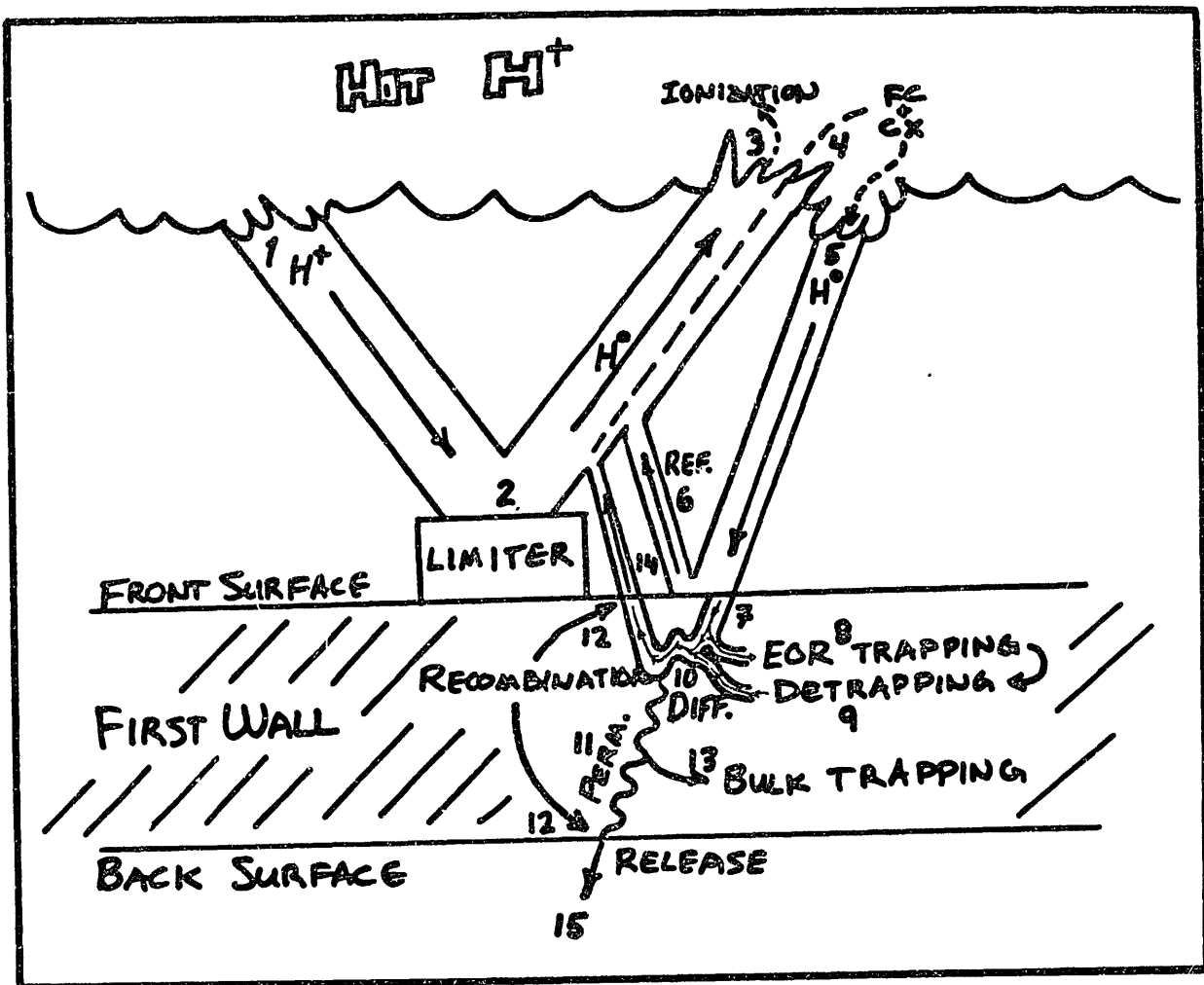


Figure 1. Schematic flow diagram of the plasma-surface interaction (PSI) at the first wall of a fusion reactor.

FIG 2. DIFFERENTIAL EQUATIONS

$$\frac{\partial c_i}{\partial t} = D \frac{\partial^2 c_i}{\partial x^2} + G_i(x) - \frac{\partial c_{ti}}{\partial t} \quad (1)$$

$$\frac{\partial c_{ti}}{\partial t} = D c_i c_e / \lambda^2 - v c_{ti} \quad (2)$$

$$A_n c_e = A_n c_t - \sum_{i=1} c_{ti} \quad (3)$$

$$A_n \cdot \frac{\partial c_t}{\partial t} = b G_i(x) - \mu A_n c_t \quad (4)$$

WHERE

$$v = v_0 e^{-(E_D + E_T)/kT} + \begin{cases} 0 & \text{not sat.} \\ \frac{G_j w}{c_t} & \text{sat. } j \neq i \end{cases} \quad (5)$$

$$D = D_0 e^{-E_D/kT} \quad (6)$$

BOUNDARY CONDITIONS

$$\Phi_{rec} = 2\sigma k_r c_0^2 \quad \begin{matrix} \text{SURFACE} \\ \text{RECOM.} \\ \text{LIMITED} \end{matrix} \quad (7)$$

$$c_0 = 0 \quad \text{DIFFUSION LIMITED} \quad (8)$$

$$\frac{\partial c}{\partial x} \Big|_0 = 0 \quad \text{NO RELEASE} \quad (9)$$

$$k_r = \left(\frac{8}{\pi m T} \right)^{1/2} \frac{\alpha' c_1}{c_0^{1/2}} \times \begin{cases} e^{-2|E_s|/kT} & |E_s + E_D| < 0 \\ e^{(E_s - E_D)/kT} & |E_s + E_D| > 0 \end{cases} \quad (10)$$

Figure 2. Differential equations used to model the PSI.

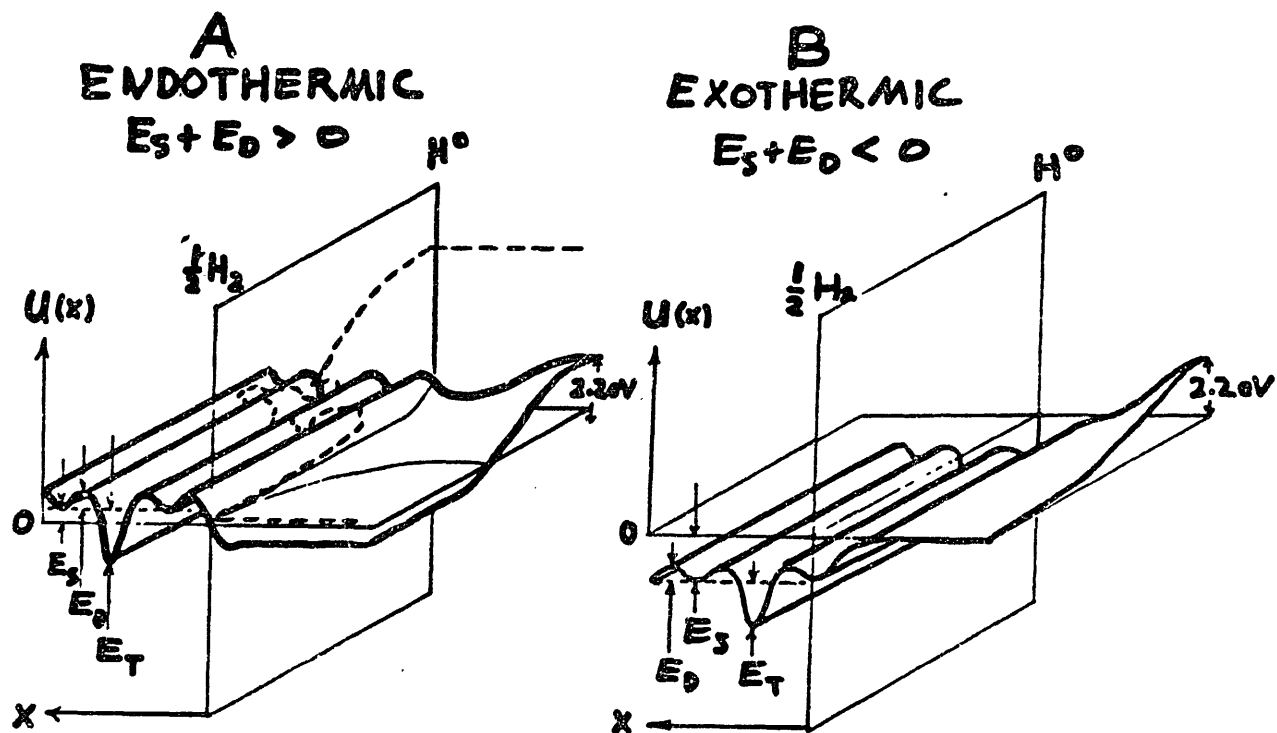


Figure 3. Diagram of potential surface in an endothermic (A) and exothermic (B) solid.

RECOMBINATION

$$\alpha\phi = -D \frac{\partial c}{\partial x} \Big|_0 + 2\sigma k_r c_0^2$$

STEADY STATE

$$c = \left(\frac{\alpha\phi}{2\sigma k_r} \right)^{1/2} \left[\frac{x_0 - x}{x_0} \right] \quad (11)$$

$$\Phi_{rec} = \alpha\phi \left[1 + \frac{2\sigma k_r}{\alpha\phi} c_0^2 (t/\tau) \right] \quad (12)$$

$$\bar{c}_{max} = \frac{1}{2} \left(\frac{\alpha\phi}{2\sigma k_r} \right)^{1/2} \quad (13)$$

$$\Phi_{in} = \frac{D}{x_0} \left(\frac{\alpha\phi}{2\sigma k_r} \right)^{1/2} \quad (14)$$

$$\tau = \frac{D}{\alpha\phi 2\sigma k_r} \quad (15)$$

NO RELEASE

$$c = 2\alpha\phi \left(\frac{t}{\pi D} \right)^{1/2} e^{-x^2/4Dt} - \frac{\alpha\phi x}{D} \operatorname{erfc} \left[\frac{x}{2\sqrt{Dt}} \right] \quad (21)$$

$$c_0 = 2\alpha\phi \left(\frac{t}{\pi D} \right)^{1/2} \quad (22)$$

$$\bar{c}_{max} = \infty \quad (23)$$

$$\Phi_{rec} = \Phi_{in} = 0 \quad (24)$$

$$\tau = \infty \quad (25)$$

$$\tau_{HYDROLYSE} \approx \frac{\pi D c_{HYDROLYSE}^2}{4 \alpha^2 \phi^2} \quad (26)$$

DIFFUSION

$$c(x=0) = 0$$

$$c = \alpha\phi \left(\frac{t}{\pi D} \right)^{1/2} \left(e^{-(x-R_p)^2/4Dt} - e^{-(x+R_p)^2/4Dt} \right) \quad (16)$$

$$\frac{2\alpha\phi}{2D} \left(|x-R_p| \operatorname{erfc} \left(\frac{|x-R_p|}{2\sqrt{Dt}} \right) + |x+R_p| \operatorname{erfc} \left(\frac{|x+R_p|}{2\sqrt{Dt}} \right) \right)$$

$$\Phi_{rec} = D \frac{dc}{dx} \Big|_0 = \alpha\phi \operatorname{erfc} \left[\frac{R_p}{2\sqrt{Dt}} \right] \quad (17)$$

$$\bar{c}_{max} = \frac{\alpha\phi R_p}{2D} \quad (18)$$

$$\Phi_{in} = \frac{\alpha\phi R_p}{x_0} \quad (19)$$

$$\tau = \frac{R_p^2}{D} \quad (20)$$

OTHER EQUATIONS

$$\tau_{lag} = \frac{x_0^2}{6D} \quad (27)$$

$$\text{McNabb Foster } D_{eff} = \frac{D}{1 + c_t k/p} \quad (28)$$

Figure 4. Solutions to differential equations in Fig. 2. for I) recombination and II) diffusion controlled transport, and III) zero release from surface conditions.

TRANSPORT PARAMETER

$$W \equiv \frac{R_p^2 \alpha \phi 2 \sigma k_r}{D^2} \quad (29)$$

$$\bar{c}'_{\max} \equiv \frac{\bar{c}_{\max}}{\left(\frac{\alpha \phi R_p}{2D}\right)} \cong 1 + W^{-1/2} \quad (30)$$

$$\Phi'_{in} \equiv \frac{\Phi_{in}}{\left(\frac{\alpha \phi R_p}{x_0}\right)} \cong 1 + W^{-1/2} \quad (31)$$

$$\tau' \equiv \frac{\tau}{\left(\frac{R_p^2}{D}\right)} \cong 1 + W^{-1} \quad (32)$$

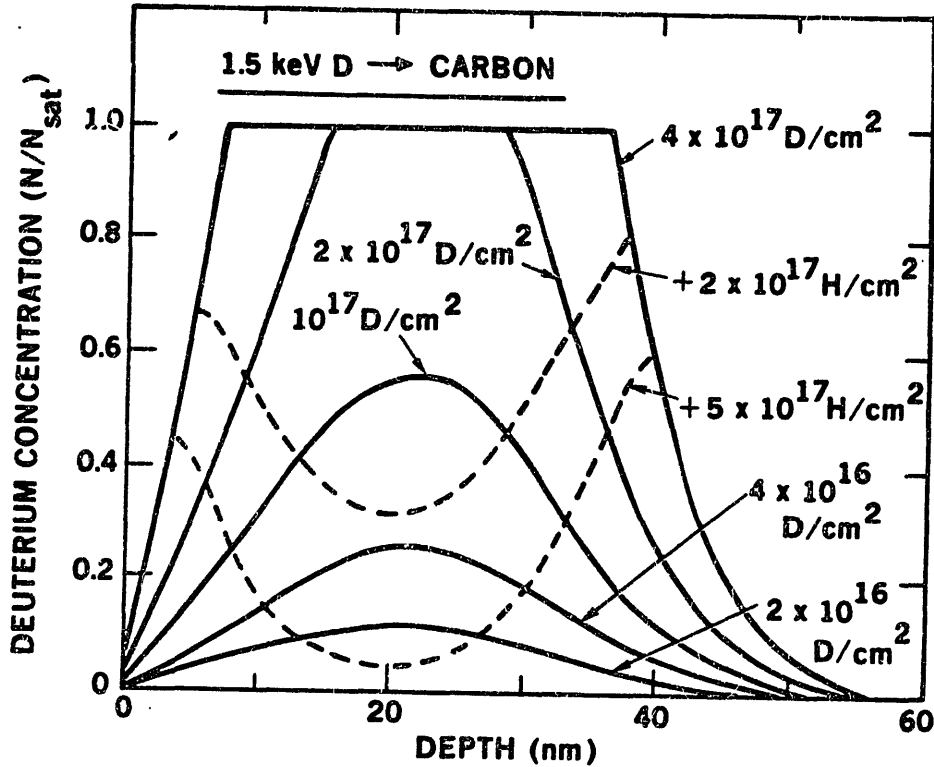
$$W > 1 \Rightarrow \text{DIFF. LIMITED} \quad (33)$$

$$W < 1 \Rightarrow \text{RECOM. LIMITED}$$

Figure 5. Definition and example uses of the transport parameter W .

LOCAL MIXING MODEL

$$\frac{\partial c_{ti}}{\partial t} = \begin{cases} G_i(x) \\ 0 \end{cases} - v c_{ti} \quad \begin{matrix} c_{ti} < n_{sat} \\ c_{ti} = n_{sat} \end{matrix} \quad (34)$$



STEADY STATE

$$c \approx \begin{cases} n_{sat} & x < R_p \\ 0 & x > R_p \end{cases} \quad (35)$$

$$\tau_{co} \approx \frac{R_p n_{sat}}{d\phi} \quad (36)$$

$$\Phi_{rec} = \int G(x) dx \quad \begin{matrix} \text{OVER} \\ \text{SAT. REGION} \\ \text{ONLY} \end{matrix} \quad (37)$$

Figure 6. Equations and example use of the Local Mixing Model (LMM).

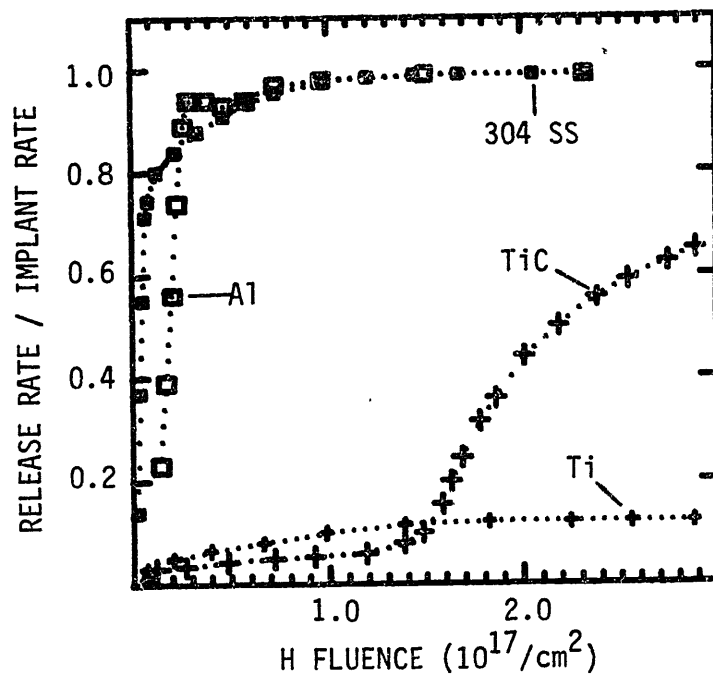


Fig. 7 H re-emission rate for 3.3 keV H ($10^{15}/\text{cm}^2\text{s}$) on 304 SS, Al, Ti and TiC. (WILSON-1981)

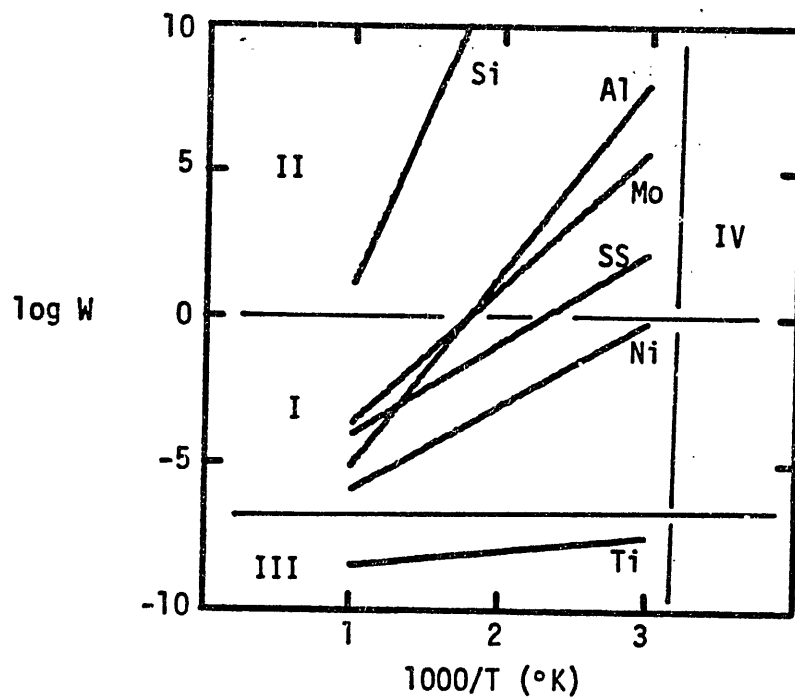
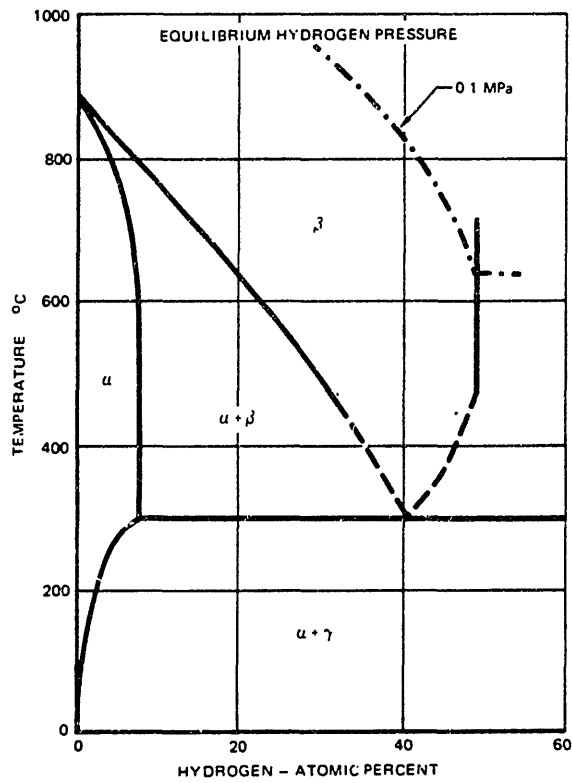


Fig. 8. Transport parameter for various materials.



13-2205A

FIGURE 9 TITANIUM-HYDROGEN BINARY PHASE DIAGRAM

WILLE-DAVIS(1981)

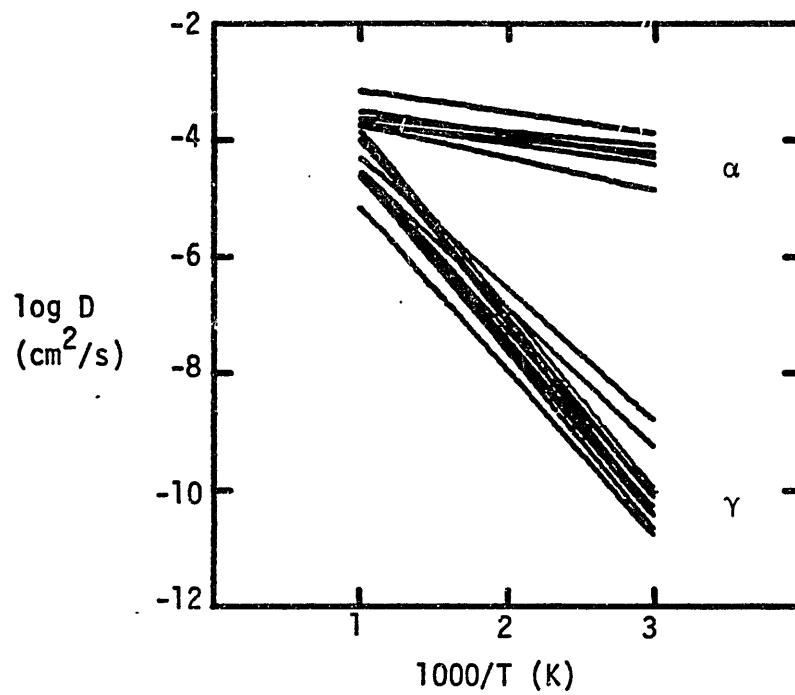


Fig. 10. Diffusivity for Fe Alloys.

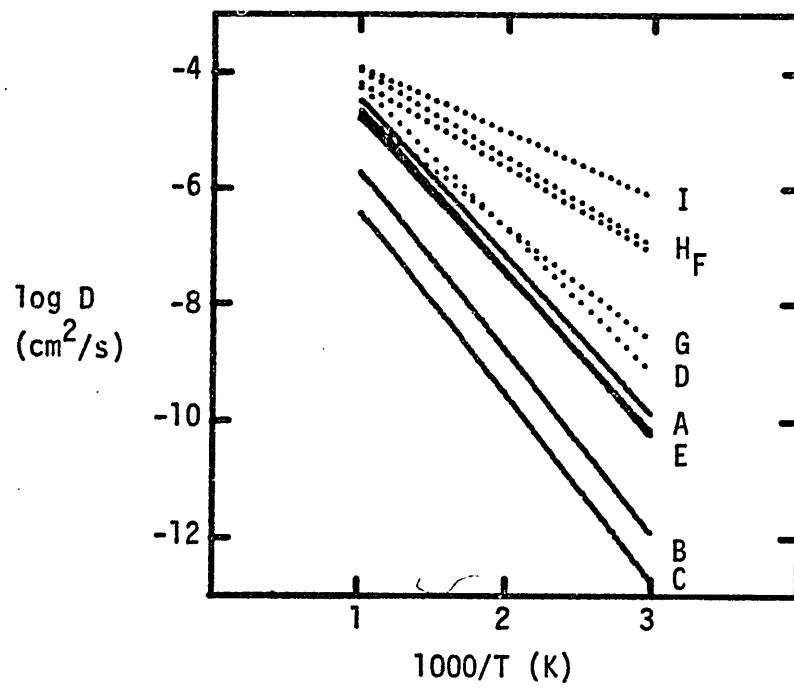


Fig. 11. Diffusivity of Ti Alloys.

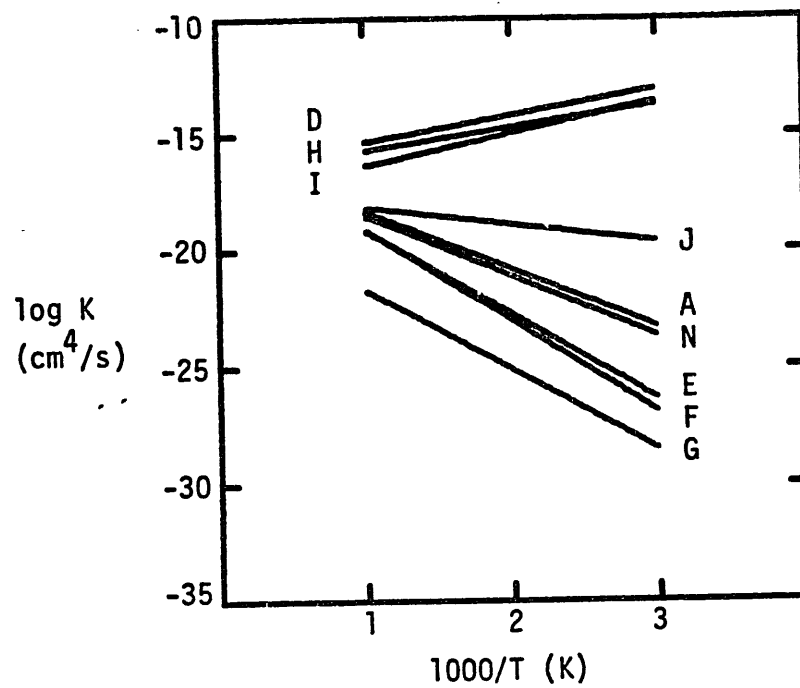


Fig. 12. Recombination Coefficient for Fe Alloys.

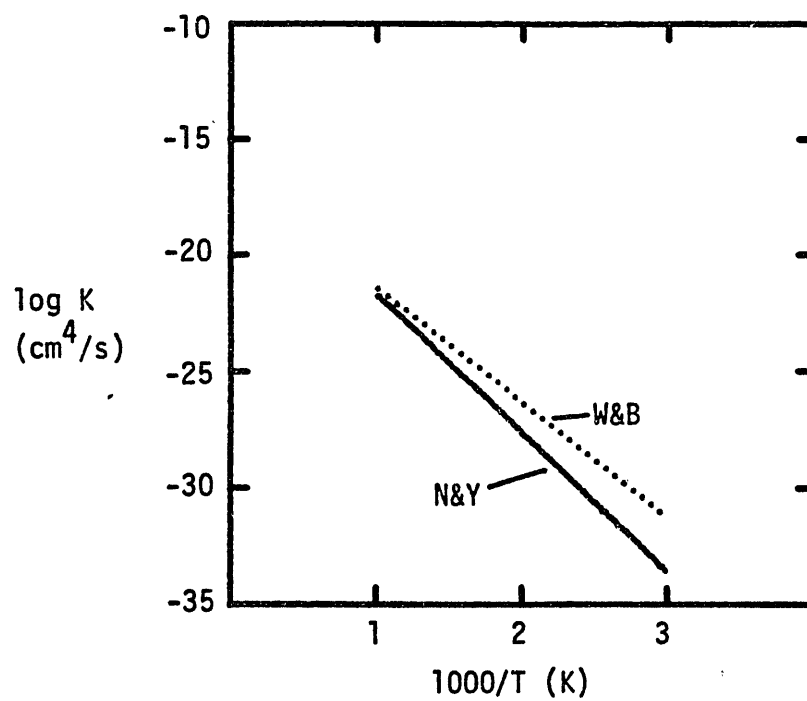


Fig. 13. Recombination Coefficient for Ti Alloys.

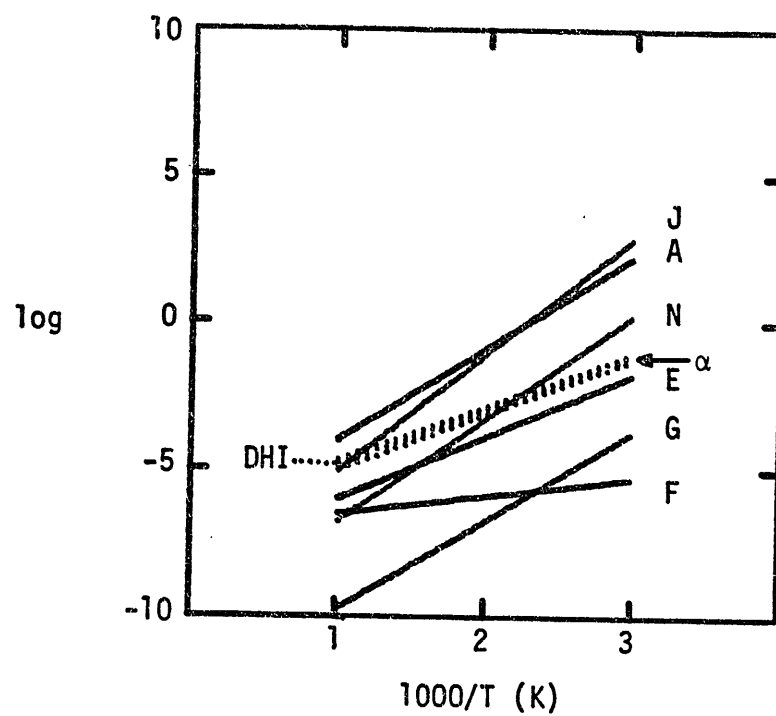


Fig. 14. Transport Parameter for Fe Alloys.

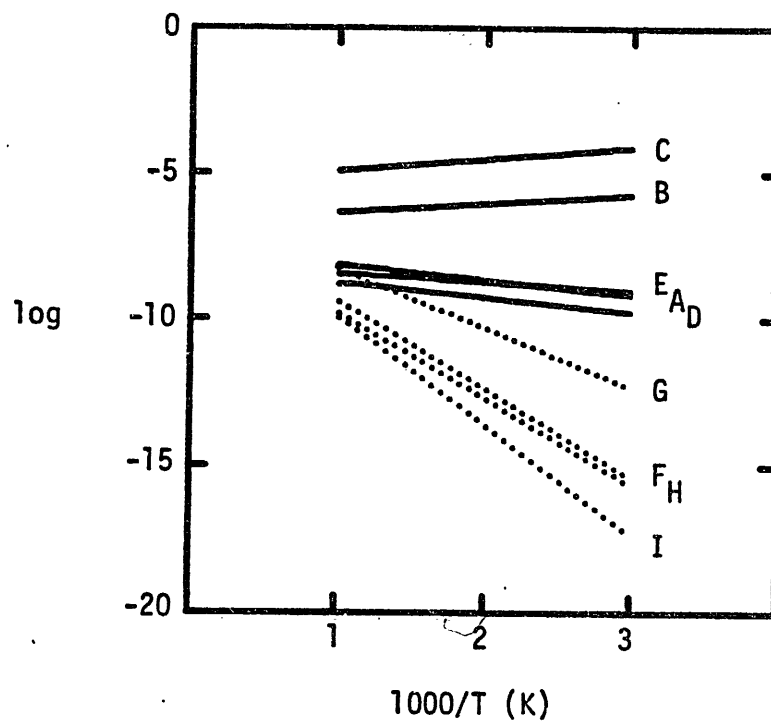


Fig. 15. Transport Parameter for Ti Alloys.

DESORPTION AND ADSORPTION

Atsushi Koma

Institute of Materials Science
University of Tsukuba
Ibaraki 305, Japan

I. Introduction

The surface of a solid is generally covered with foreign atoms and molecules. Those foreign atoms leave the surface and go into the vacuum due to the heat or the impact of incident atoms, electrons and photons. This is so-called desorption and plays significant roles in the plasma-wall interactions in two ways, which occur at the surface of the first wall of the nuclear fusion devices. One is the impurity introduction process. Such impurity atoms as C and O on the first wall go into the plasma due to the desorption and cause the serious radiation loss. The other is the fuel gas recycling process. The hydrogen isotopes are adsorbed on the surface of the first wall and go back to the plasma due to the desorption. This process makes important contributions to the energy and particle balances of the plasma. Thus it is urgently needed to make clear the desorption and adsorption processes on the surface of the first wall.

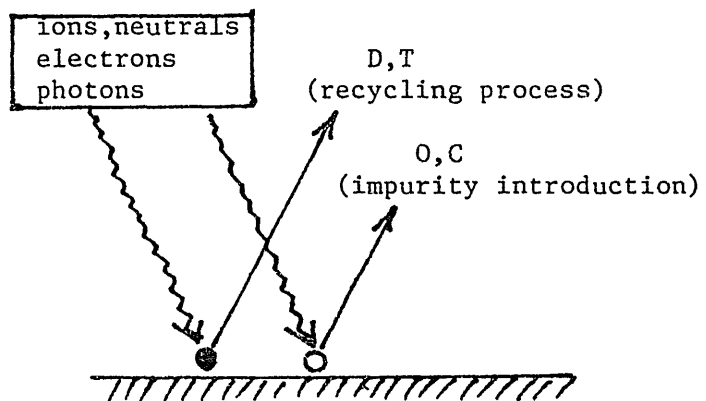


Fig. 1 Desorption on the Surface of the First Wall

II. Characteristic Features of the Desorption on the Surface of the First Wall

As for the impurity introduction process from the first wall into the plasma, sputtering has been mostly notified. But the desorption occurs much more easily than the sputtering. One of the reasons is the low binding energy (usually less than 1 eV) of the impurity atoms adsorbed to the surface of the first wall. This binding energy is considerably lower than the one involved in the sputtering. Even if such impurity atoms as C and O are chemically and strongly bound to the first wall, they react with impinging hydrogen isotopes and are changed into the form of CD_4 or D_2O , which are bound physically and loosely. Thus the detailed understanding of desorption process is urgently needed to reduce the impurity in-

roduction into the plasma. That knowledge is also useful to the effective discharge cleaning of nuclear fusion devices.

Even if a clean surface is once obtained by the discharge cleaning, there remains another problem. There is a large amount of impurities inside the first wall materials, and large gradient of impurity concentration is formed by the removal of the impurity on the first wall. That concentration gradient acts as a motive force for the diffusion of the impurity from the inside of the wall to the surface. Thus the desorption process on the first wall must be made clear in connection with the diffusion process in the first wall materials.

Most investigations on the desorption have been made on the well-defined single-crystalline surfaces. But the surface of the first wall of the nuclear fusion devices is far from the single-crystalline surface, and there is difficulty in the estimation of the desorption yield for the actual surface of the first wall.

III. Various Desorption Processes on the Surface of the First Wall

The desorption which has been most intensively investigated is thermal desorption. Thermal desorption occurs on the surface of the first wall as well. But ion-induced, electron-induced and photon-induced desorptions will be discussed in the followings, because they are characteristic desorptions on the surface of the first wall.

3.1 Ion-induced desorption

This is a desorption due to the impact of ions (and neutrals) impinging on the surface. Three processes are considered in the ion-induced desorption. (a) Adsorbed atoms receive the momentum directly from the impinging ions, and leave the surface after the reflection at the top surface of the wall material. (b) Incident ions are reflected on the surface and knock off the adsorbed atoms. (c) Atoms sputtered by incident ions knock off the adsorbed atoms. Desorption cross section has been measured mainly on the surfaces of refractory metals. They fall between 10^{-14} cm² and 10^{-17} cm². The cross section is larger for the heavier ions. Dependence on the energy of the incident ions is not simple. In some cases desorption cross section is larger for higher incident energy, but the dependence is inverse in another case.

3.2 Electron-induced desorption

As for electron-induced desorption, there are considerable numbers of data for metal surfaces. The adsorbed atoms are excited into the unbound states and go out into vacuum by the incident electrons. The cross section of electron-induced desorption is about 10^{-17} cm² in loosely bound systems and $10^{-21} \sim 10^{-19}$ cm² in tightly bound systems. Clear angle dependence in the outgoing direction of the desorbed atoms is seen on some single-crystalline surfaces.

3.3 Photo-desorption

Details of the photo-desorption process has not been well investigated. Thermal and quantum mechanical processes are consi-

dered in photo-desorption. In the thermal mechanism photo-desorption is essentially same as thermal desorption. In the quantum mechanical mechanism the adsorbed atoms are knocked off by direct interactions with incident light or by photoelectron produced by incident light. Although only limited amount of data are available, the cross section of photo-desorption is estimated as about 10^{-20} cm^2 .

Comparison of yield for each desorption mechanism is shown in Table 1 and Table 2. Table 1 is the result of Bauer's estimation [1] for C and O on stainless steel. This indicates that ion-induced desorption will make the largest contribution to the impurity introduction into plasma. Table 2 shows results of Wilson's estimation [2] on numbers of desorbed deuterium, which contribute to the fuel gas recycling. Ion-induced desorption seems to be leading desorption process in the fuel gas recycling.

Incident Particles	Desorption Yield (atoms/particle)	Incident Flux $(\text{cm}^{-2} \text{s}^{-1})$	Released Impurity $(\text{cm}^{-2} \text{s}^{-1})$
D	2	1×10^{16}	2×10^{16}
electron	5×10^{-3}	4×10^{16}	2×10^{14}
photon	4×10^{-4}	10^{17}	4×10^{13}

Table 1. Evaluation of desorption of C and O on stainless steel[1]

Incident Particle	Cross Section (cm^2)	Incident Flux $(\text{cm}^{-2} \text{s}^{-1})$	Desorbed D / Adsorbed D
D	10^{-16}	10^{16}	1
electron	10^{-17}	5×10^{16}	0.5
photon	$10^{-20} - 10^{-18}$	10^{18}	0.01 - 1

Table 2 Evaluation of fuel gas recycling due to desorption[2]

IV. Data Needed for the Desorption on the First Wall Surfaces

Such low z material as graphite is a promising candidate material as limiter or armour material. But there are few data on the desorption on low z material surfaces. It is urgently requested to compile desorption data for low z materials.

Data for photo-desorption are also lacking. In addition to the data for cross section, informations about intensity and energy

distributions of photons impinging on the first wall are needed as well.

Auger electron spectroscopy (AES) and ion scattering spectroscopy have been successfully used in the investigations of desorption. But unfortunately those techniques are insensitive to hydrogen isotopes, which play main roll in the plasma-surface interactions. Development of new technique is needed to detect hydrogen isotopes on the surface with high sensitivity.

Desorption and adsorption is much more sensitive to the surface conditions than sputtering. The surface of the first wall changes their forms by sputtering and blistering etc.. In some compound materials, the surface composition changes as well by sputtering. Thus data for those "technical" surfaces are needed in the design of the first wall, which are lacking as well.

REFERENCES

- [1] W. Bauer, J. Nucl. Mater. 76 & 77 (1978) 3-15.
- [2] K. L. Wilson, presented at the Topical Meeting on Nuclear Fusion Materials, Seattle, 1981.

Review of Discussions on Mechanism of PWI

B. L. Doyle

Sandia National Laboratories

Albuquerque, New Mexico 87185

This session was held Wednesday morning and was chaired by B. L. Doyle. E. Thomas presented a short talk in which 17 subcategories used to specify the particle-solid interaction by the ORNL Data Center were spelled out. This list can be found in Table 1. In addition, the various parameters used to describe each process were listed and included:

1. Energy (incident and final)
2. Angle (incident and exit)
[note: in some cases the exit angle was integrated.]
3. Temperature
4. Surface Structure (ie. crystal, polycrystal, amorphous etc)

Thomas then proceeded to present a critique on each topic based upon 1) the importance to fusion reactor development and 2) a characterization of the existing data and/or theoretical base. Because this list was originally prepared in 1976, several additional topics were added which are of current interest such as 1) H in metal phenomena and 2) radiation induced damage or composition modification. A questionnaire was distributed to each participant in order to get a general opinion as to the importance and data resources of each subject. The results of this is shown in Table II.

Two important points can be inferred from this table.

1) Most of the processes were considered very important and, unfortunately perhaps, 2) the current data compilations were deemed inadequate. This indicates that a significant amount of experimental work will be required in the next few years to insure that the data base for PWI will meet the near future needs of both plasma modelers and experimentalists. Incidentally, the majority opinion expressed by the participants was remarkably similar to that of Thomas.

Table I

Bibliography Categorization List on Particle Interactions with Solids

1. General
2. Sputtering by Electrons, Neutrons, and Heavy Particles
(total removal coefficients)
3. Sputtered Particle Charge and Quantum (Excited) State
Distribution
4. Secondary Electron Ejection by Heavy Particle and Electrons
5. Photoelectric Ejection of Electrons (coefficients)
6. Reflection of Electrons from Surfaces (coefficients)
7. Reflection of Heavy Particles from Surfaces
(total reflection coefficients)
8. Charge and Quantum State Distributions of Reflected
Heavy Particles at Macroscopic Distances from Surfaces
9. De-Excitation, Neutralization, Ionization, or Dissociation
of Particles Interacting with Surfaces
10. Interaction Potentials Between Surfaces and Free Particles
Located External to the Surface (electrons and heavy
particles)
11. Sticking Coefficients (thermal energies)
12. Electromagnetic Radiation Induced by Electron or Heavy
Particle Impact on Surfaces
13. Desorption of Gases from Surfaces
14. Blistering, Voids, and Surface Strain in Metals
15. Radiation Damage in Metals
16. Particle Implantation in Metals
17. Electron-, Ion-, and Photon-Induced Chemical Changes
to Surfaces

Table II
Ranking of Various PWI Processes

Process	Importance	Under- standing Status	Data Quality	Existing Compendia adequate
Sputtering by Electrons, Neutrons, and Heavy Particles (total removal coefficients)	1.1	1.2	1.3	Yes
Sputtered Particle Charge and Quantum (Excited) State Distribution	1.7	2.3	2.5	No
Sputtering of Alloy	1.3	2.4	2.4	No
Chemical Sputtering	1.0	2.3	2.4	No
Secondary Electron Ejection by Heavy Particle and Electrons	1.5	1.9	2.3	No
Photoelectric Ejection of Electrons (coefficients)	1.9	1.7	2.1	No
Reflection of Electrons from Surfaces (coefficients)	1.7	1.7	2.3	No
Reflection of Heavy Particles from Surfaces (total reflection coefficients)	1.1	1.4	1.5	Yes
Charge and Quantum State Distributions of Reflected Heavy Particles at Macroscopic Distances from Surfaces	1.8	2.4	2.4	No
De-Excitation, Neutralization, Ionization, or Dissociation of Particles Interacting with Surfaces	2.0	2.7	2.8	No
Interaction Potentials Between Surfaces and Free Particles Located External to the Surface (electrons and heavy particles)	2.2	2.5	3.0	No
Sticking Coefficients (thermal energies)	1.4	2.1	2.5	No
Electromagnetic Radiation Induced by Electron or Heavy Particle Impact on Surfaces	2.4	2.2	2.5	No
Desorption of Gases from Surfaces	1.2	2.0	2.2	Maybe
Blistering, Voids, and Surface Strain in Metals	1.9	1.9	1.9	No
Precipitation of voids or bubbles	1.9	2.3	2.3	No
Radiation Damage in Metals	1.5	1.8	1.9	No
Particle Implantation in Metals	1.4	1.3	1.9	Maybe
Electron-, Ion-, and Photon-Induced Chemical Changes to Surfaces	1.4	2.4	2.6	No
Hydrogen Diffusion	1.1	2.0	2.2	Yes
Hydrogen Recombination	1.3	2.2	2.4	No
Hydrogen Permeation	1.1	2.1	2.4	No
Hydrogen Saturation concentration	1.2	1.8	2.1	No
Hydrogen Trap binding energies	1.4	2.2	2.3	No
Radiation enhanced diffusion and/or surface segregation	1.3	2.4	2.6	No
Synergistic effects	1.1	2.7	2.8	No

1=very
3=not

1=good
3=bad

Review of Data Center Activities

E. W. Thomas
Georgia Institute of Technology
Atlanta, GA 30332 , U.S.A.

Short presentations were made to review activities of the data centers contributing to the meeting. This included the Oak Ridge Data Center (presented by E.W. Thomas, center lead by D.H. Crandall), the IPP-Nagoya center (presented by Y. Itikawa, the center's director) and the JAERI data center (presented by K. Ozawa, the center's director).

The Oak Ridge data center devotes most of its effort to searching journals and producing an annual bibliography concerning relevant processes. This is supplied to IPP-Nagoya as a computer tape and acts as a major source of information for their data compilations. The data center produced a handbook of data as report ORNL-5207 in 1977 and the surface physics section was updated in 1979 by report ORNL-5207/R1. The center also publishes a "Newsletter" four times per year that carries a bibliography of recent important data and news of recent developments.

The IPP-Nagoya data center concentrates on collecting data with the Oak Ridge bibliography as a primary reference source. Working groups of specialists correlate the information and develop semi-empirical equations to represent the published information and to guide both interpolation as well as extrapolation. The major outputs in the area of surfaces are data compendia as sputtering (Report IPP-AM 14) and on reflection of ions (Report IPP-AM 18). A review on desorption is complete and will be published shortly. Reviews are also being made of how sputtering and back scattering depending on incidence and exit angles. Reports are planned for 1982. The area of hydrogen recycling has been discussed in a workshop and data collection in selected areas will start soon.

The JAERI data center under Dr. Ozawa has a number of working groups concentrating on materials properties such as damage, impurity implantation and trapping. Activity in the trapping areas is co-ordinated with the Nagoya center to prevent overlap; a report is planned for 1982.

All three centers have extensive efforts in atomic and molecular physics data as well as data related to PWI. No significant overlap of activities was apparent and active collaboration exists in certain areas. The Japanese centers benefit from the active part-time participation of large numbers of scientists through the numerous working groups and frequent workshops. By contrast the U.S. center relies on a very small group of permanent consultants and in practise only one person is active in the area of surfaces.

It was generally agreed that the plasma physics community is not sufficiently aware of the activities by these centers. It was suggested that we seek the opportunity to present a short review of our activities to relevant plasma physics conference such as the PWI conference that will next be held in Gatlinburg, 1982. It was also agreed that we should seek input from plasma modellers as to the relative importance of different mechanisms so that we may focus attention on the processes that are most significant.

Review of Discussions on PWI Data for Specific Cases
— Reflection and Sputtering —

D. M. Gruen
Chemistry Division
Argonne National Laboratory, Argonne, IL 60439, U.S.A.

I. Reflection: H^+ on C and on SS.

E. W. Thomas and K. Morita

There appears to be general agreement that data compilation (DC) and the availability of empirical formulae (EF) to describe data are satisfactory for total reflection coefficients. This is not, however, the case for reflected charge state fractions. It was felt that the data basis set (DBS) is satisfactory for total reflection coefficients but needs to be augmented by data on well characterized surfaces for charge state fractions. Emphasis was placed on *critical* evaluation of existing data before inclusion in numerical tables or as part of a data set to be represented by a smoothed curve.

II. Sputtering Coefficients of H^+ on SS, O^+ and Fe^+ on SS.

D. M. Gruen and N. Matsunami

For total sputtering yields, the DC and EF on stainless steel are sufficient. The DBS is satisfactory for *clean* surfaces at normal incidence but deficient at oblique angles. A seminal study on the dependence of light ion-sputtering yields of Fe on ion fluence and oxygen partial pressure [J. Nucl. Mat. 93 & 94, 645 (1980)] shows changes in sputtering yields by factors of

10-15 due to oxygen contamination. More work is needed on sputtering yields as a function of surface contamination.

III. Charge State and Energy Distribution of Sputtered

Particles: H^+ on SS, O^+ and Fe^+ on SS.

D. Gruen and Y. Yamamura

Charge state and energy distributions of sputtered particles are potentially extremely important parameters for impurity control. The DBS in this area is very meager and must be augmented by careful work on well characterized surfaces. Monolayer oxygen contamination can change the charge fraction by orders of magnitude. A combination of LFS and SIMS measurements can provide empirical numbers for $R^+(E)$, the surface ionization coefficient as a function of energy. Empirical equations, perhaps, along the lines suggested by Schelton [Z. Naturforschung, 23a, 109 (1968)] should be applied to the data.

IV. Effects of Metal Structure on Sputtering of Binary Alloys.

H. Simizu

Since first walls and limiters are alloys or compounds rather than elementary metals, preferential sputtering must be considered. Because of surface segregation driven by Gibbsian and radiation enhanced diffusion, sputtering of alloys is a very complicated process. Data in this area relevant to fusion materials is almost wholly lacking and there are no empirical formulas as yet to serve as a means for data reduction. Both theoretical and experimental studies are underway in a number of laboratories.

Review of Discussions on PWI Data for Specific Cases
— Trapping, Re-Emission, Desorption and Adsorption —

K. Kamada
Institute of Plasma Physics
Nagoya University
Nagoya 464, Japan

Data reviews on re-emission and desorption, as important contributions to the hydrogen isotope recycling process, were made together with the discussions about the underlying physical and chemical mechanisms, by Doyle and Tanabe (re-emission) and by Thomas and Kamada (desorption of H and O from SS), with an additional supplement for the re-emission by Sone.

Doyle described the recycling process throughout the plasma and wall materials. Basically he employed the plasma transport code due to Howe, which includes kinetic reflection on the surface, thermal diffusion and beam induced detrapping in the wall, giving a set of coupled differential equations which represent the concentration of hydrogen isotope implanted into a solid. These differential equations are hybridization of several theories plus a modification of the isotope exchange term. Special cases of the equations are useful to give insight into 1) the complex relationships which exist between the plasma parameters (i.e. flux and energy) and materials parameters (i.e. diffusion constant D and surface recombination coefficient K_r), 2) how both sets of these variables affect important issues such as recycle time, tritium inventory and tritium permeation flux through wall.

Effects of the two materials parameters D and K_r are represented by the transport parameter W which govern whether diffusion or surface recombination limited effects

dominate the hydrogen transport into the plasma. According to the magnitude of the transport parameter, taking into account of its temperature dependence at the same time, candidate materials are classified into four groups:

1. "Surface recombination" limited materials; SS, Ni, Ni alloy, Mo and Al at relatively high temperature region which is quite relevant in fusion reactors.
2. "Diffusion" limited materials; Al, Cu and Mo at relatively low temperature region.
3. "Total H retention" materials; when the transport parameter $W \ll 1$, injected hydrogen is essentially prohibited from being re-emitted as H_2 molecule. A typical example of this class of materials is titanium. Another candidates are vanadium and zirconium which have exothermic heat of solution for hydrogen.
4. "End of range trapping" materials:
All materials change over to this class at sufficiently low temperatures. This is because the thermal detrapping of hydrogen from lattice defects, which are formed near the end of range of the implanted hydrogen, becomes ineffective. Doyle gave $T < [(E_D + E_T) \cdot 400]K$ for the temperature range, where E_D and E_T are activation energy for thermal diffusion and the de-trapping expressed in eV, Low Z materials, including C, TiC, TiB₂, VB₂, SiC, B, B₄C, and Si, belong to this class of materials even at room temperature and above.

Tanabe supplemented the Doyle's talk with a complex re-emission phenomenon having larger hydrogen retention with increasing temperature in Ni above 500K, suggesting the reconstruction of radiation damage. He also mentioned super-permeation and super-inventory observed by transmission experiment under glow discharge condition.

Tanabe summarized the data so far obtained concerning the retention and re-emission behaviour of hydrogen isotopes in SS and Ti.

Sone presented his own results of deuteron trapping and re-emission in carbon in the energy range of 100 ~ 1000 eV. He pointed out the effect of pre-bombardment damage on the re-emission behaviour, describing the result as a reduction of detrapping cross-section due to the presence of lattice defects.

On the desorption of H and O from SS, Thomas pointed out that reliable desorption study is very lacking. Further he pointed out that many experiments have involved the desorption of naturally occurring impurity atoms from technical steel, being likely to be different from the case of hydrogen or oxygen deliberately adsorbed onto steel. The only data worth reviewing are those involving well outgassed surface deliberately exposed to a single contaminant. For photodesorption, he insisted that there is no basis for performing any meaningful review. For electron and ion impact desorption, he referred the data due to Drinkwine-Lichman and Bastasz, respectively.

Specifically on ion induced desorption, Kamada talked about the compilation of data so far obtained for the combinations of various kinds of adsorbates and substrate materials, together with the discussions on underlying physical mechanisms. He classified the desorption cross-sections so far obtained into two groups; one of which is a group of data which nearly fit to the theory of Winters and Sigmund, and the another group which includes data, mainly measured on single crystalline substrates, showing anomalously large desorption cross-sections at a certain energy range. The latter group of the data was presumed to be related to the shadowing by the surrounding substrate atoms of an adsorbate, making the probe ion to focus on the adsorbate so as to make the desorption much easier. However, the desorption of D from SS was ascertained to be included in the first group.

Conclusion

E.W. Thomas

Georgia Institute of Technology
Atlanta, GA 30332, U. S. A.

In his opening paper N. Itoh drew a valuable distinction between the phenomena associated with energetic particle (energy greater than 100 eV) impact on the wall and phenomena associated with low energy (less than 100 eV) impact on the wall. The former can be readily understood in terms of atomic collision theory, and have been the subject of a number of data reviews. By contrast the behaviour of low energy particles, down to thermal energies, lies in the realm of solid state physics being intimately related to diffusion, trapping at defects and to chemical reactions. This area is not well understood by the PWI (Plasma Wall Interaction) community, the data is sparse and reviews unobtainable. Indeed it is not immediately clear what parameters are relevant and how they are inter-related. B. Doyle provided a detailed analysis of the relationship between implantation, diffusion, trapping and re-emission. This can be used to set the stage for further consideration of the problem.

As part of the workshop's deliberations a poll was taken as to how the participants ranked the various processes contributing to PWI. It was concluded that thermal energy processes, diffusion, recombination, permeation, saturation, trapping and chemical sputtering were most important to PWI in present machines but were-least understood. By contrast the energetic processes of physical sputtering and reflection were considered to be of lesser importance and relatively well understood.

The major reviews and data compendia provided by the IPP Nagoya data center (and similar reports from MPI Garching)

provide adequate coverage of reflection and physical sputtering. There remains a need to consider charge and excited states of reflected and sputtered particles; the quantum state of the emerging particle will influence its penetration into the plasma. Data compendia for these areas are being undertaken by IPP Nagoya and reports are planned for 1982. In general the reports include provision of algebraic formulae to represent the phenomenon; these formulae may be directly incorporated into PWI simulation codes. A criticism of the work published to date is that data are accepted uncritically so that both good and bad data contributes to the derived algebraic representation. In summary the areas of reflection and sputtering are well covered and only refinement is needed.

Thermal energy processes include trapping, re-emission, recombination and chemical processes. The Japanese data centers are both entering into consideration of these areas. In general the data coverage is weak, the quality is poor and it is not clear whether an assessment is feasible at this time. With the continuing clarification of these subject areas the situation is improving rapidly. There is need for the PWI community to become better acquainted with existing compendia for such processes as diffusion and precipitation which are the province of the metallurgist. These areas are under review and require continued effort.

Largely neglected by the data centers are the areas of secondary electron ejection and electron reflection. The flux of electrons from the wall will influence sheath potential and this in turn alters the energy of ions impinging on the surface. The energy governs sputtering, reflection, retention and other processes. The area of electron processes was reviewed some thirty years ago but has been largely ignored since. It is to be proposed that the Oak Ridge Data Center will undertake a data compendia and review in that area. Also largely neglected is the area of adsorption and desorption. It was agreed that further scientific work needs to be done here before any review is attempted.

It was generally agreed that we need to better publicize the activities of the data centers so that the plasma physicist, who represents the customer for the information becomes better acquainted with the availability of data compendia. Specifically, we suggest that reviews of data center activities may be presented as papers to the international conferences such as the PWI conference in Gatlinburg next May. We propose also to arrange a short informal discussion group at such conferences where representatives of data producing groups, data users and data centers can meet to discuss what data collection activities are most appropriate for the immediate future. The Japanese and US data centers will annually write short reviews of their present and proposed activities which can be published in the newsletters of various data centers. The US participants considered it desirable that the present data handbook(Atomic and Molecular Data for Fusion ORNL/5207)be updated using as a basis the data compendia published by IPP Nagoya and by MPI Garching.

There is generally a continuing need to assess the relative importance of these various processes to PWI. One requires an improved diagnostics of the particle fluxes to the wall followed by incorporation of this data into a model for PWI. Certain mechanisms may prove to be quantitatively unimportant. For the important processes it is necessary to vary the magnitudes of the various coefficients and cross sections to determine the sensitivity of device operation to these parameters. In this way one may assess the accuracy with which the parameters need to be determined. The two characteristics of importance and accuracy should be a guide for further work by the data centers. At the present time data centers choose subjects primarily for the ease with which they may be considered not for their importance. Moreover no real attention is paid to the evaluation of accuracy.

In general the workshop showed that the processes contribution to PWI are now being well defined and certain areas have reached a maturity where compendia and assessment are justified. The subject does however remain volatile and there is a continuing need for better data and for assessment in the area of thermal energy processes, chemical effects, synergistic effects, adsorption, desorption and electron processes.

✓

U.S. - Japan Surface Data Review Workshop

IPP, Nagoya, Japan
December 14-18, 1981

Section I: Overview of PWI Data Needs and Production for Fusion

	chairman:	K. Kamada
Dec. 14 (Monday)	13:30-14:00 p.m.	Registration and opening K. Kamada
	14:00-15:00	PWI data needs — T. Amano
	15:00-16:00	Atomic interaction in plasma E.W. Thomas
	16:00-16:30	Coffee
	16:30-17:30	Plasma-wall interaction N. Itoh
	17:30-18:00	Survey of activities in U.S. E.W. Thomas
	18:00-18:30	Survey of activities in Japan T. Yamashina
	19:00	Workshop outing

Section II: Mechanisms of PWI

	chairman:	E.W. Thomas
Dec. 15 (Tuesday)	9:00-10:00	Particle Reflection T. Tabata
	10:00-11:00	Sputtering---materials removal rate R. Shimizu
	11:00-11:30	Coffee
	11:30-12:30	Sputtering---quantum state and energy of ejected material D. Gruen

12:30-14:00 Lunch

 chairman T. Yamashina

14:00-15:00 Chemical reaction and chemical
 sputtering
 R. Yamada

15:00-16:00 Hydrogen trapping, detrapping and
 re-emission
 B. Doyle

16:00-16:30 Coffee

16:30-17:30 Desorption and adsorption
 A. Koma

 chairman B. Doyle

Dec. 16 9:00-10:30 General discussions on mechanisms
(Wednesday)

10:30-11:00 Coffee

Section III: Data Center Interactions

11:00-11:20 ORNL Data Center activities
 E.W. Thomas

11:20-11:40 JAERI Data Center activities
 K. Ozawa

11:40-12:00 IPP Data Center activities
 Y. Itikawa

12:00-12:30 Discussions on Data Center
 interactions

12:30-14:00 Lunch

Section IV: Discussion on PWI Data for Specific Cases

chairman	S. Ishino
14:00-15:00	Reflection: H^+ on C and on SS. E.W. Thomas and K. Morita
15:00-16:00	Sputtering coefficients H^+ on SS, O^+ and Fe^+ on SS D. Gruen and N. Matsunami
16:00-16:30	Coffee
16:30-17:30	Charge State and energy distribution of sputtered particles H^+ on SS O^+ and Fe^+ on SS D. Gruen and Y. Yamamura

	chairman	D. Gruen
Dec. 17 (Thursday)	9:00-10:00	Trapping and re-emission H^+ on Ti and on SS B. Doyle and T. Tanabe
	10:00-11:00	Desorption and adsorption H and O on SS E.W. Thomas and K. Kamada
	11:00-12:30	General discussions on data evaluation
	12:30-14:00	Lunch

Section V: New Proposals and Summary

	chairman	E.W. Thomas and N. Itoh
Dec. 18 (Friday)	9:00-9:30	Comments on evaluation of trapping and re-emission data K. Sone
	9:30-10:00	Effects of metal structure on sputtering of binary alloys H. Simizu
	10:00-12:30	General Discussion and Summary

List of Participants

U.S.- Japan Workshop on Surface Data Review

Institute of Plasma Physics, Nagoya University

December 14-18, 1981

From the U.S.

Barney L. Doyle	Sandia National Laboratories Albuquerque, NM 87185
Dieter Gruen	Chemistry Division Argonne National Laboratory Argonne, IL 60439
Edward W. Thomas	School of Physics Georgia Institute of Technology Atlanta, GA 30332

From Japan

Susume Amamiya	Department of Nuclear Engineering Nagoya University Nagoya 464
Tsuneo Amano	Institute of Plasma Physics Nagoya University Nagoya 464
Junji Fujita	Institute of plasma Physics Nagoya University Nagoya 464
Shiori Ishino	Department of Nuclear Engineering University of Tokyo Bunkyo, Tokyo 113

Yukikazu Itikawa	Institute of Plasma Physics Nagoya University Nagoya 464
Noriaki Itoh	Department of Crystalline Materials Science Nagoya University Nagoya 464
Shuichi Iwata	Department of Nuclear Engineering University of Tokyo Bunkyo, Tokyo 113
Koji Kamada	Institute of Plasma Physics Nagoya University Nagoya 464
Atsushi Koma	Institute of Materials Science The University of Tsukuba Sakuramura, Ibaraki 305
Noriaki Matsunami	Department of Crystalline Materials Science Nagoya University Nagoya 464
Kenji Morita	Department of Crystalline Materials Science Nagoya University Nagoya 464
Kunio Ozawa	Physics Division Japan Atomic Energy Research Institute Tokaimura, Ibaraki 319-11

Masahiro Saidoh	Division of Thermonuclear Fusion Research Japan Atomic Energy Research Institute Tokaimura, Ibaraki 319-11
Hazime Shimizu	Electrotechnical Laboratory Sakuramura, Ibaraki 305
Ryuichi Shimizu	Department of Applied Physics Osaka University Yamadaoka, Suita 565
Kazuho Sone	Division of Thermonuclear Fusion Research Japan Atomic Energy Research Institute Tokaimura, Ibaraki 319-11
Tatsuo Tabata	Radiation Center of Osaka Prefecture Shinkecho, Sakai 593
Tetsuo Tanabe	Department of Nuclear Engineering Osaka University Yamadaoka, Suita 565
Reyji Yamada	Division of Thermonuclear Fusion Research Japan Atomic Energy Research Institute Tokaimura, Ibaraki 319-11
Yasunori Yamamura	Department of Applied Physics Okayama University of Science Ridaicho, Okayama 700
Toshiro Yamashina	Department of Nuclear Engineering Hokkaido University Kitaku, Sapporo 060

LIST OF IPPJ-AM REPORTS

- IPPJ-AM-1* "Gross Sections for Charge Transfer of Hydrogen Beams in Gases and Vapors in the Energy Range 10 eV–10 keV"
by Tawara (1977)
- IPPJ-AM-2* "Ionization and Excitation of Ions by Electron Impact –Review of Empirical Formulae–"
by T. Kato (1977)
- IPPJ-AM-3 "Grotrian Diagrams of Highly Ionized Iron FeVIII-FeXXVI"
by K. Mori, M. Otsuka and T. Kato (1977) AD NDT 23, 196 (1979)
- IPPJ-AM-4 "Atomic Processes in Hot Plasmas and X-Ray Emission"
by T. Kato (1978)
- IPPJ-AM-5* "Charge Transfer between a Proton and a Heavy Metal Atom"
by S.Hiraide, Y. Kigoshi and M. Matsuzawa (1978)
- IPPJ-AM-6* "Free-Free Transition in a Plasma –Review of Cross Sections and Spectra–"
by T. Kato and H. Narumi (1978)
- IPPJ-AM-7* "Bibliography on Electron Collisions with Atomic Positive Ions: 1940 Through 1977"
by K. Takayanagi and T. Iwai (1978)
- IPPJ-AM-8 "Semi-Empirical Cross Sections and Rate Coefficients for Excitation and Ionization by Electron Collision and Photoionization of Helium"
by T. Fujimoto (1978)
- IPPJ-AM-9 "Charge Changing Cross Sections for Heavy-Particle Collision in the Energy Range from 0.1 eV to 10 MeV I. Incidence of He, Li, Be, B and Their Ions"
by Kazuhiko Okuno (1978)
- IPPJ-AM-10 "Charge Changing Cross Sections for Heavy-Particle Collision in the Energy Range from 0.1 eV to 10 MeV II. Incidence of C, N, O and Their Ions"
by Kazuhiko Okuno (1978)
- IPPJ-AM-11 "Charge Changing Cross Sections for Heavy-Particle Collision in the Energy Range from 0.1 eV to 10 MeV III. Incidence of F, Ne, Na and Their Ions"
by Kazuhiko Okuno (1978)
- IPPJ-AM-12* "Electron Impact Excitation of Positive Ions Calculated in the Coulomb-Born Approximation –A Data List and Comparative Survey–"
by S. Nakazaki and T. Hashino (1979)
- IPPJ-AM-13 "Proceedings of the Nagoya Seminar on Atomic Processes in Fusion Plasmas Sept. 5-7, 1979" (1979)
- IPPJ-AM-14 "Energy Dependence of Sputtering Yields of Monatomic Solids"
N. Matsunami, Y. Yamamura, Y. Itikawa, N. Itoh, Y. Kazumata, S. Miyagawa, K. Morita and R. Shimizu (1980)
- IPPJ-AM-15 "Cross Sections for Charge Transfer Collisions Involving Hydrogen Atoms"
Y. Kaneko, T. Arikawa, Y. Itikawa, T. Iwai, T. Kato, M. Matsuzawa, Y. Nakai, K. Okuno, H. Ryufuku, H. Tawara and T. Watanabe (1980)

- IPPJ-AM-16 "Two-Centre Coulomb Phaseshifts and Radial Functions"
by H. Nakamura and H. Takagi (1980)
- IPPJ-AM-17 "Empirical Formulas for Ionization Cross Section of Atomic Ions for
Electron Collisions –Critical Review with Compilation of Experimental
Data–"
by Y. Itikawa and T. Kato (1981)
- IPPJ-AM-18 "Data on the Backscattering Coefficients of Light Ions from Solids"
T. Tabata, R. Ito, Y. Itikawa, N. Itoh and K. Morita (1981)
- IPPJ-AM-19 "Recommended Values of Transport Cross Sections for Elastic Collision and
Total Collision Cross Section for Electrons in Atomic and Molecular Gases"
M. Hayashi (1981)
- IPPJ-AM-20 "Electron Capture and Loss Cross Sections for Collisions between Heavy
Ions and Hydrogen Molecules"
Y. Kaneko, Y. Itikawa, T. Iwai, T. Kato, Y. Nakai, K. Okuno and H. Tawara
(1981)
- IPPJ-AM-21 "Proceedings of the U.S.–Japan Workshop on Surface Data Review
Dec. 14-18, 1981" (1982)

Available upon request to Research Information Center, Institute of Plasma Physics, Nagoya University, Nagoya 464, Japan, except for the reports noted with*.